TR–230–1963 15 MAY 1979

SPACE SHUTTLE PLUME/SIMULATION APPLICATION

FINAL REPORT

RESULTS AND MATH MODEL SUPERSONIC DATA

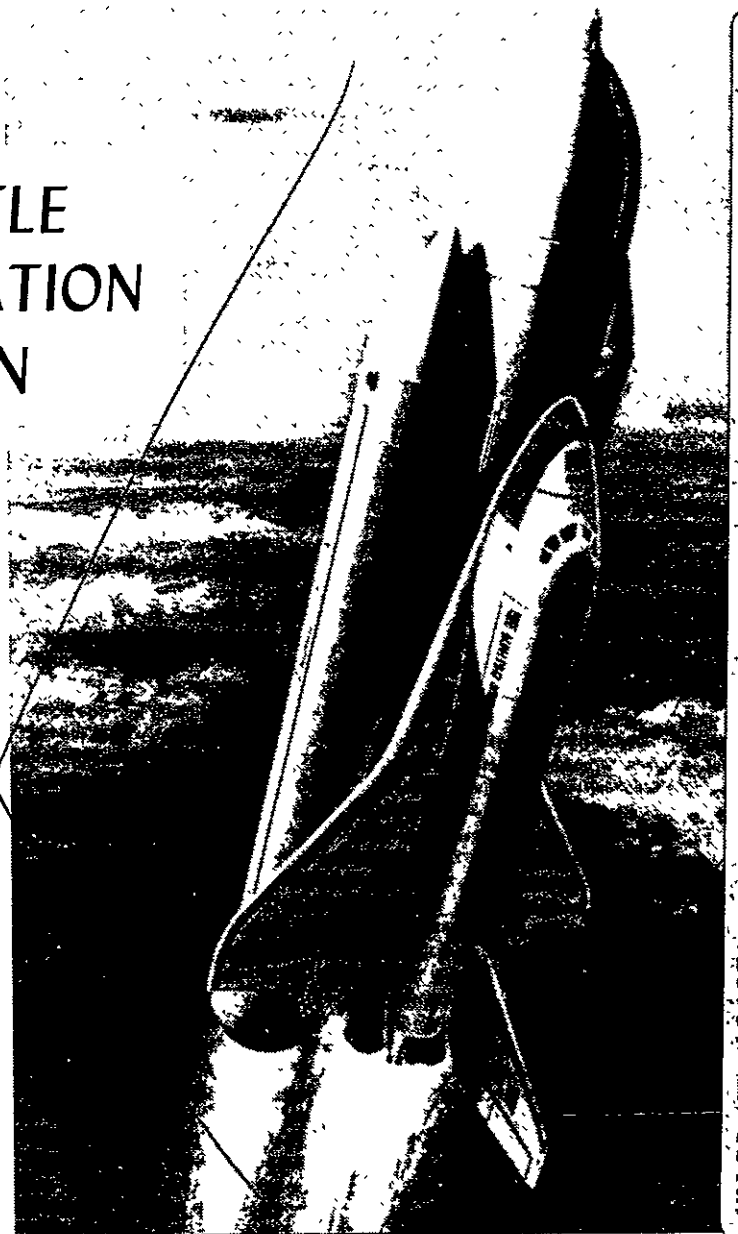

Prepared for:

NATIONAL AERONAUTICS AND SPACE ADMINISTRATION
GEORGE C. MARSHALL SPACE FLIGHT CENTER
Science and Engineering Directorate
Under Contract NAS8-32524

Prepared by:

NORTHROP SERVICES, INC.
P. O. Box 1484 Huntsville, Alabama 35807 (205) 837-0580

NSI

TR–230–1963

SPACE SHUTTLE PLUME SIMULATION APPLICATION FINAL REPORT

RESULTS AND MATH MODEL SUPERSONIC DATA

15 MAY 1979

by

W. Boyle
B. Conine
G. Bell

Prepared for:

NATIONAL AERONAUTICS AND SPACE ADMINISTRATION
GEORGE C. MARSHALL SPACE FLIGHT CENTER
SCIENCE AND ENGINEERING DIRECTORATE

Under Contract NAS8-32524

Reviewed and Approved by:

M. A. Sloan, Jr., Manager
Technology

NORTHROP SERVICES, INC.
ENGINEERING AND TECHNOLOGY CENTER
P.O. BOX 1484
HUNTSVILLE, ALABAMA 35807
(205)837-0580

FOREWORD

This report presents the results of work performed by Northrop Services, Inc. Engineering Technology Center for the Marshall Space Flight Center under Contract NAS8-32524. The NASA technical monitor for this contract is Mr. J. Sims. The authors wish to acknowledge their valuable assistance, direction and contributions to the successful completion of this study.

TABLE OF CONTENTS

LIST OF ILLUSTRATIONS

LIST OF ILLUSTRATIONS (Concluded)

LIST OF TABLES

LIST OF TABLES (Continued)

LIST OF TABLES (Concluded)

GENERAL NOMENCLATURE

SYMBOL	DEFINITION
ET	Space Shuttle external tank
O	Space Shuttle Orbiter
SRB	Space Shuttle Solid Rocket Booster
SSLV	Space Shuttle Launch Vehicle
Base	Locations on the Space Shuttle where the nozzle exhaust plumes are the primary influence in determining the local pressure environment
Components	Portions of the Orbiter; wing, body flap, etc.
Elements	Primary elements of the SSLV, Orbiter, ET, SRB's
Forebody	Locations on the Space Shuttle where the nozzle exhaust plumes are the secondary influence in determining the local pressure environments

TEST NOMENCLATURE

Symbol General:	Definition
C_A	Axial force coefficient
C_{B_V}	Vertical tail bending moment coefficient
C_{B_W}	Wing-root bending-moment coefficient
C_H	Hinge moment coefficient
$C_{H_{E_I}}$	Hinge-moment coefficient for inboard elevon.
$C_{H_{E_O}}$	Hinge-moment coefficient for outboard elevon.
C_ℓ	Rolling moment coefficient
C_M	Pitching moment coefficient
C_N	Normal force coefficient
C_{N_W}	Wing normal-force coefficient
C_{T_V}	Vertical tail torsion moment coefficient
C_{T_W}	Wing-root torsion-moment coefficient
C_Y	Side force coefficient
C_{Y_N}	Yawing moment coefficient
C_{Y_V}	Vertical tail shear force coefficient
L	Reference length, in. or ft. defined in Table 6-10
S	Reference area, ft^2 defined in Table 6-10
	SUBSCRIPTS
B	Base
F	Forebody - fuselage
C_P	Determined using power on pressure coefficient
DEL	Determined using power-on minus power-off delta pressure coefficient
O	Orbiter

TEST NOMENCLATURE

ET	ET
SRB	SRB
PON	Power On
POF	Power Off

GAS DYNAMIC NOMENCLATURE

Symbol	Definition
P_i	Pressure (absolute) at model surface tap i, psia
C_{P_i}	Pressure coefficient for model surface tap i.
ΔC_{P_i}	$C_{P_{\text{Power On}}} - C_{P_{\text{Power Off}}}$
P_{c_j}	Chamber pressure (absolute) for nozzle j, psia
P_{e_j}	Exit pressure (absolute) for nozzle j. psia
CPR_j	Chamber-pressure ratio for nozzle j, P_c/P_∞
γ_j	Ratio of specific heats for nozzle J
$P_c/P_{\infty_{ORB}}$	SSME chamber to freestream pressure ratio
$P_c/P_{\infty_{SRB}}$	SRB chamber to freestream pressure ratio
P_c/P_e	Chamber to exit nozzle pressure ratio
P_c/P_{wall}	Chamber to nozzle wall pressure ratio
M_j	Plume boundary Mach number at nozzle lip
M_E	Nozzle exit Mach number at nozzle wall (inviscid)
N	Exponent of ratio of specific heats and in similarity paramet
δ_j	Initial plume expansion angle
Deflections:	
δ_{E_I}	Left inboard elevon setting, corrected for load deflection, c
δ_{E_O}	Left outboard elevon setting, corrected for load deflection,

Test Operations:

M	Freestream Mach number.
Re/ft	Freestream unit Reynolds number, ft^{-1}.
q	Freestream dynamic pressure, psf.
P_∞	Freestream static pressure, psia.
P_T	Freestream total pressure, psia.
T	Freestream static temperature, ^oR.
T_T	Freestream total temperature, ^oR.
α	Model angle-of-attack, deg.
β	Model angle-of-sideslip, deg.
$T_{T_{SRB}}$	SRB supply total temperature, ^oR.
$T_{T_{MPS}}$	MPS supply total temperature, ^oR.
$P_{c_{MPS}}$	MPS supply total pressure, psia.
$P_{c_{SRB}}$	SRB supply total pressure, psia.

REVISIONS			
REV SYM	DESCRIPTION	DATE	APPROVAL

Section I

INTRODUCTION

The analysis of pressure and gage wind tunnel data from Space Shuttle wind tunnel test IA138 was performed to define the aerodynamic influence of the main propulsion system (MPS) and solid rocket booster (SRB) plumes on the total vehicle, elements, and components of the Space Shuttle vehicle during the supersonic portion of ascent flight.

Wind tunnel test IA138 was a supersonic test of a 0.01-scale model of the Space Shuttle launch vehicle. The wind tunnel test was conducted in the 9 x 7-foot section of the NASA/AMES Research Center Unitary Plan Wind Tunnel. Pressure data were obtained over the aft portions of the wind tunnel model. Wing and elevon gage data were also obtained.

Air was used as a simulant gas to develop the model exhaust plumes. A portion of the test was devoted to testing at various power levels. Data from the power level portion was used in conjunction with prototype base pressure possibility curves to evaluate nominal power levels to be used during the investigation of changes in model attitude, and elevon deflections. The simulation parameter used to develop nominal power levels was $[\delta_j \gamma_j^N]_{PROT} = [\delta_j \gamma_j^N]_{MODEL}$ where N varies with Mach number.

The plume induced aerodynamic loads were developed for the Space Shuttle base areas and forebody areas. The base areas include the orbiter base including nozzles, ET base and SRB base. The forebody includes the orbiter areas forward of the base, including the blody flap, the wings and elevons, and ET and SRB areas forward of the base.

A math model of the plume induced aerodynamic characteristics was developed for a range of Mach numbers to match the forebody aerodynamic math model. The base aerodynamic characteristics are presented in terms of forces and moments versus attitude. Total vehicle base and forebody aerodynamic characteristics are presented in terms of aerodynamic coefficients for Mach numbers from 1.55 to 2.5. Element and component base and forebody aerodynamic characteristics ar

presented for Mach numbers of 1.55, 1.8, 2.2 and 2.5. These Mach numbers are compatible with defined forebody aerodynamic characteristics.

Tolerances were developed for all plume induced aerodynamic characteristics. The tolerances are developed in terms of a math model and include simulation parameter uncertainties, model instrumentation uncertainties, model configuration uncertainties including tunnel-model support interference uncertainties and Reynolds number effects.

Section II

WIND TUNNEL MODEL

The wind tunnel model was a 0.01 scale space shuttle launch vehicle configuration. The wind tunnel model is designated - 75 OTS Configuration 140C (modified) Jet - Plume Integrated Space Shuttle Vehicle. The orbiter model was the 140C model configuration which generally represents the OV101 orbiter mold lines. The OV102 mold lines have significant differences in the canopy contour, the wing section near the glove-wing fairing, and the elevon contour. Details of the model configuration can be obtained from the pretest report (reference 1).

The model was strut mounted as shown in Figure 2-1. Cold air was supplied through the strut to the SSME and SRB nozzles. An air supply strut was mounted between the ET and orbiter to supply air to the simulated SSME nozzles as shown in Figure 2-2. The SSME nozzles were conical with an exit plane lip angle of 11.0 degrees. The SRB nozzles were conical with a lip angle of 27.5 degrees. Schmatics of the SSME and SRB nozzle internal contour are presented in Figures 2 and 2-4. Calibration data for the nozzles are presented in Section IV. Details of the model configuration can be obtained from the pretest report (reference 1)

A partial right orbiter wing was strain-gage instrumented to obtain wing shear forces, root bending moments and torsion moments. The inboard and outboard elevons on the left wing were also separately strain-gage instrumented to obtain hinge moments. All base, nozzle, and portions of each element forebody were pressure instrumented.

Figure 2-1. WIND TUNNEL MODEL INSTALLATION PHOTOGRAPH - IA138 TEST

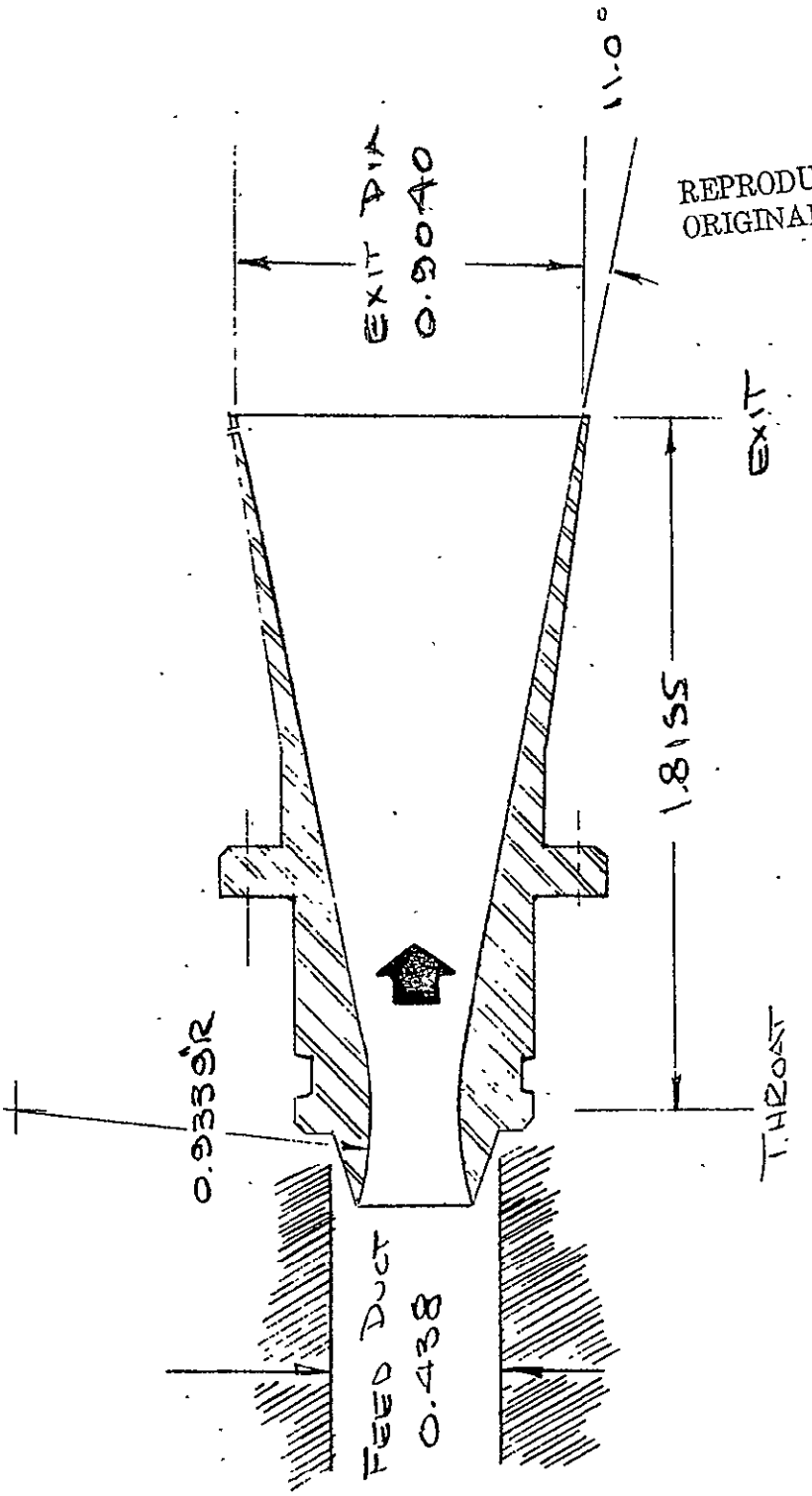

Figure 2-3. SSME NOZZLE (N_{87})

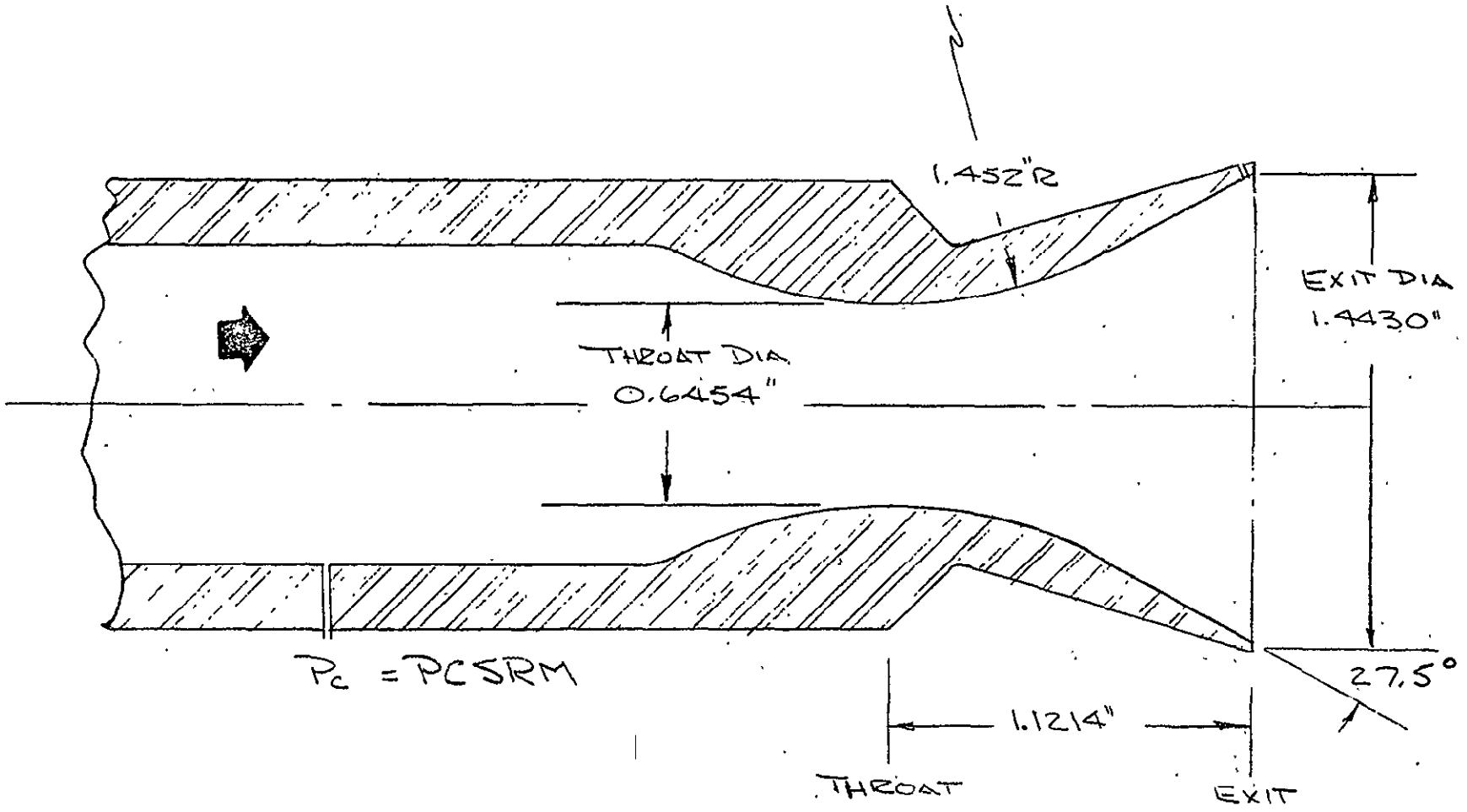

Figure 2-4. SRM NOZZLE (N_{88})

Section III

TEST CONDITIONS

The IA138 wind tunnel test program was essentially conducted in two parts. Part one was a power variation test at zero attitude, where chamber pressure of the MPS and SRB model nozzles was varied. Part two was a test program at a nominal power level that included testing the model at various elevon deflections and attitudes.

Base pressure data, from the power variation test (Part 1), was evaluated at the test site along with prototype plume characteristics to evaluate the nominal model nozzle plume characteristics and model chamber pressures. (See Section V for plume simulation discussion). These tests were conducted at zero angle of attack and zero angle of sideslip. Tests were conducted for a series of Mach numbers from 1.55 to 2.5.

Part 2 of the test program consisted of testing the model using the nominal power levels developed in Part 1 over a range of attitudes and elevon deflections. Data were obtained at nominal angles of attack of -8, -6, -4, 0, and +4 degrees. The angles of sideslip were nominally 0, and ± 4 degrees.

The data analysis procedure required a power-on and a power-off run sequence. The power-on data was required to obtain the power-on base pressure environments. The power-off data is used to evaluate the influence of power on changes in local pressure environments for use in the analysis of forebody plume induced aerodynamic characteristics. The development of the plume induced aerodynamic characteristics also required testing at positive and negative sideslip angles, since portions of the model had pressure instrumentation on only one side of the model. Thus four sets of test data were required to develop the plume induced aerodynamic data. The power-on and power-off run data sets used for analysis are presented in Tables 3-1 through 3-4. These tables show the angle of sideslip schedule and the elevon deflection run sets for each Mach number. The run numbers are arranged in terms of the model configuration at nominal power levels (elevon deflection), then the power variation run numbers.

Each power run number has a sequence slash number that denotes a particular MPS and SRB power level. Figures 3-1 through 3-4 show the power level for each power run-sequence combination. The square shows the nominal power value used for the testing of the various elevon settings.

Tests were conducted at various elevon deflections corresponding to Schedule 6 and probable variations about schedule 6. Schedule 6 elevon deflections are presented in Figure 3-5. Plots of the various inboard and outboard elevon deflection angles evaluated during the test along with the nominal schedule 6 value are presented in Figures 3-6 through 3-9. The elevon deflection closest to schedule 6 that was used to develop the plume induced aerodynam data base is shown in each figure.

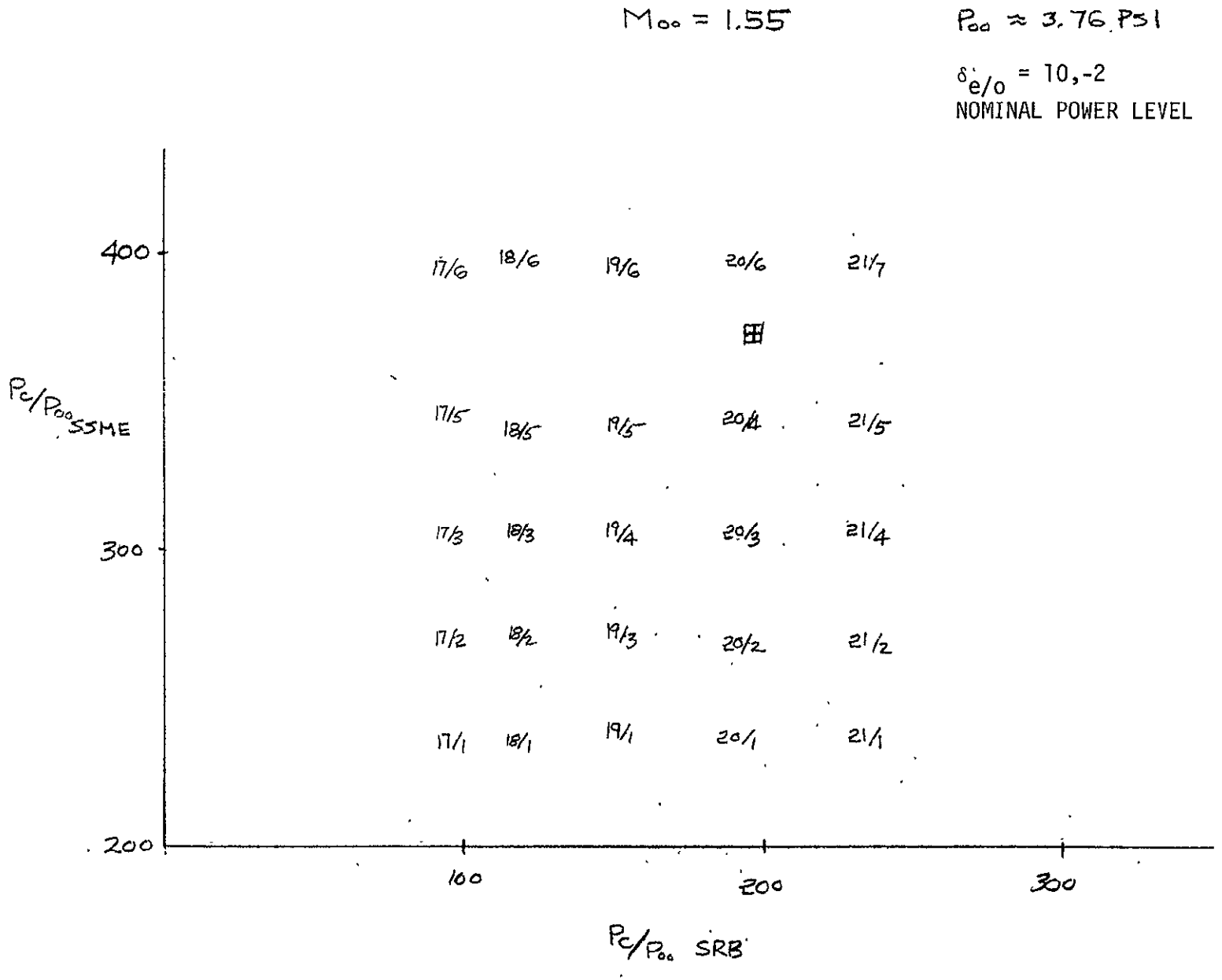

Figure 3-1. POWER VARIATION RUNS (M_{∞} = 1.55)

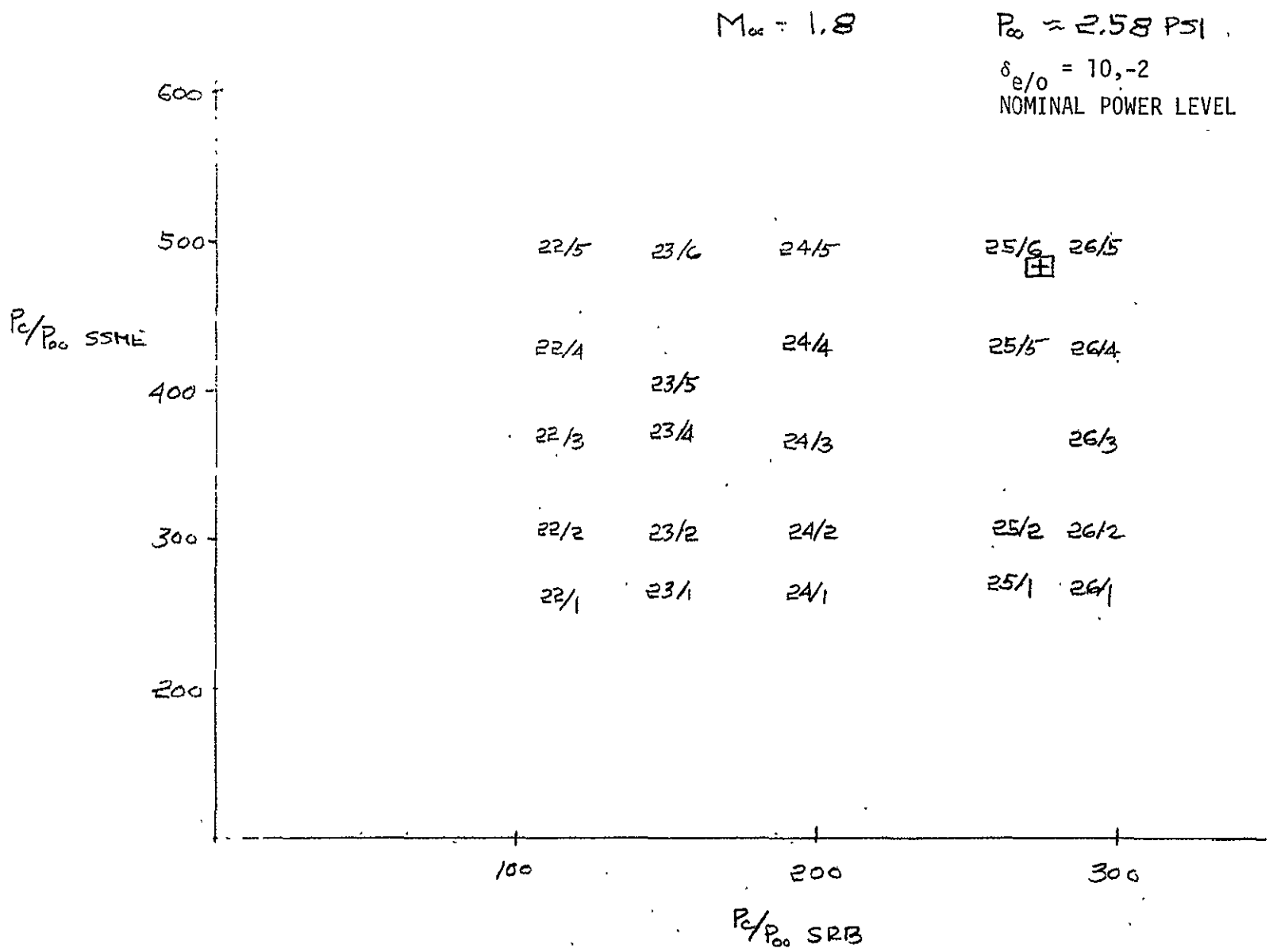

Figure 3-2. POWER VARIATION RUNS (M_∞ = 1.80)

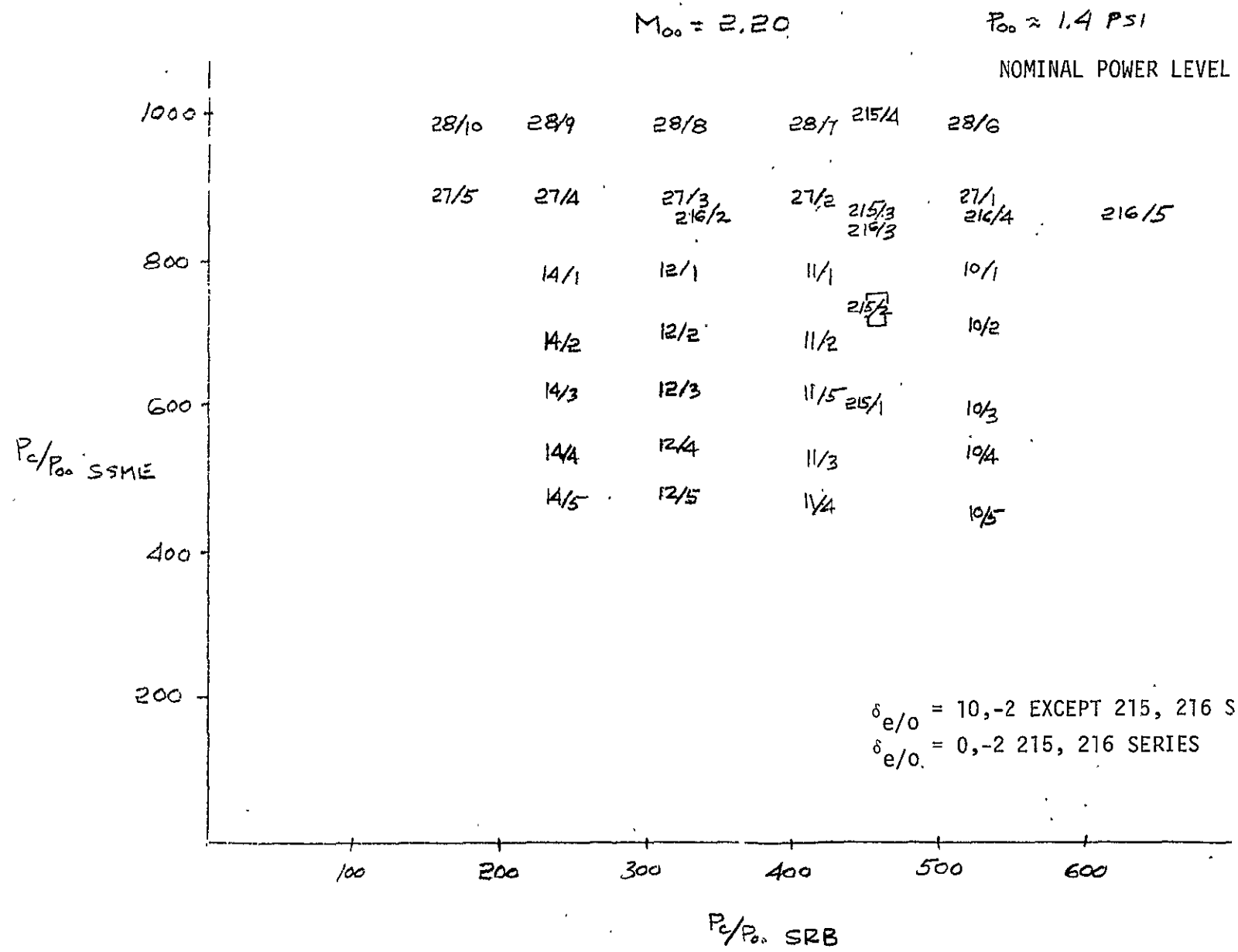

Figure 3-3. POWER VARIATION RUNS (M_{∞} = 2.20)

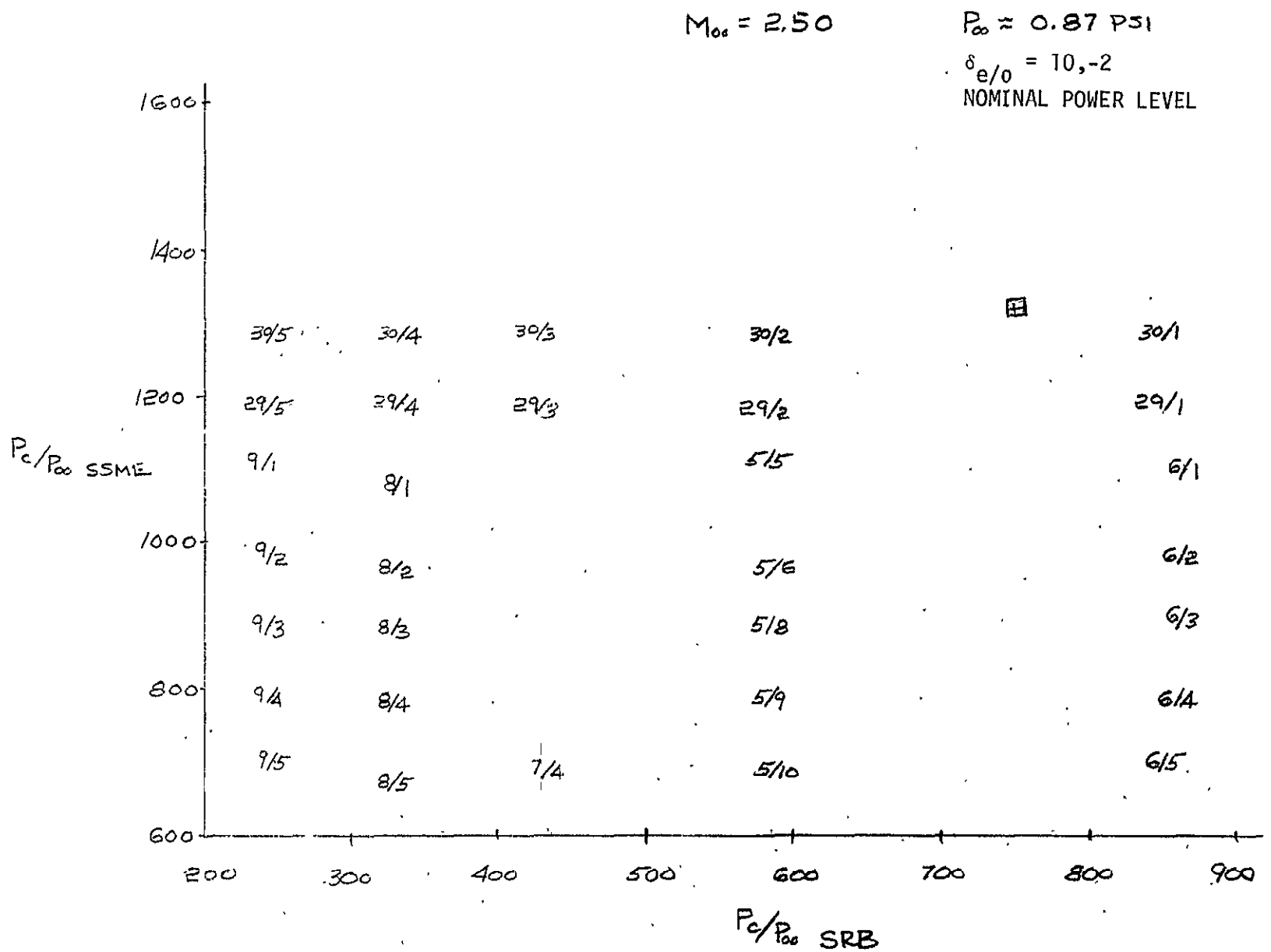

Figure 3-4. POWER VARIATION RUNS (M_{∞} = 2.50)

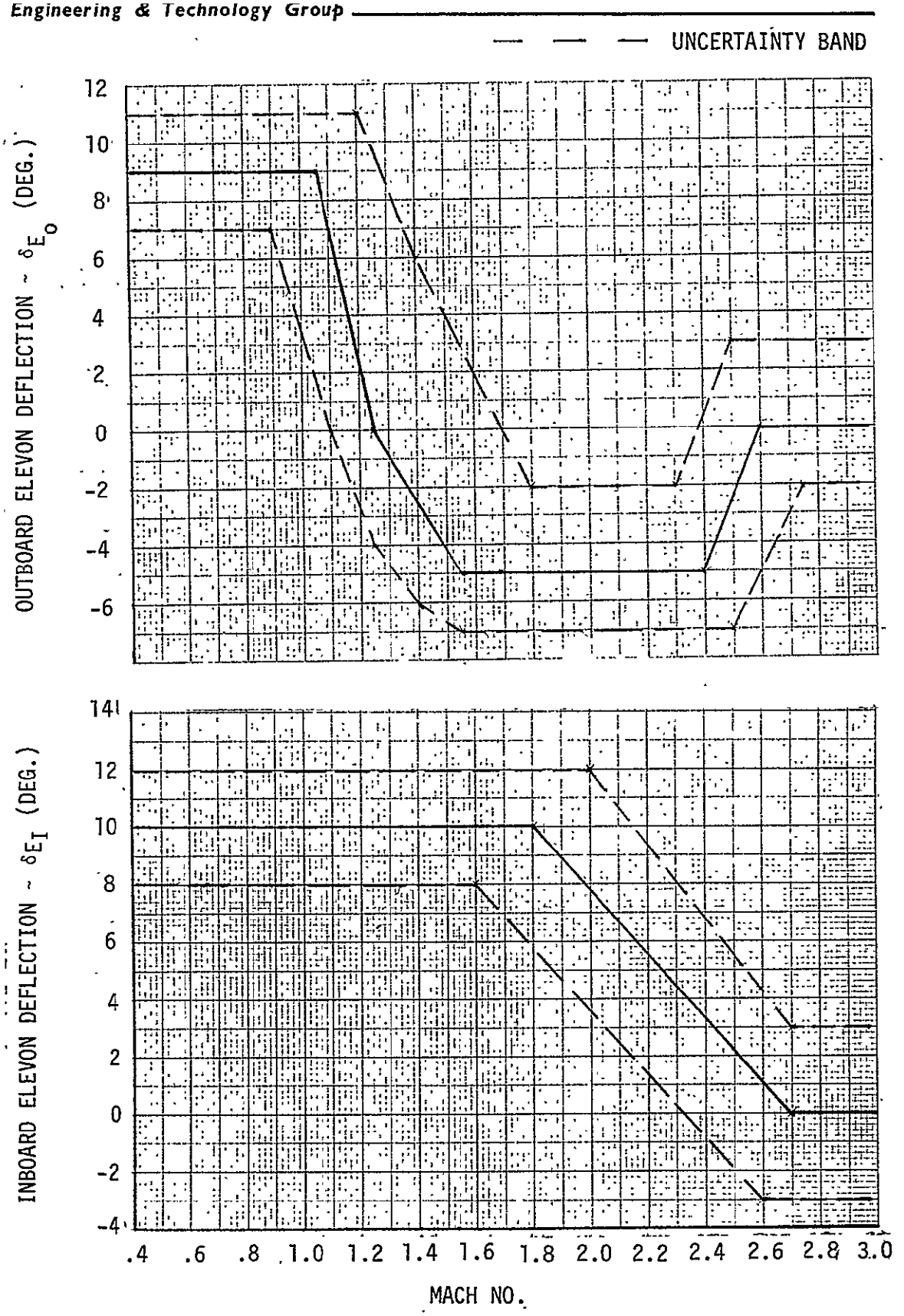

Figure 3-5. SCHEDULE 6 ELEVON DEFLECTIONS

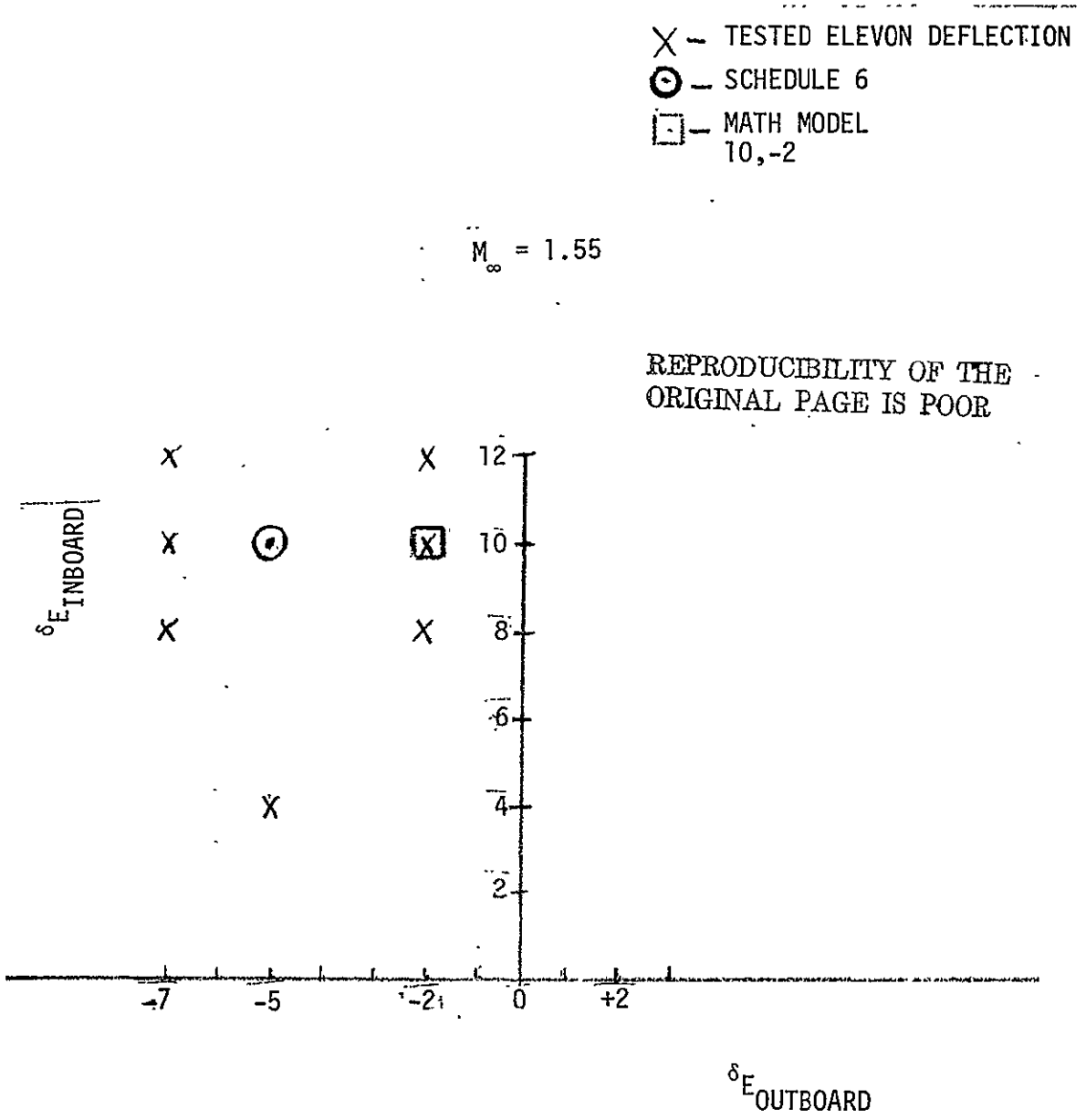

Figure 3-6. ELEVON DEFLECTION MATRIX (M_∞ = 1.55)

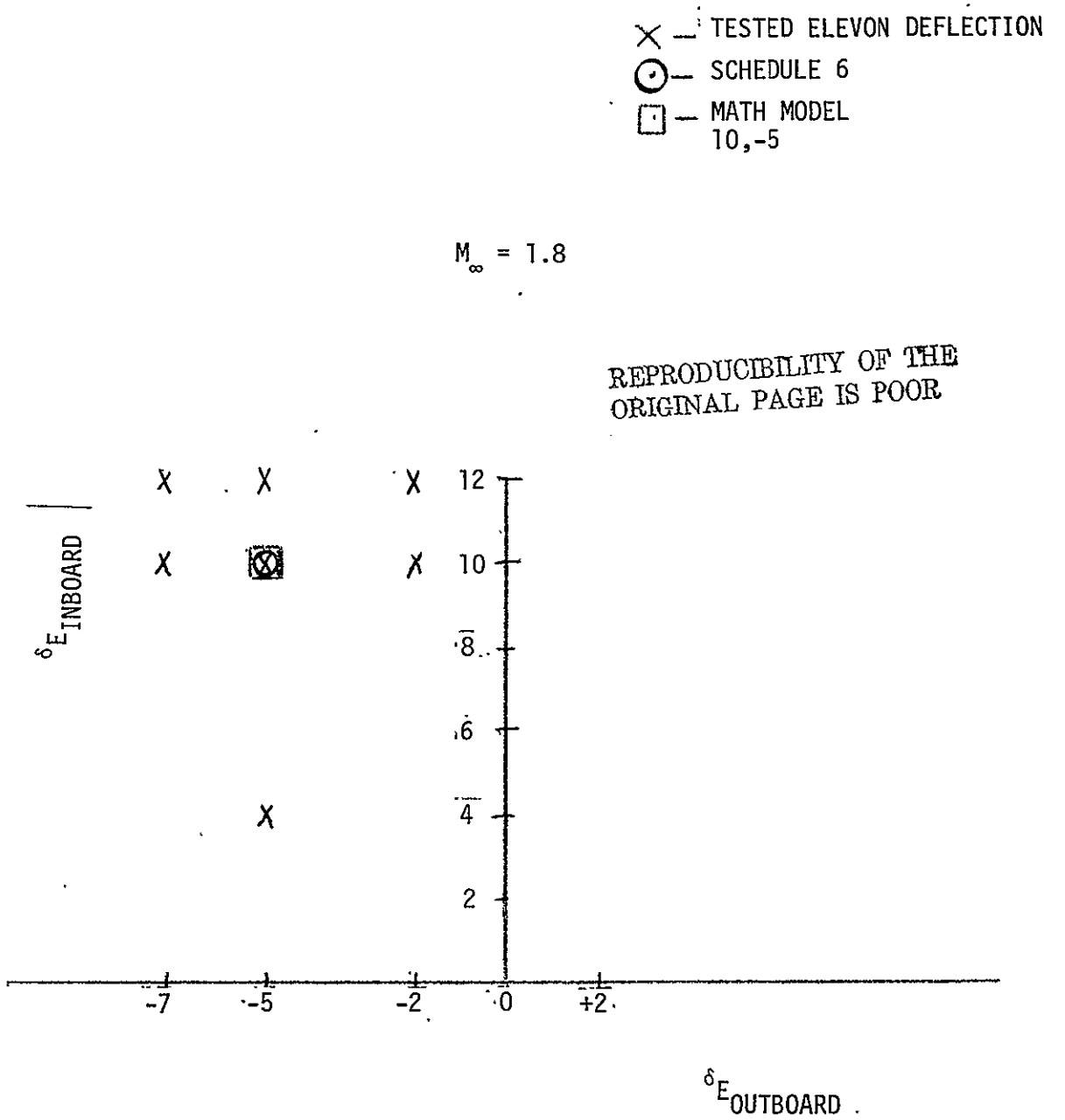

Figure 3-7. ELEVON DEFLECTION MATRIX (M_∞ = 1.80)

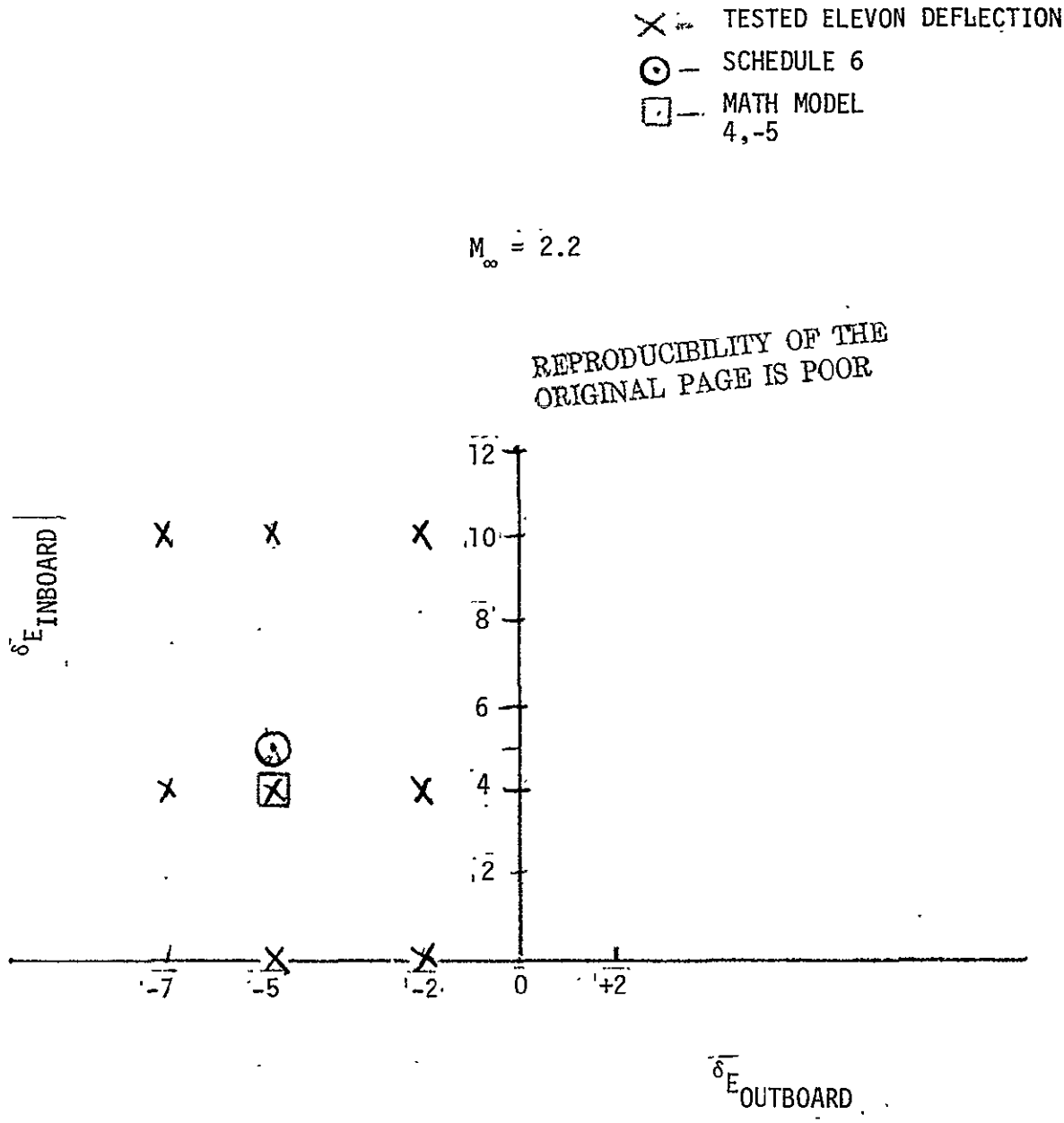

Figure 3-8. ELEVON DEFLECTION MATRIX (M_∞ = 2.20)

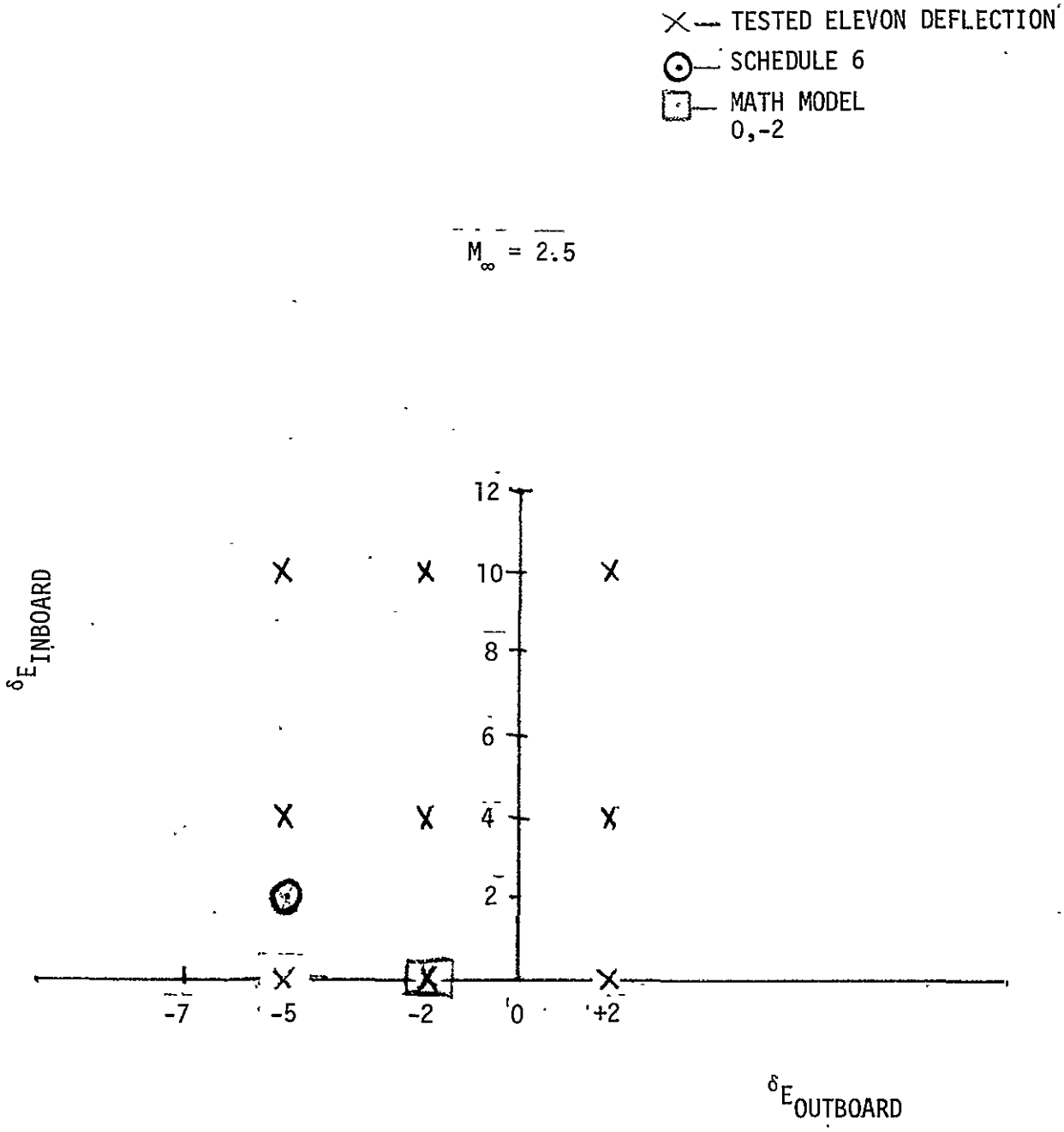

Figure 3-9. ELEVON DEFLECTION MATRIX (M_∞ = 2.50)

Table 3-1

IA138.

POWER ON-OFF DATA SETS (M_∞=1.55)

α	SRB/SSME POWER	β -4	β 0	β +4	δ_{EI}/δ_{EO}	GIM
C	NN	35	36	37	10/-2	N
C	OF OF	31	32	33	10/-2	N
C	NN	82	81	80	10/-7	N
C	OF OF	77	78	79	10/-7	N
C	NN	96	97	98	12/-2	N
C	OF OF	101	100	99	12/-2	N
C	NN	133	132	131	12/-7	N
C	OF OF	130	129	128	12/-7	N
C	NN	147	146	145	8/-7	N
C	OF OF	142	143	144	8/-7	N
A	NN OF OF	154			4/-5	N
C	NN	177	178	179	8/-2	N
C	OF OF	176	175	174	8/-2	N
			POWER			
0	OF OF		32/5		10/-2	N
↓	N1V		17		↓	↓
	N2V		18			
	N3V		19			
↓	N4V		20		↓	↓
0	N5V		21		10/-2	N

N = CONSTANT
V = VARIABLE
OF = OFF

A.) α = -6, -4, 0, +4, +6
B.) β = -4, 0, +4
C.) α = -8, -6, -4, 0, +4

Table 3-2

IA138

POWER ON-OFF DATA SETS (M_∞=1.80)

α	SRB/SSME POWER	β -4	β 0	β +4	δ_{EI}/δ_{EO}	GIM
A	NN	63	62	61	10/-5	N
A	OF OF	58	59	60	10/-5	N
C	NN	38	39	40	10/-2	N
C	OF OF	43	42	41	10/-2	N
A	NN	83	84	85	10/-7	N
A	OF OF	88	87	86	10/-7	N
C	NN	107	106	105	12/-2	N
C	OF OF	102	103	104	12/-2	N
A	NN	134	135	136	12/-7	N
A	OF OF	139	138	137	12/-7	N
A	NN	148	149	150	12/-5	N
A	OF OF	153	152	151	12/-5	N
A	NN	155	156	157	4/-5	N
A	OF OF	160	159	158	4/-5	N
			POWER			
0	OF OF		42/3		10/-2	N
↓	N1V		22		↓	↓
	N2V		23			
	N3V		24			
↓	N4V		25		↓	↓
0	N5V		26		10/-2	N

N = CONSTANT
V = VARIABLE
OF = OFF

A.) α = -6, -4, 0, +4, +6
B.) β = -4, 0, +4
C.) α = -8, -6, -4, 0, +4

Table 3-3

IA138

POWER ON-OFF DATA SETS (M_∞=2.20)

α	SRB/SSME POWER	β -4	β 0	β +4	δ_{EI}/δ_{EO}	GIM
A	NN	166	165	164	4/-5	N
A	OF OF	161	162	163	4/-5	N
A	NN	64	65	66	10/-5	N
A	OF OF	69	68	67	10/-5	N
A	NN	94	93	92	10/-7	N
A	OF OF	89	90	91	10/-7	N
A	NN	126	125	124	4/-2	N
A	OF OF	121	122	123	4/-2	N
A	NN	44	45	46	10/-2	N
A	OF OF	49	48	47	10/-2	N
A	NN	186	185	184	0/-5	N
A	OF OF	181	182	183	0/-5	N
A	NN	194	195	196	4/-7	N
A	OF OF	199	198	197	4/-7	N
A	NN	214	213	212	0/-2	N
A	OF OF	209	210	211	0/-2	N
			POWER			
0	OF OF		48/3		10/-2	N
↓	N1V		10		↓	↓
↓	N2V		11		↓	↓
↓	N3V		12		↓	↓
↓	N4V		14		↓	↓
↓	V N1		27		↓	↓
0	V N2		28		10/-2	N
			210/3			
0	V N3		215		0/-2	N
0	V N4		216		0/-2	N

N = CONSTANT
V = VARIABLE
OF = OFF

A.) α = -6, -4, 0, +4, +6
B.) β = -4, 0, +4
C.) α = -8, -6, -4, 0, +4

Table 3-4

IA138

POWER ON-OFF DATA SETS (M_∞=2.50)

α	SRB/SSME POWER	β -4	β 0	β +4	δ_{EI}/δ_{EO}	GIM
A	NN	217	218	219	0/-2	N
A	OF OF	222	221	220	0/-2	N
A	NN	187	188	189	0/-5	N
A	OF OF	192	191	190	0/-5	N
A	NN	75	74	73	10/-5	N
A	OF OF	70	71	72	10/-5	N
A	NN	113	112	111	4/+2	N
A	OF OF	108	109	110	4/+2	N
A	NN	115	116	117	4/-2	N
A	OF OF	120	119	118	4/-2	N
A	NN	167	168	169	4/-5	N
A	OF OF	172	171	170	4/-5	N
A	NN	224	225	226	10/+2	N
A	OF OF	229	228	227	10/+2	N
A	NN	55	54	53	10/-2	N
A	OF OF	50	51	52	10/-2	N
A	NN	206	205	204	0/+2	N
A	OF OF	201	202	203	0/+2	N
			POWER			
0	OF OF		51/3		10/-2	N
↓	N1V		5		↓	↓
↓	N2V		6		↓	↓
↓	N3V		7		↓	↓
↓	N4V		8		↓	↓
↓	N5V		9		↓	↓
↓	V N1		29		↓	↓
0	V N2		30		10/-2	N

N = CONSTANT
V = VARIABLE
OF = OFF

A.) α = -6, -4, 0, +4, +6
B.) β = -4, 0, +4
C.) α = -8, -6, -4, 0, +4

Section IV

WIND TUNNEL MODEL NOZZLE CALIBRATION ANALYSIS

An analysis of the model nozzle calibration data was performed to determi nozzle flow characteristics for the evaluation of model power levels. A range of model power levels were required for the power level variation portion of the test. Model nozzle wall pressures and exit plane pressures were plotted and compared with MOC results to evaluate the nozzle flow characteristics and to evaluate chamber to exit pressure ratios. The chamber to exit pressure ratios were required to evaluate the model plume characteristics.

The IA138 test program used a 1% conical SSME nozzle configuration and a 1% conical SRB nozzle configuration. The nozzle internal contours are shown in Figures 2-3 and 2-4 of Section II. The nozzle calibration data and instrumentation layout was obtained from references 2 through 7.

Summary post test and pre test model nozzle performance data are presente in Figures 4-1 and 4-2 for the SSME model nozzles and the SRB model nozzles respectively. The average chamber to exit plane pressure for the model SSME nozzle was approximately 265. The average chamber to exit plane pressure for the SRB nozzle was approximately 78.

The SSME nozzle calibration data is compared with MOC results in Figures 4-3 through 4-8. The range of chamber to exit plane pressure ratios is from 240 to 320 which covers the post test results.

A potential problem with the SSME nozzle performance was a change in chamber to exit plane pressure ratio that occurred during the test. The performance of the SSME nozzle versus run sequence is shown in Figure 4-9. The difference in performance of the SSME nozzles is evident by comparing the values of P_c/P_e for run sequences 10 through 14 obtained early in the test program with run sequences 27 and 28 which occurred toward the end of the test program. The early runs have an average P_c/p_e of approximately 275 while the

later runs have an average P_c/P_e near 260. A comparison of the measured exit plane pressure from several runs is presented in Figure 4-10. This figure shows that the exit plane pressure from several of the early runs at Mach 2.2 was potentially low. The accuracy of the exit plane pressure is estimated to be approximately $\pm$.05 PSI. This accuracy range covers a large portion of the variation, but does not explain the consistency of the change from the early Mach 2.2 runs and the late Mach 2.2 runs shown in Figure 4-9.

The SRB nozzle calibration data is compared with MOC results in Figures 4-11 and 4-12. The SRB nozzle chamber to exit plane pressure ratio from the calibration test was approximately 60 which is lower than the post test result of approximately 75 shown in Figure 4-2. The reason for this difference is unknown.

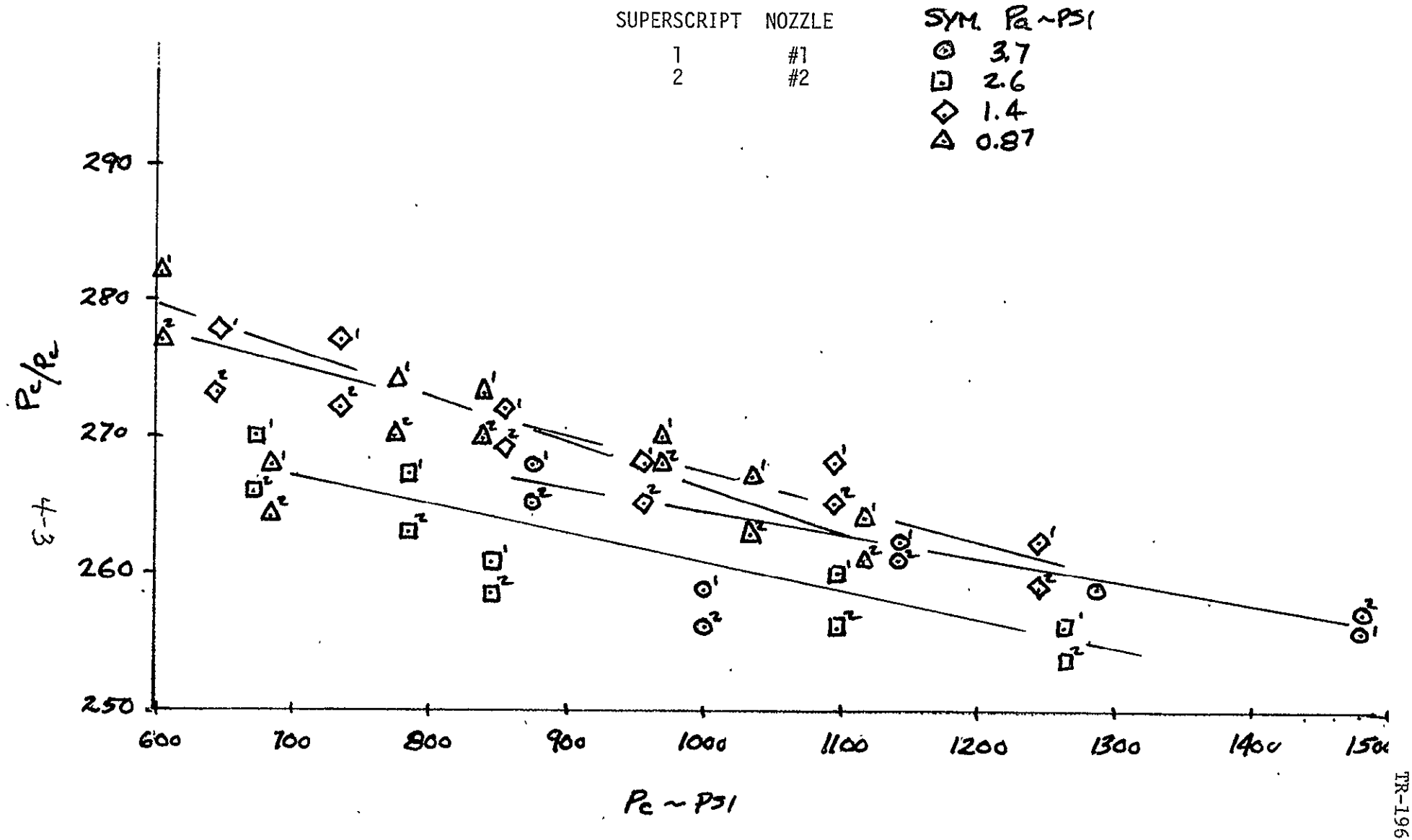

Figure 4-1. SSME NOZZLE CHAMBER TO EXIT PRESSURE RATIO

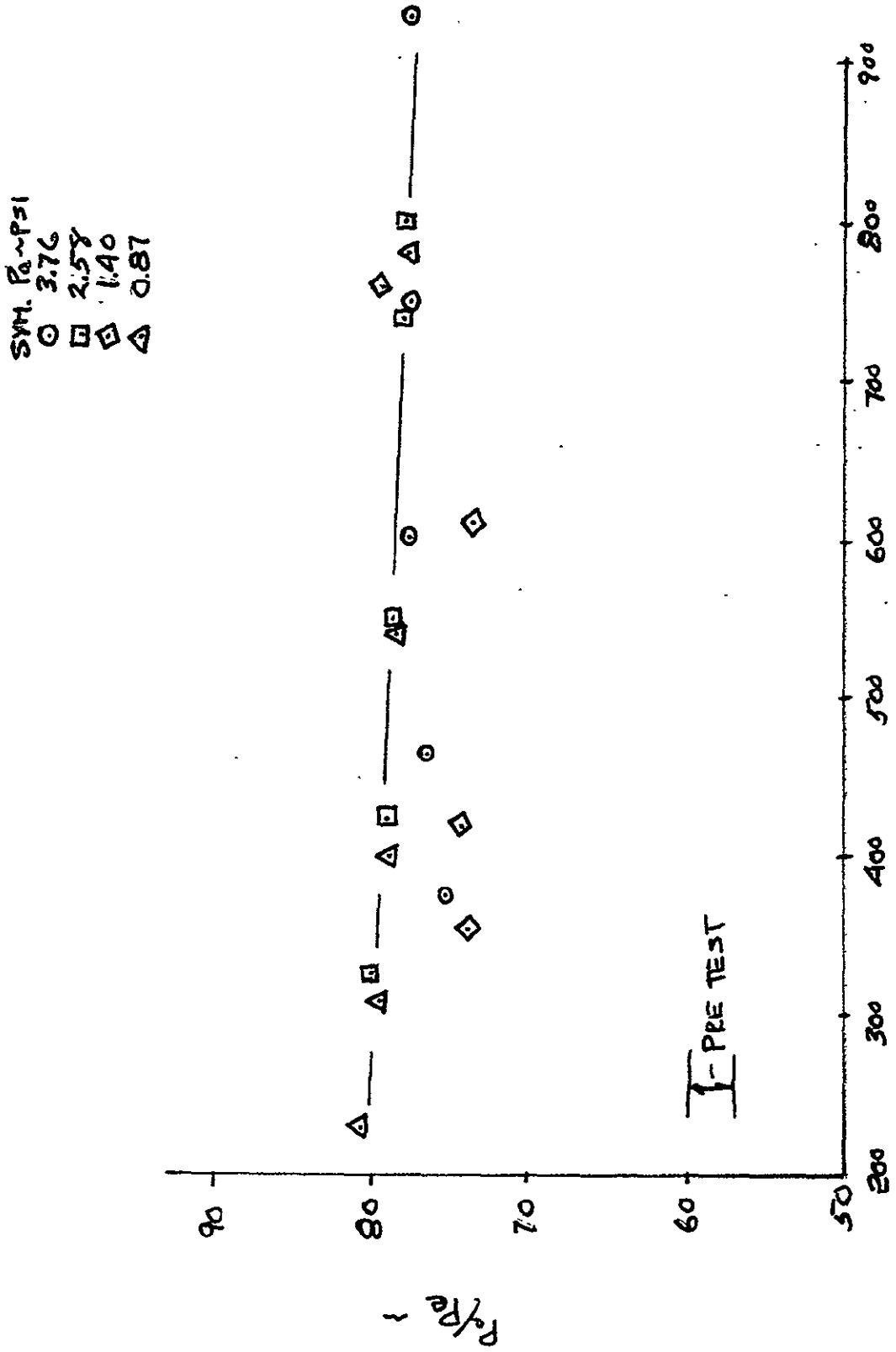

Figure 4-2. SRB NOZZLE CHAMBER TO EXIT PRESSURE RATIO

Figure 4-3. SSME NOZZLE CALIBRATION DATA - NOZZLE #1 P_a LOW

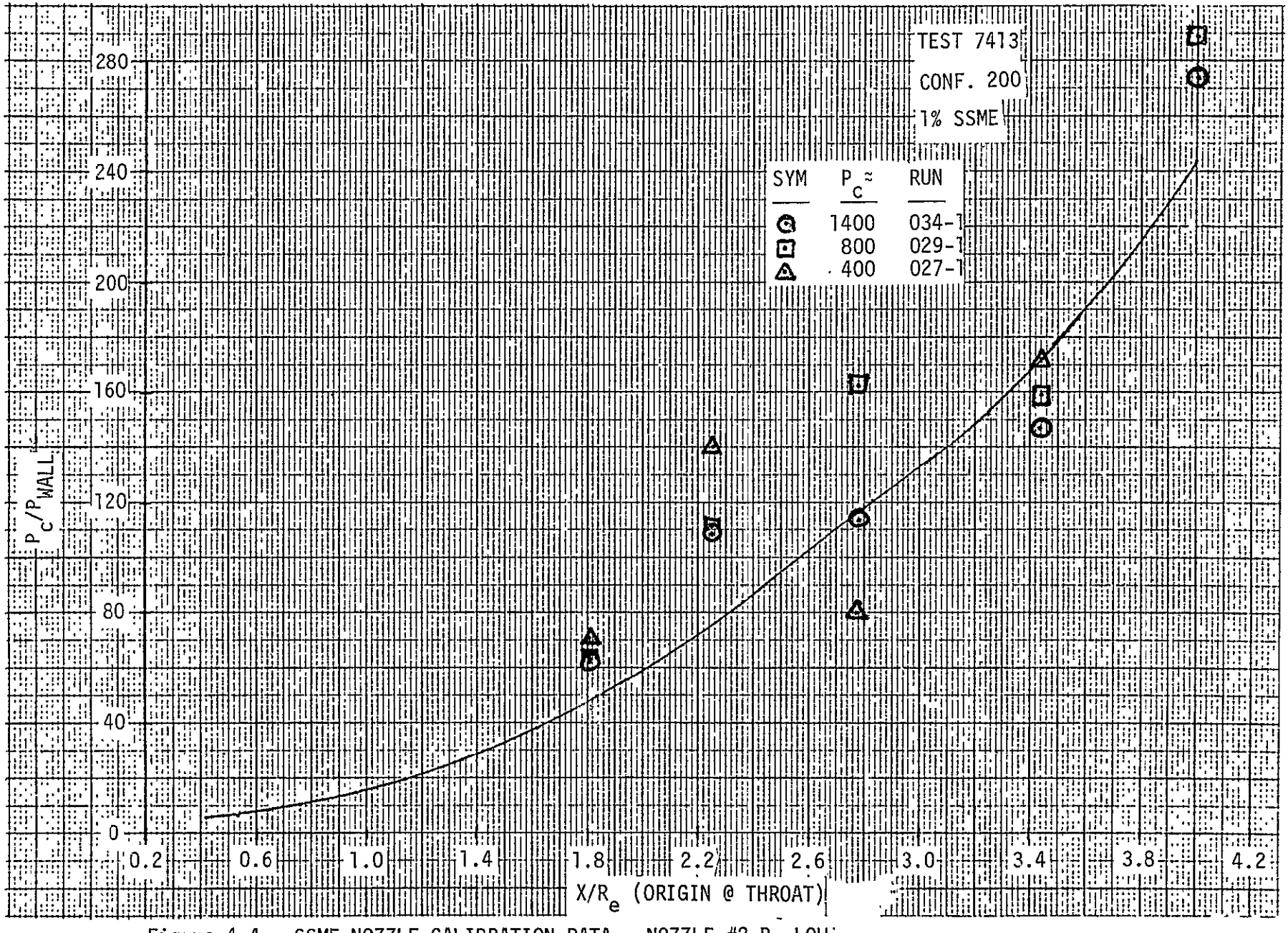

Figure 4-4. SSME NOZZLE CALIBRATION DATA - NOZZLE #2 P_a LOW

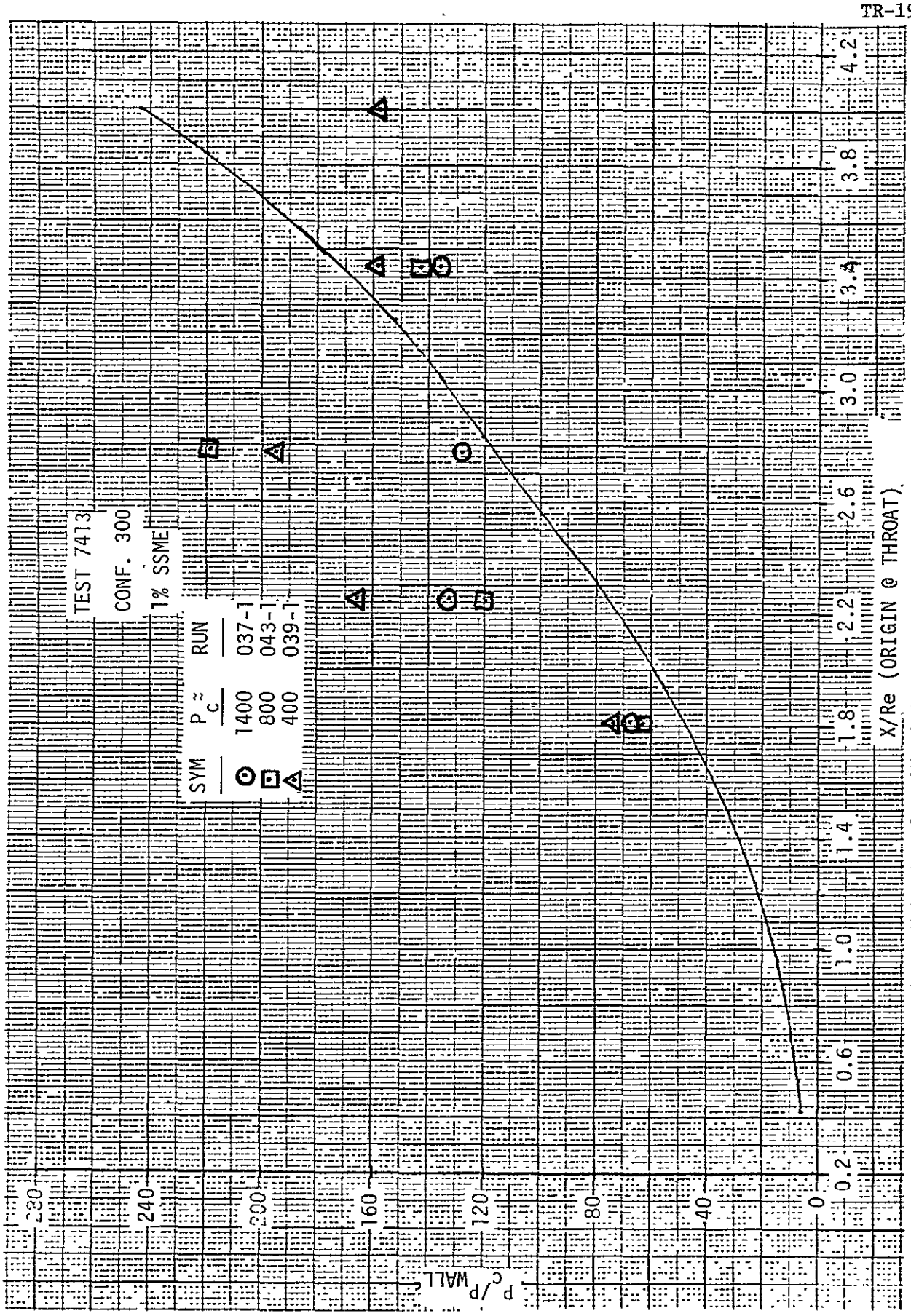

Figure 4-5. SSME NOZZLE CALIBRATION DATA - NOZZLE #3 P_a LOW

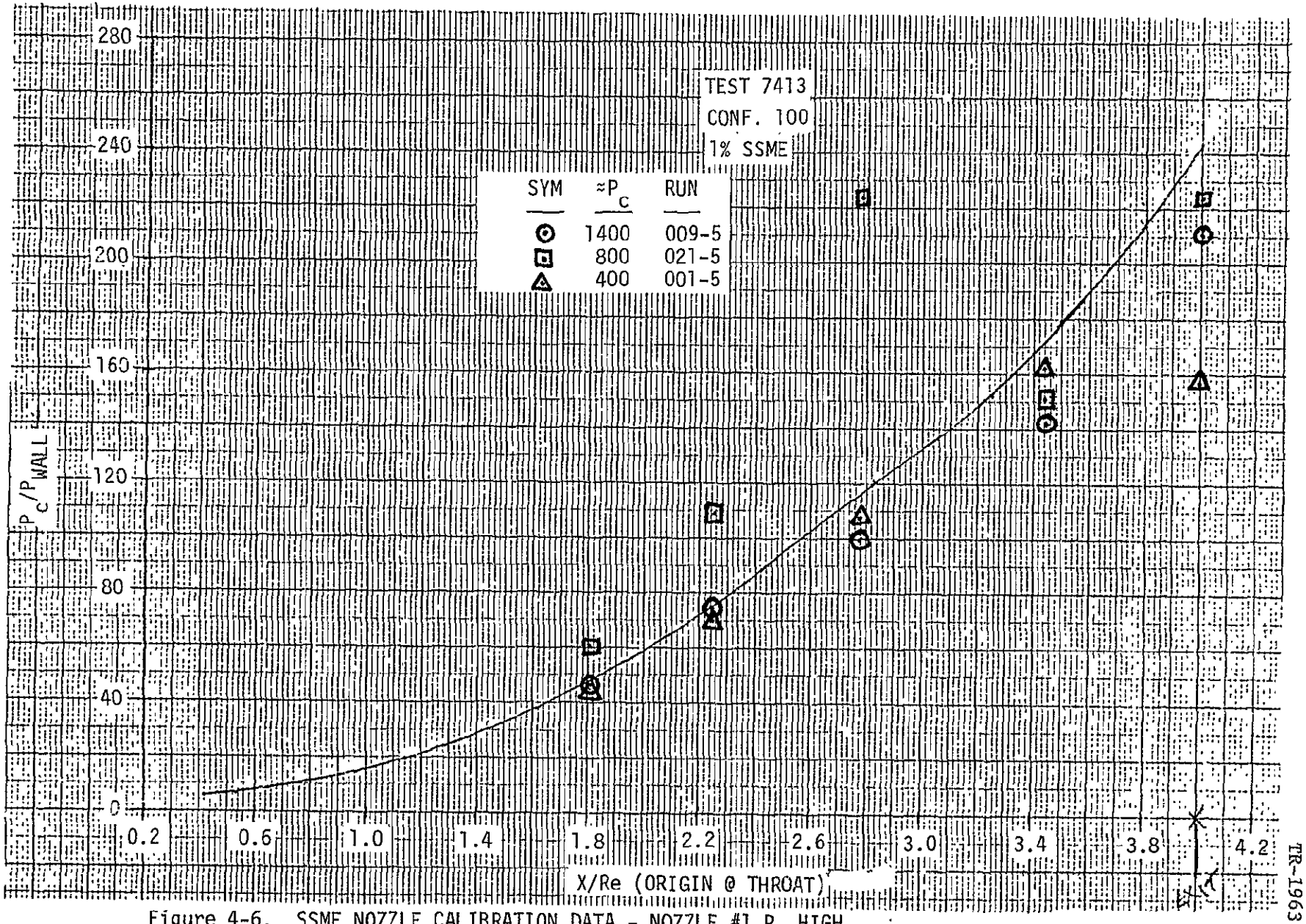

Figure 4-6. SSME NOZZLE CALIBRATION DATA - NOZZLE #1 P_a HIGH

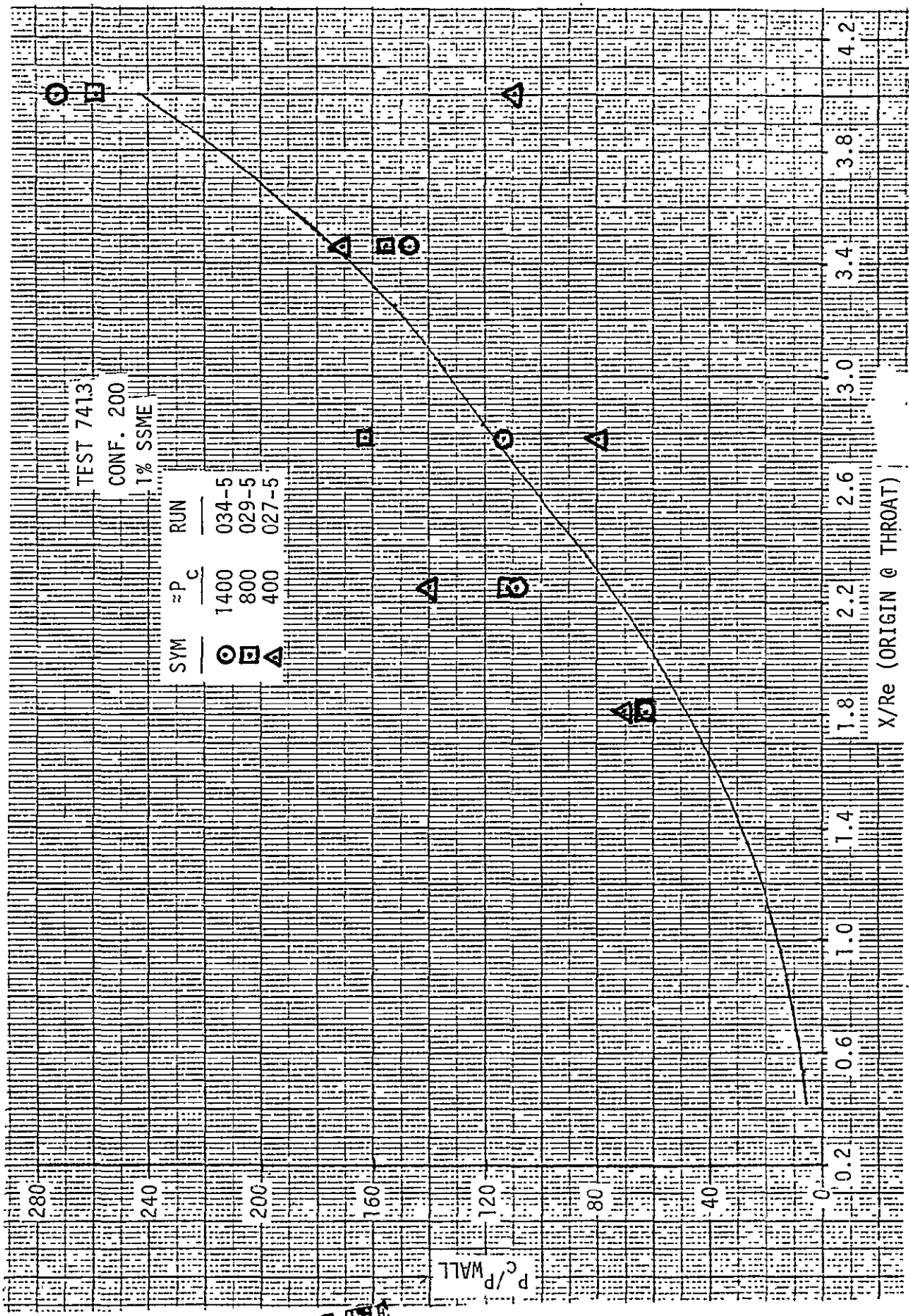

Figure 4-7. SSME NOZZLE CALIBRATION DATA - NOZZLE #2 P_a HIGH

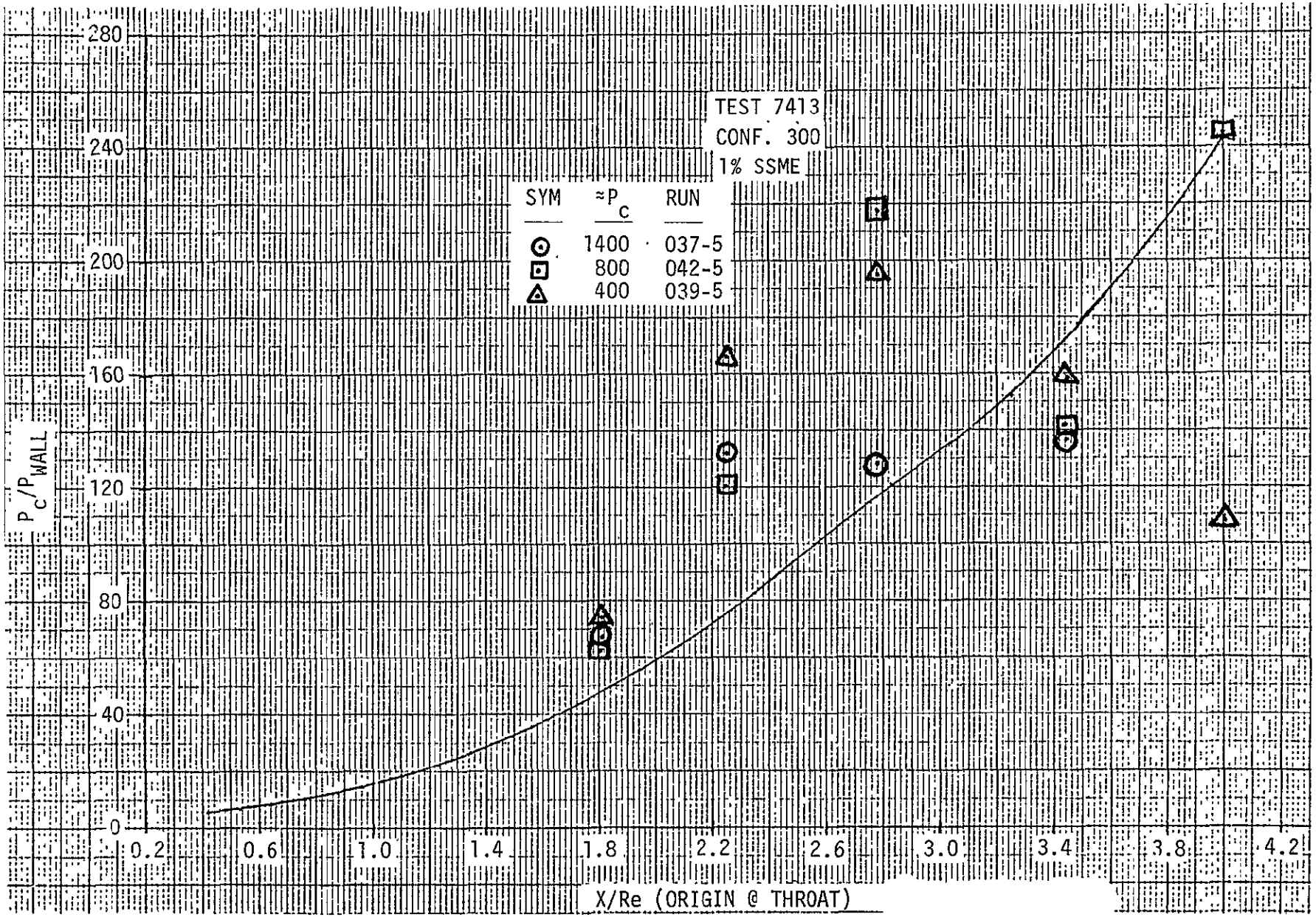

Figure 4-8. SSME NOZZLE CALIBRATION DATA - NOZZE #3 P_a HIGH

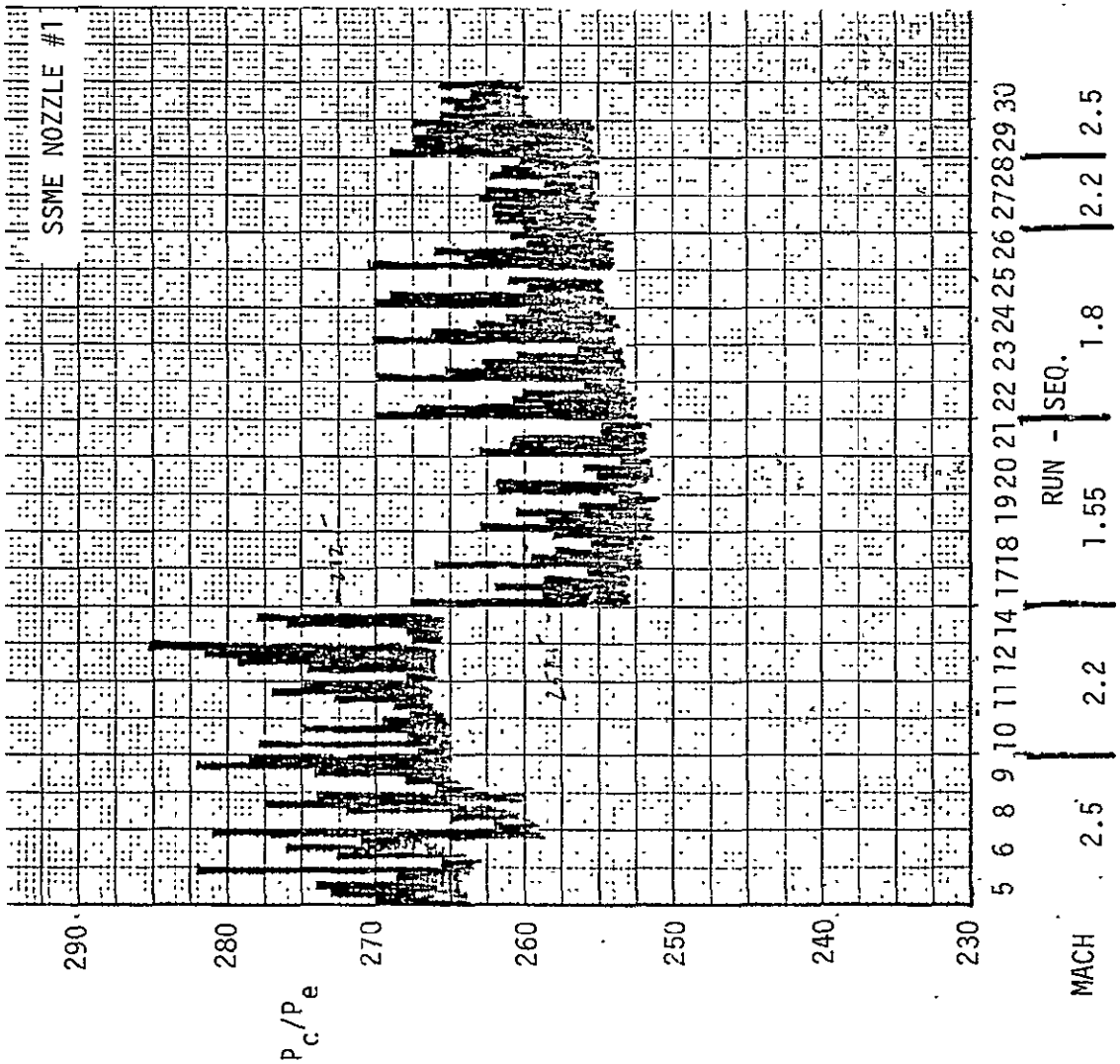

Figure 4-9. SSME NOZZLE PERFORMANCE VERSUS RUN SEQUENCE

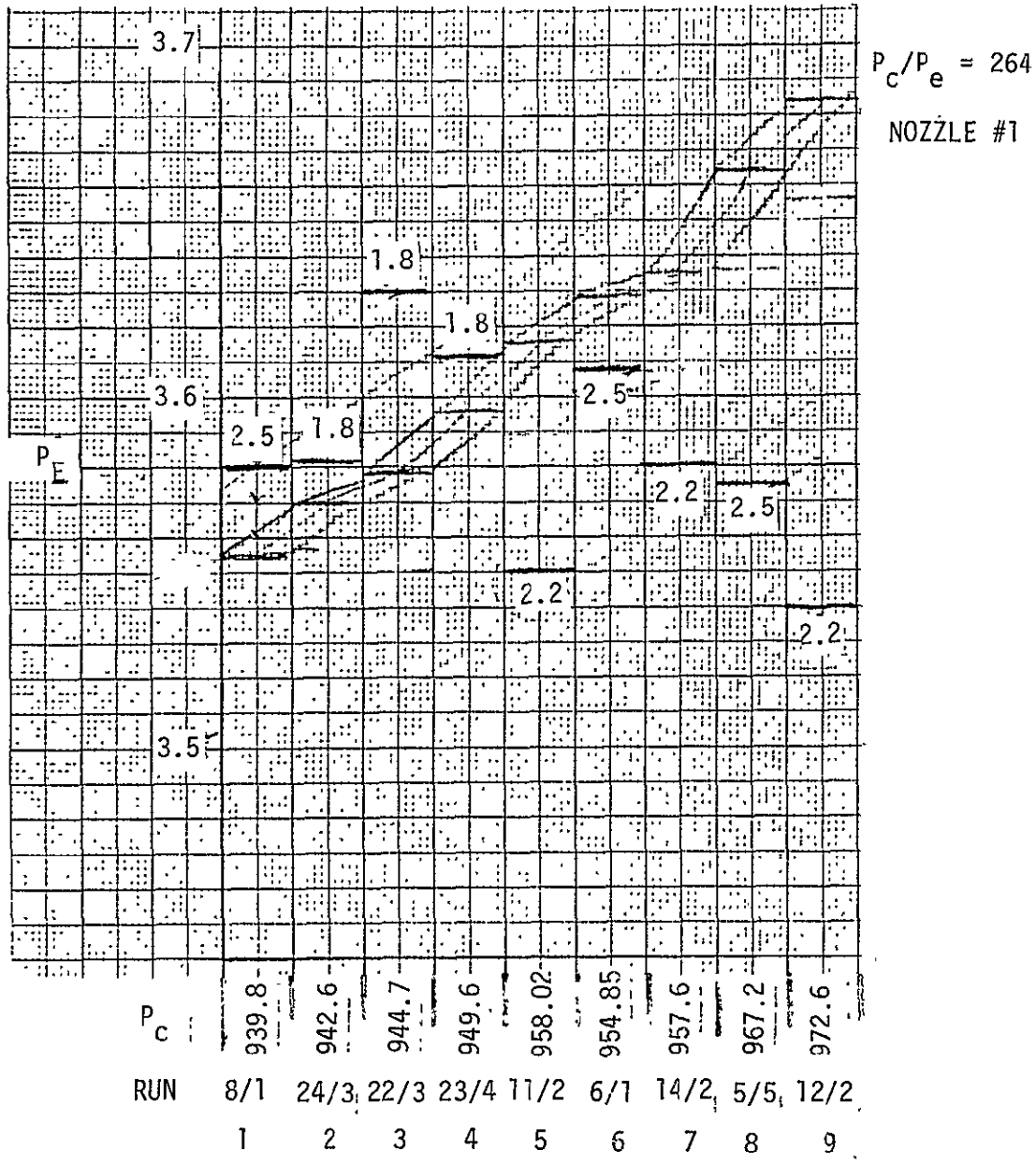

Figure 4-10. SSME NOZZLE EXIT PLANE PRESSURE VERSUS CHAMBER PRESSURE

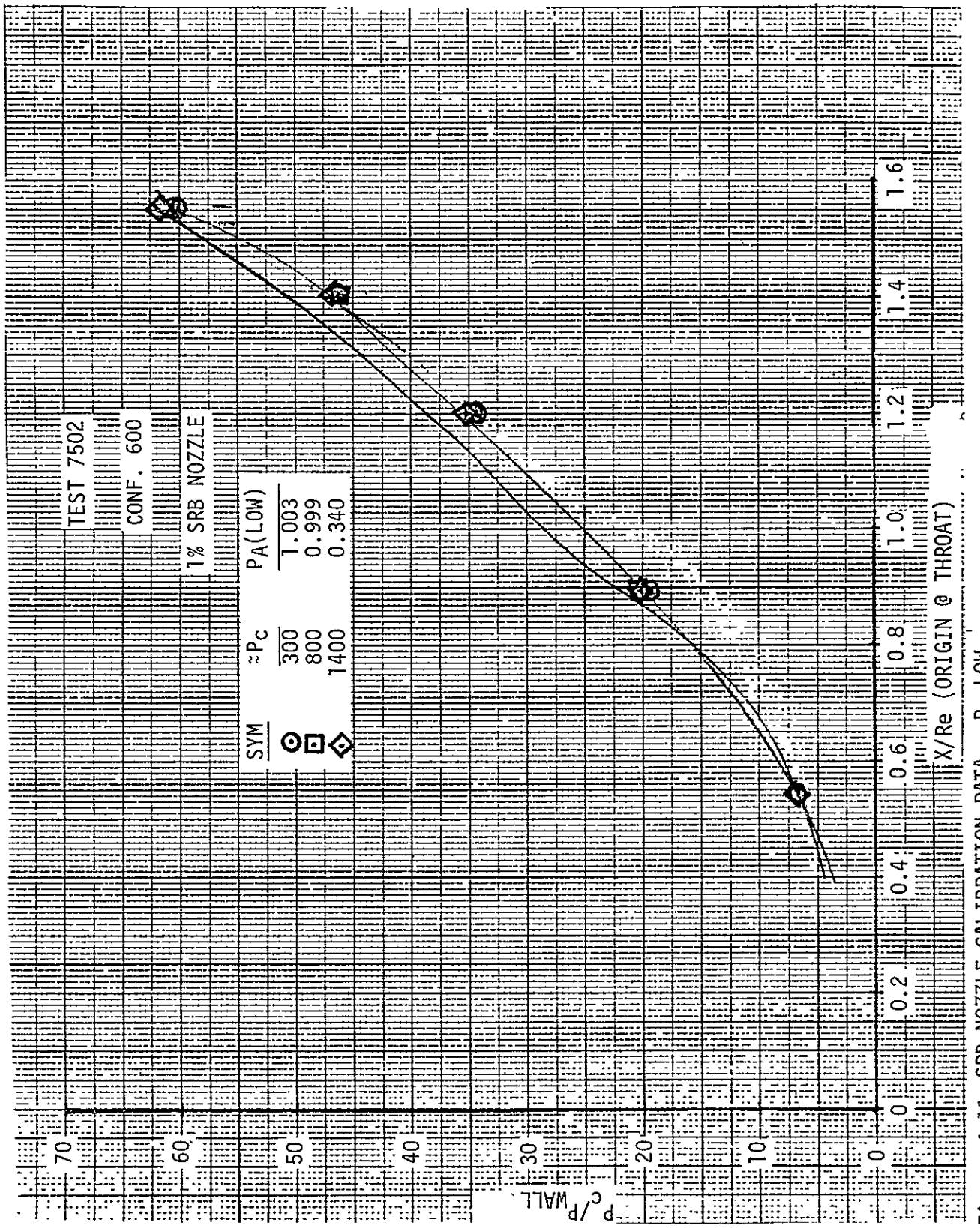

Figure 4-11. SRB NOZZLE CALIBRATION DATA - P_A LOW

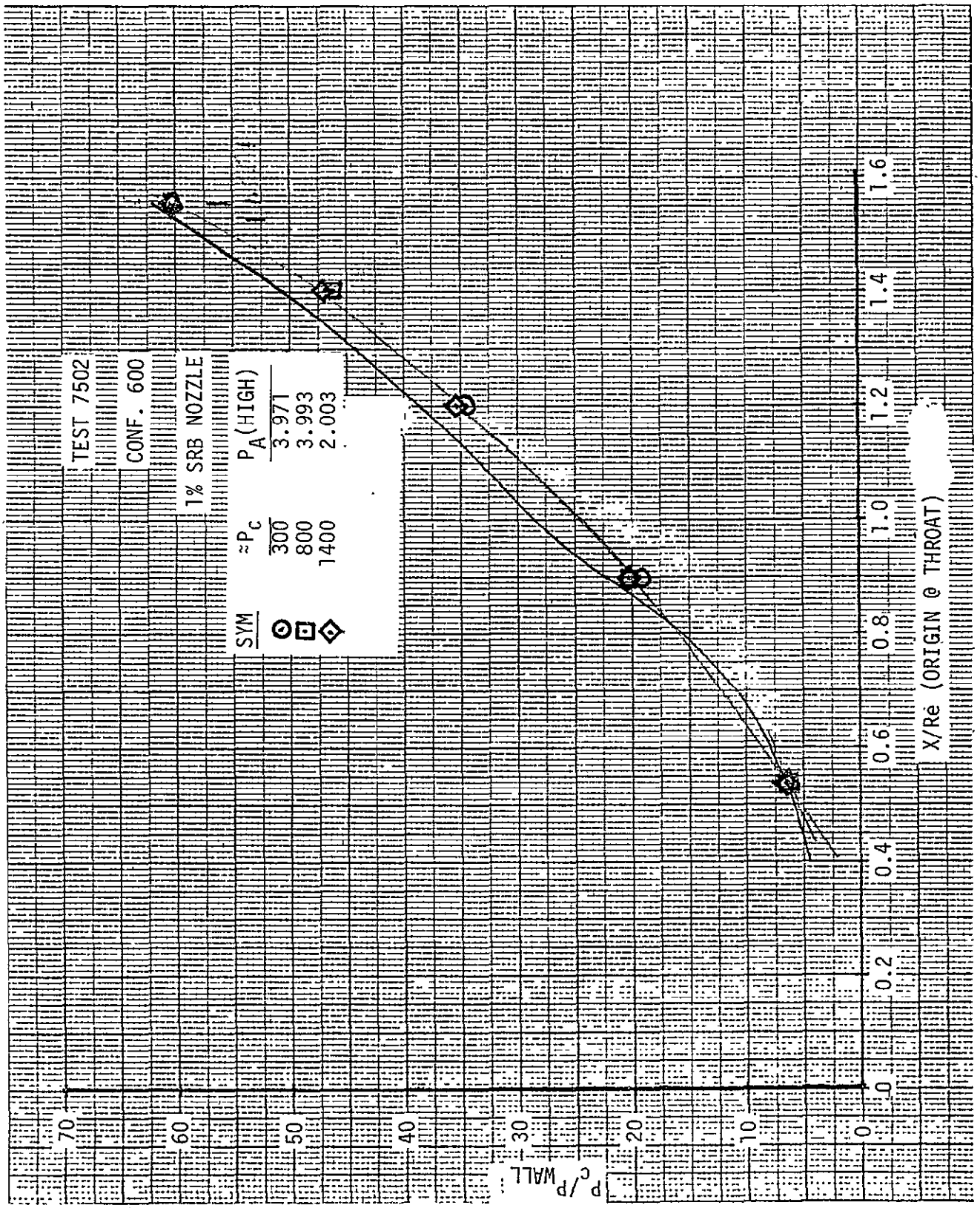

Figure 4-12. SRB NOZZLE CALIBRATION DATA - P_c HIGH

Section V

PLUME SIMULATION

The Space Shuttle plumes were simulated using cold air flowing through model nozzles. The model plume characteristics required to develop base and forebody pressure environments were determined using an iteration procedure requiring the development of "PROTOTYPE POSSIBILITY CURVES". Prototype possibility curves are curves of base pressure or base pressure coefficient versus prototype plume characteristics. An example prototype possibility curve is shown in Figure 5-1. The curve is called possibility curve since it is developed for a range of possible prototype base pressure environments. These curves were developed prior to the wind tunnel test for both the SSME and SRB prototype nozzles. The SSME possibility curves were developed using possible orbiter base pressure coefficients and the SRB possibility curves were developed using SRB possible base pressure environments. During the power level portion of the test, model base pressure data are plotted on the prototype possibility curves as shown in Figure 5-1. The model power level is determined where the model pressure curve crosses the prototype pressure curve. An iteration procedure is used when there are two variables involved that influence the base pressure, i.e. SSME power level and SRB power level. The possibility curves and the model pressure data used to determine the nominal power levels at each Mach number are presented in the Appendix.

The form of the plume simulation equation used during the IA138 test program was the following (reference 8)

$$\delta_j \gamma_j^N{}_{PROT.} = \delta_j \gamma_j^N{}_{MODEL}$$

where N is a function of Mach number. A plot of N versus Mach number is shown in Figure 5-2 and was obtained from reference 9. This curve was developed by correlating the base pressure in the near field and the far field developed from cold gas air and CF_4 plumes. The plume induced near field and far field areas considered are shown in Figure 5-3. The model configurations used were single body single nozzle, single body triple nozzle and triple body configurations. The triple body configuration was similar to the ET-SRB space shuttle

configuration. The band on the curve represents the range of N for the various models used in the plume technology test (i.e., single body, triple body, etc.) The criteria used for correlation of the plume technology data was that the same base pressure occur for a five percent or less change in similarity parameter. The band represents the total spread of N for the various model and nozzle configurations considered in the plume technology program.

Recent analysis (Reference 10) has identified a new similarity paramter that has the functional form

$$\frac{M_j \delta_j}{f(M_{EX})\ g(\gamma_j)}$$

where f, g appear to depend weakly upon M_∞ and configuration. The functions f and g have been defined for several model configurations and Mach numbers. The form of the various base pressure correlation parameters is presented in Table 5-1. These new similarity parameters, namely

$\frac{M_j \delta_j}{M_E^{(.25)\gamma_j}}$, $\frac{M_j \delta_j}{M_E^{(.25)\gamma_j (.5)}}$, and $\frac{M_j \delta_j}{\gamma_j}$ have been tabulated on the data pages along with the value of $\delta_j \gamma_j^N$ (see Section VII).

The similarity parameter $\delta_j \gamma_j^N$ requires the development of "PROTOTYPE POSSIBILITY CURVES" using prototype MPS and SRB plume characteristics. The δ_j and γ_j characteristics of the MPS and SRB plumes used to develop the prototype similarity parameters are presented in Figures 5-4 through 5-6. The "PROTOTYPE POSSIBILITY CURVES" are presented in the appendix.

The prototype plume characteristics are a function of the motor chamber pressure and altitude and are therefore dependent on the ascent trajectory. The 3A ascent trajectory characteristics were used as a reference trajectory. The ascent trajectory characteristics that influence the prototype plume characteristics are presented in Table 5-2.

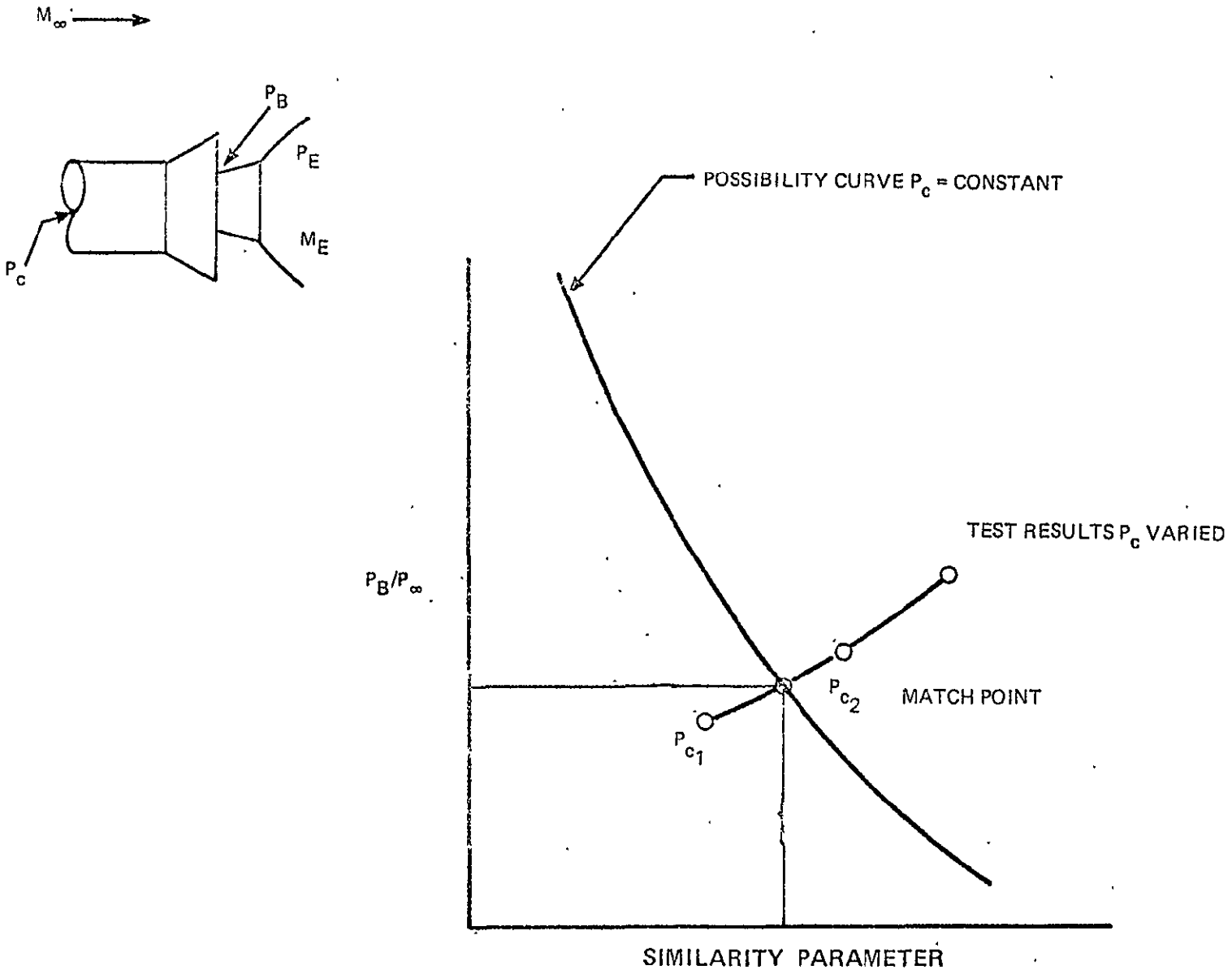

Figure 5-1. PROTOTYPE POSSIBILITY CURVE

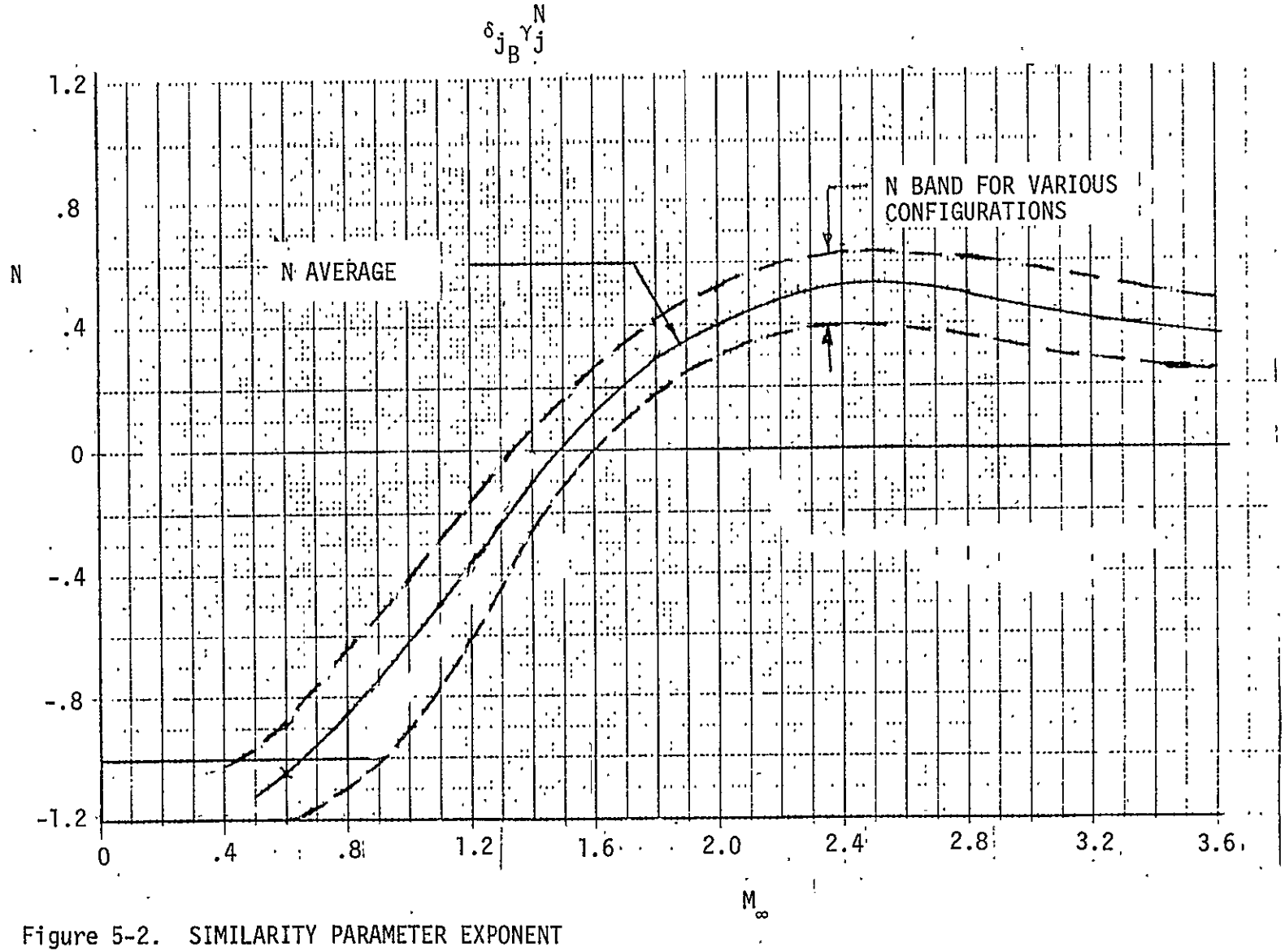

Figure 5-2. SIMILARITY PARAMETER EXPONENT

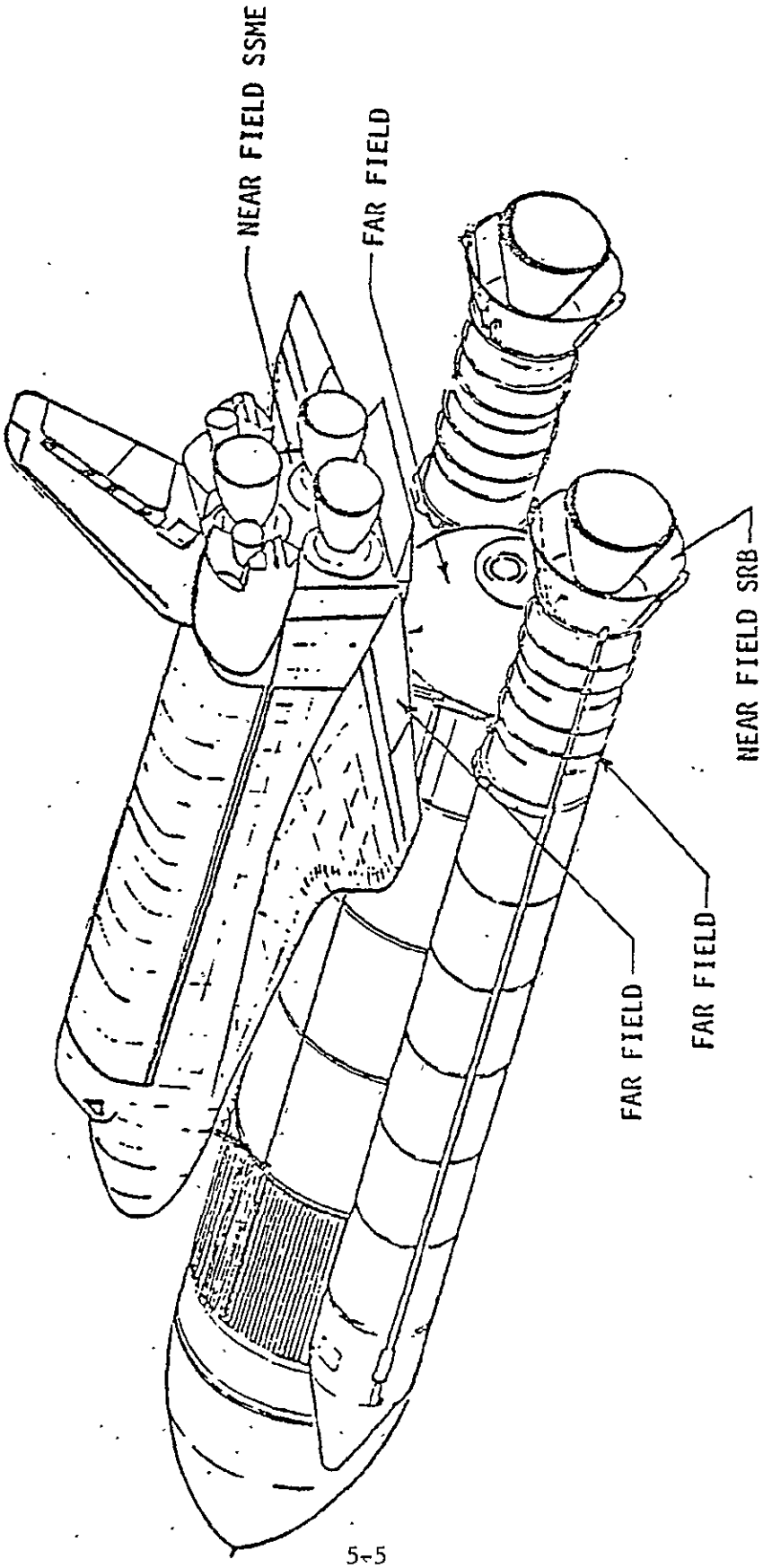

Figure 5-3. PLUME FLOW FIELD AREAS

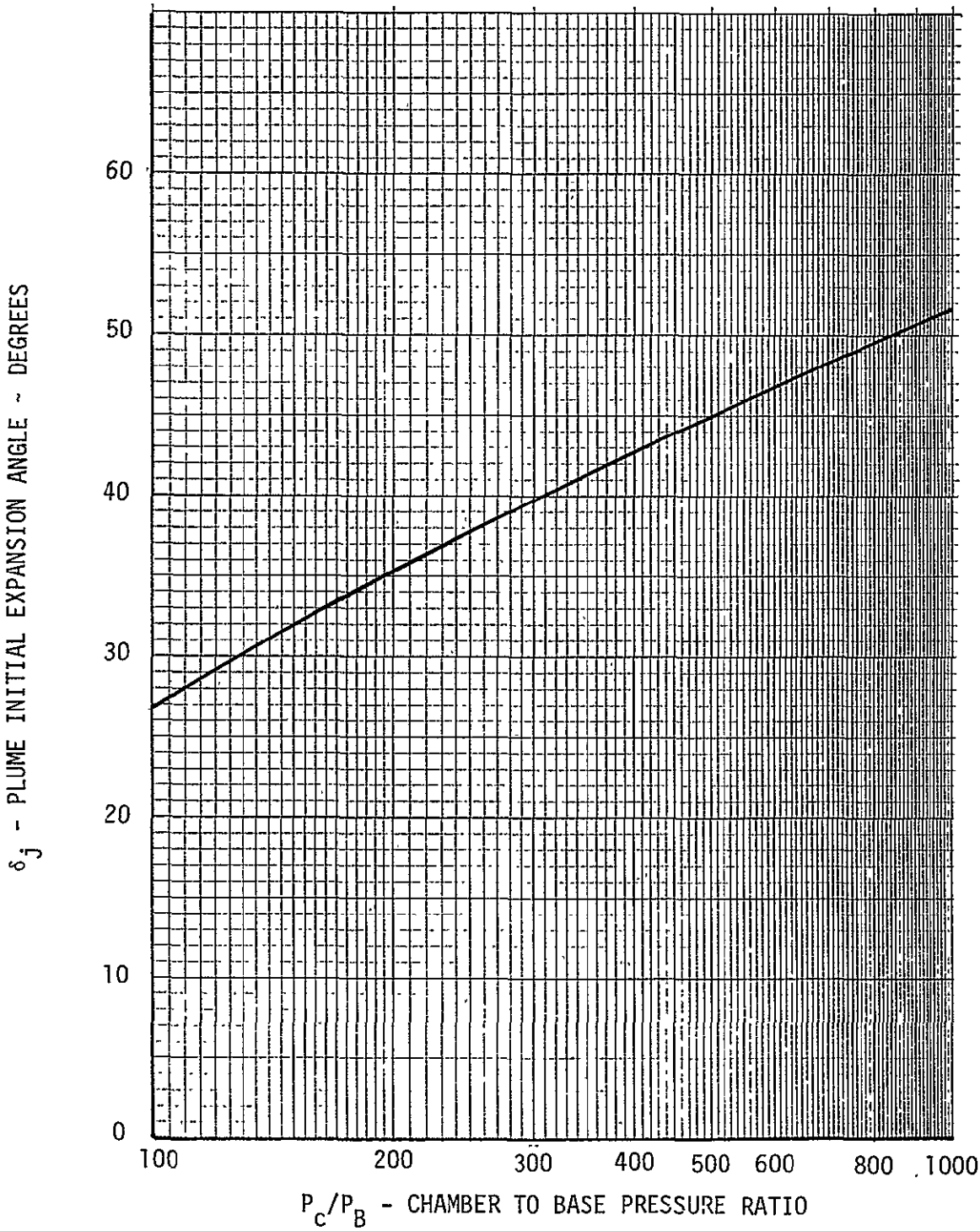

Figure 5-4. SRB PROTOTYPE PLUME ANGLE

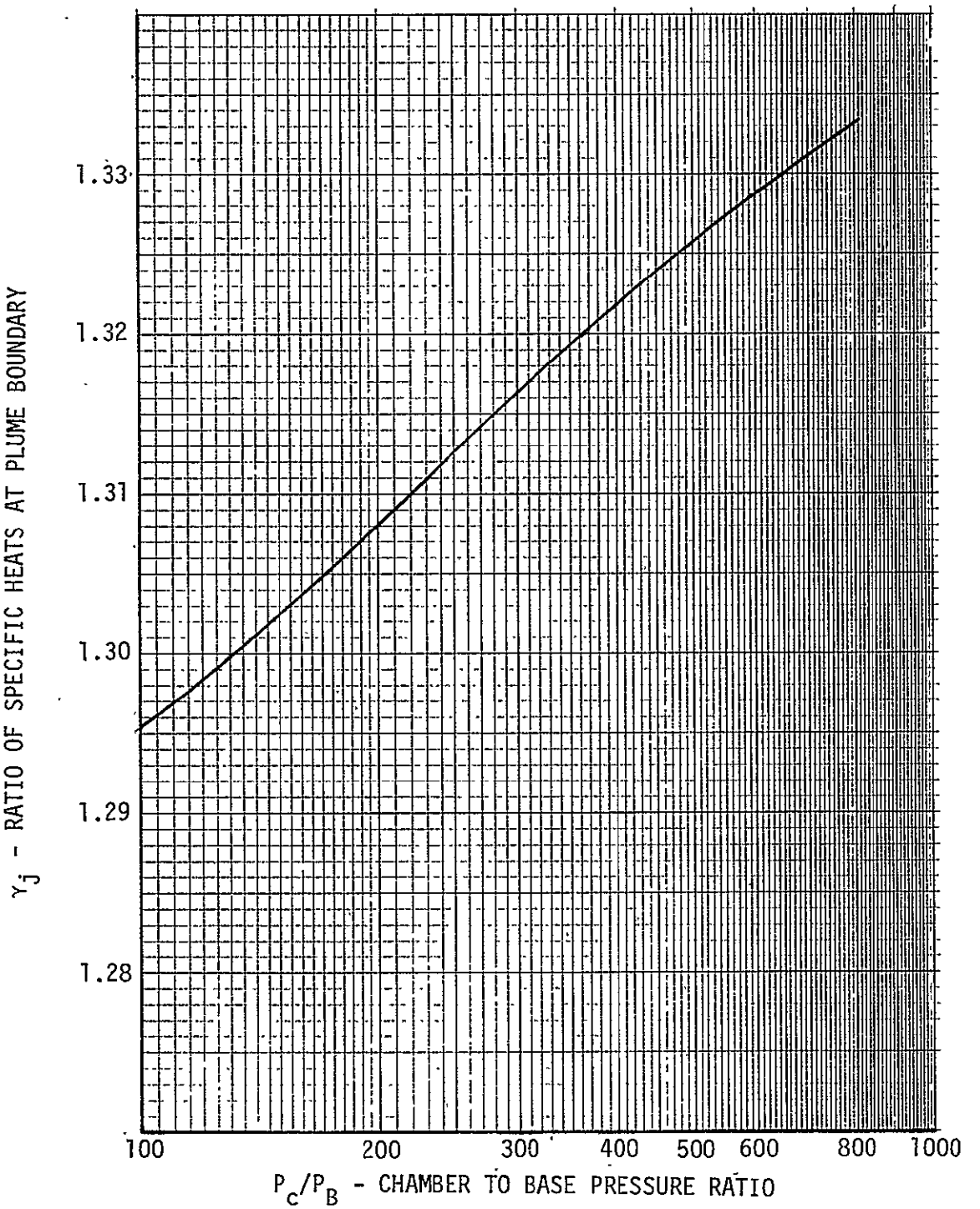

Figure 5-5. SRB PROTOTYPE PLUME RATIO OF SPECIFIC HEATS

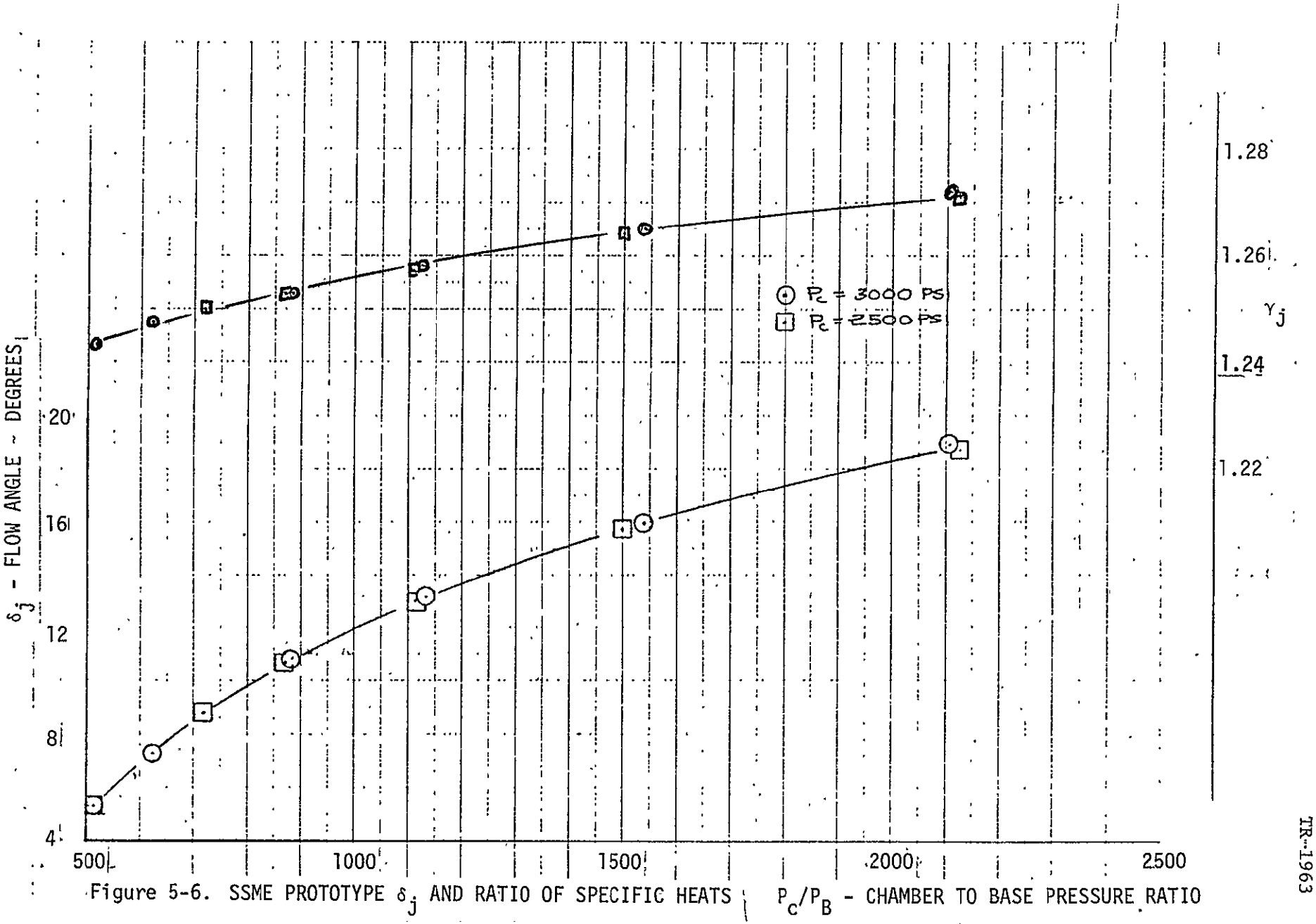

Figure 5-6. SSME PROTOTYPE δ_j AND RATIO OF SPECIFIC HEATS

Table 5-1
CORRELATION PARAMETERS

M_∞	CONFIGURATION		
	SINGLE BODY SINGLE NOZZLE	SINGLE BODY TRIPLE NOZZLE	TRIPLE BODY
0.9	$\frac{M_j \delta_j}{M_{EX}^{0.25} \gamma_j}$	$\frac{M_j \delta_j}{M_{EX}^{0.25} \gamma_j}$	$\frac{M_j \delta_j}{M_{EX}^{0.25} \gamma_j}$
1.2	$\frac{M_j \delta_j}{M_{EX}^{0.25\ 0.5} \gamma_j}$	$\frac{M_j \delta_j}{M_{EX}^{0.25} \gamma_j}$	$\frac{M_j \delta_j}{M_{EX}^{0.25} \gamma_j}$
1.46	$\frac{M_j \delta_j}{M_{EX}^{0.25\ 0.5} \gamma_j}$	$\frac{M_j \delta_j}{M_{EX}^{0.25} \gamma_j}$	
3.48	$\frac{M_j \delta_j}{\gamma_j}$	$\frac{M_j \delta_j}{\gamma_j}$	

Table 5-2

ASCENT TRAJECTORY AND SRB — SSME CHAMBER PRESSURE

TIME	MACH NO.	P_∞(PSIA)	q_∞(PSF)	$P_{C_{SRB}}$(PSIA)	SSME PERCENT THROTTLE %
66.0	1.55	2.66	648.0	613	109
72.0	1.80	1.90	621.0	630	109
80.0	2.20	1.09	533.0	637	109
86.0	2.50	0.69	443.0	600	109

Section VI

DATA ANALYSIS

Various computer codes were used to analyze the IA138 data. These programs are: 1. SORT program, 2. Power Delta program, and 3. Plume Integration. A brief discussion of each of these programs is presented below.

SORT PROGRAM

The SORT Program was used to sort the run and sequence data sets into basic groups of four. The four run groups consist of +β power-on, +β power-off, -β power-on and -β power off. The four run data sets were arranged in angle of attack sets of -8, -6, -4, 0, +4, +6 degrees. Flags were set to note α, β, Mach, gimbal and configuration incompatibility of the four run sets. (See Tables 3-1 through 3-4. Section III).

The following tolerances were put on the data sets to check compatibility.

VARIABLE	TOLERANCE
MACH	.03
α	.25
β	.25
β	Sign
Gimbal	≠0
CONFIGURATION NO. DO NOT AGREE	
RUN NUMBER/SEQUENCE OUT OF PLACE	
δ_{INB}	±.25
δ_{OUT}	±.25

The SORT program proved very useful in identifying errors in the post test run schedule and differences between the power-on and power-off model attitude.

POWER DELTA PROGRAM

The Power Delta program was used to evaluate the change in the pressure data due to power. The program lists all data from the power on run and all

data from the power off run and then subtracts the two data sets and lists the power delta's. This allows a rapid survey of the power delta's for abnormal numbers and a reference to the power on run and power off run to determine the error source.

PLUME INDUCED PRESSURE INTEGRATION

The IA-119 Plume Integration Program was modified and used as the main tool to analyze the IA138 pressure data. This computer program was developed specifically to analyze the IA119 pressure data and was used to integrate the pressure data to obtain base and forebody plume induced aerodynamic loads and moments. The computer program was developed to analyze four run sequences of positive and negative β sets. This operation is required since portions of the model have pressure data on only one side. Thus, to analyze the effects of sideslip required the evaluation of + and - β runs. An example of a four run data set used for analysis at Mach 1.55 would be run sets 37, 33, 35 and 31. These four sets are shown at the top of Table 3-1 as positive and negative sideslip data sets for elevon deflections of 10/-2 and nominal nozzle gimbal angles. Both power-on and power-off data sets are required since a portion of the plume induced data uses power on pressure coefficients while other portions require only the change in pressure coefficient due to power.

The analysis of the plume induced aerodynamic characteristics was performed using different pressure data over different portions of the vehicle. This type of analysis was required because of the unique configuration of the Space Shuttle and the model configurations used to obtain the forebody aerodynamic characteristics. The two types of pressure data used for analysis are: 1) The power on C_p's for nominal SSME and SRB model power settings; and 2) The power delta C_p's where $\Delta C_{p_{Power}} = C_{p_{Power\ on}} - C_{p_{Power\ off}}$.

The power on C_p's were used to evaluate the power-on base forces and moments. The power delta C_p's were used to evaluate the change in forebody aerodynamic characteristics. The location on the Space Shuttle vehicle where the different types of pressure data were used is shown in Figure 6-1. Following is a brief discussion of the analysis technique used to evaluate the plume induced aerodynamic characteristics.

ORBITER ANALYSIS

BASE

A photograph of the IA138 model orbiter base is shown in Figure 6-2. The orbiter base includes the base plate, upper body flap area, and SSME nozzle bells. The lower portions of the OMS pods are also included in the orbiter base.

A complex base pressure integration procedure was used to develop base force and moment coefficients. The base pressure coefficients were integrated over the base areas and nozzles to determine base axial force coefficients. The nozzle configuration corresponded to the prototype external nozzle contour, not the model external contour. The rationale used was that the external model contour was sufficiently scaled to develop the base pressure environment, but not of the correct shape for the integration of the pressures to determine nozzle axial forces. A schematic of the SSME model and prototype nozzle configurations is shown in Figure 6-3.

A different technique was used for the determination of nozzle normal forces and pitching moments. The Space Shuttle forebody aerodynamic characteri tics include power-off nozzle forces and moments. Thus, only the power delta forces and moment on the nozzles are included. The model nozzle configuration was used to develop the nozzle forces and moments since the normal forces and moments are developed near the exit plane where model nozzle geometric similitude is the best. The SSME nozzle hinge moments were not determined.

The SSME instrumentation layout is shown in Figure 6-4. The SSME tap-line-item and effective axial nozzle area is presented in Tables 6-1 through 6-3.

The orbiter base plate pressure instrumentation locations are shown in Figure 6-5. The base plate orifice, tap-line-items numbers, vertical locations and areas used to analyze the base plate are presented in Table 6-4. A schematic showing the relative area size assigned to each pressure is shown in Figure 6-6. The base plate total area was checked from several drawings as noted at the bottom of the tables.

OMS PODS

The OMS pods were analyzed using the effective areas and orientation as shown in Figure 6-7. Since only one OMS pod was instrumented, the effective area is for both pods. The base pressures were averaged at + and - β angle for a β run. Close proximity orbiter base plate pressures were used for the pod overhang areas.

BODY FLAP

The orbiter body flap instrumentation is shown in Figure 6-8. The effective areas are presented in Table 6-5. Only the upper portion of the body flap is included as part of the orbiter base.

ORBITER FOREBODY

The orbiter forebody pressure instrumentation layout is shown in Figure 6-9. The forebody plume induced aerodynamic characteristics were evaluated using the power delta C_p's. Radial ring locations are presented in Table 6-6.

WING AND ELEVONS

The gaged wing and elevon arrangement is shown in Figure 6-10. A partial right wing was instrumented to measure wing shear, and root bending and torsion moments. Gaged inboard and outboard elevons were located on the left wing. The elevons were instrumented to measure elevon hinge moments. The sign convention used for the wing and elevon plume induced aerodynamic characteristics is presented in Figure 6-11.

SRB BASE

The SRB nozzle instrumentation layout is shown in Figure 6-12. The prototype nozzle configuration was used to determine external aerodynamic loads. The nozzle configuration used is shown in Figure 6-13. The nozzle pressure integration was terminated at the compliance ring shown in Figure 6-14. The nozzle axial areas assigned to each pressure location is presented in Table 6-7.

SRB FOREBODY

The SRB forebody instrumentation layout is shown in Figure 6-15 and the pressure integration area layout in Table 6-8. No consistent trend in

power-delta pressure could be determined except on the skirt. Thus only the skirt area was used to determine power-induced forebody aerodynamic characteristics.

ET BASE

The ET base instrumentation layout is shown in Figure 6-16. The area assignment is presented in Table 6-9. The area assignments were determined by plotting the ET base pressures and determining pressure contours for selected Mach numbers. The areas were then evaluated using the base pressure contours.

The results of integration of the base pressure and the forebody power delta pressures have been listed in a special format which is discussed in Section VII. Reference areas, lengths, and moment reference locations used for all aerodynamic characteristics are presented in Table 6-10.

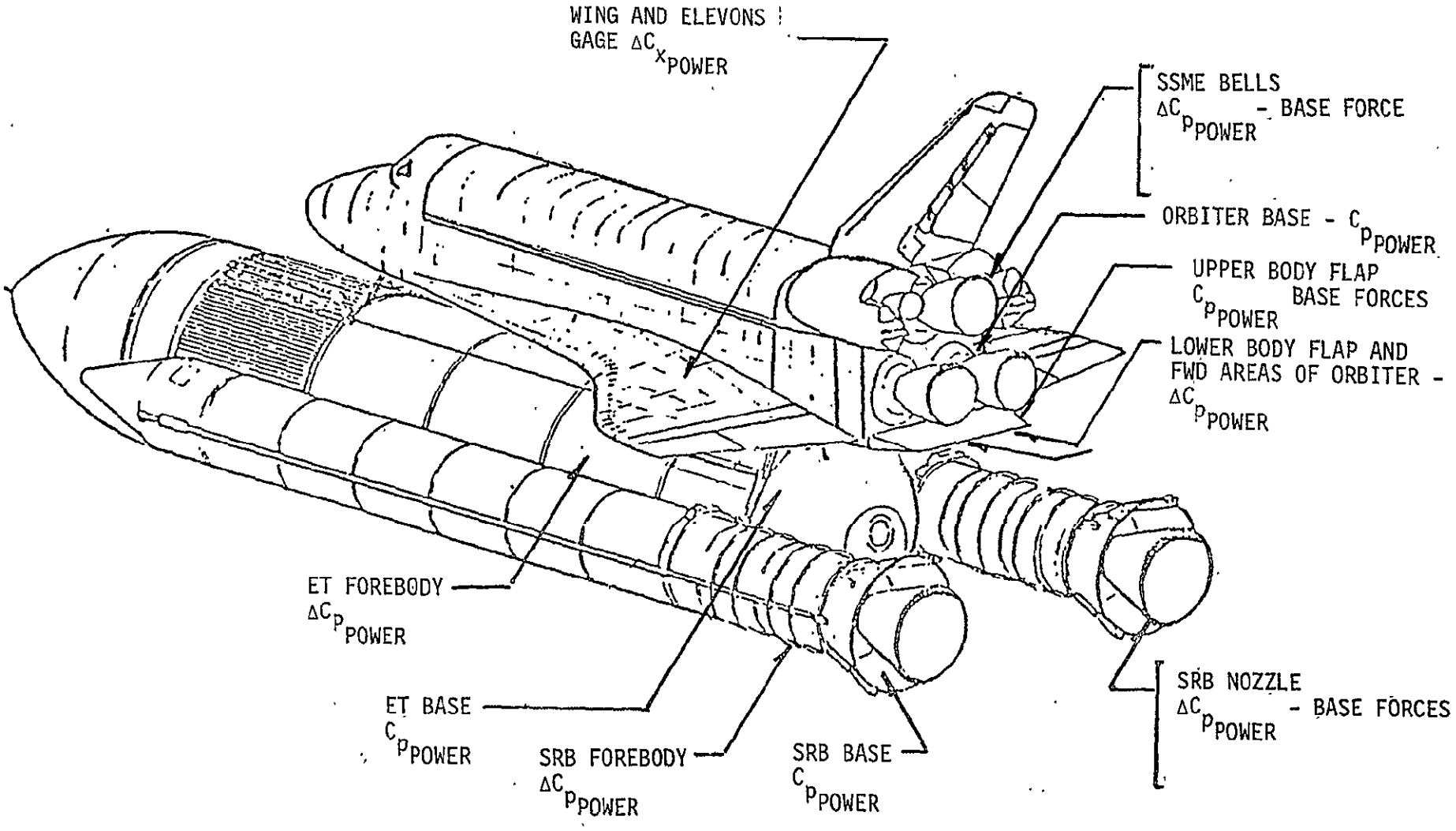

Figure 6-1. PLUME FLOW FIELD AREAS

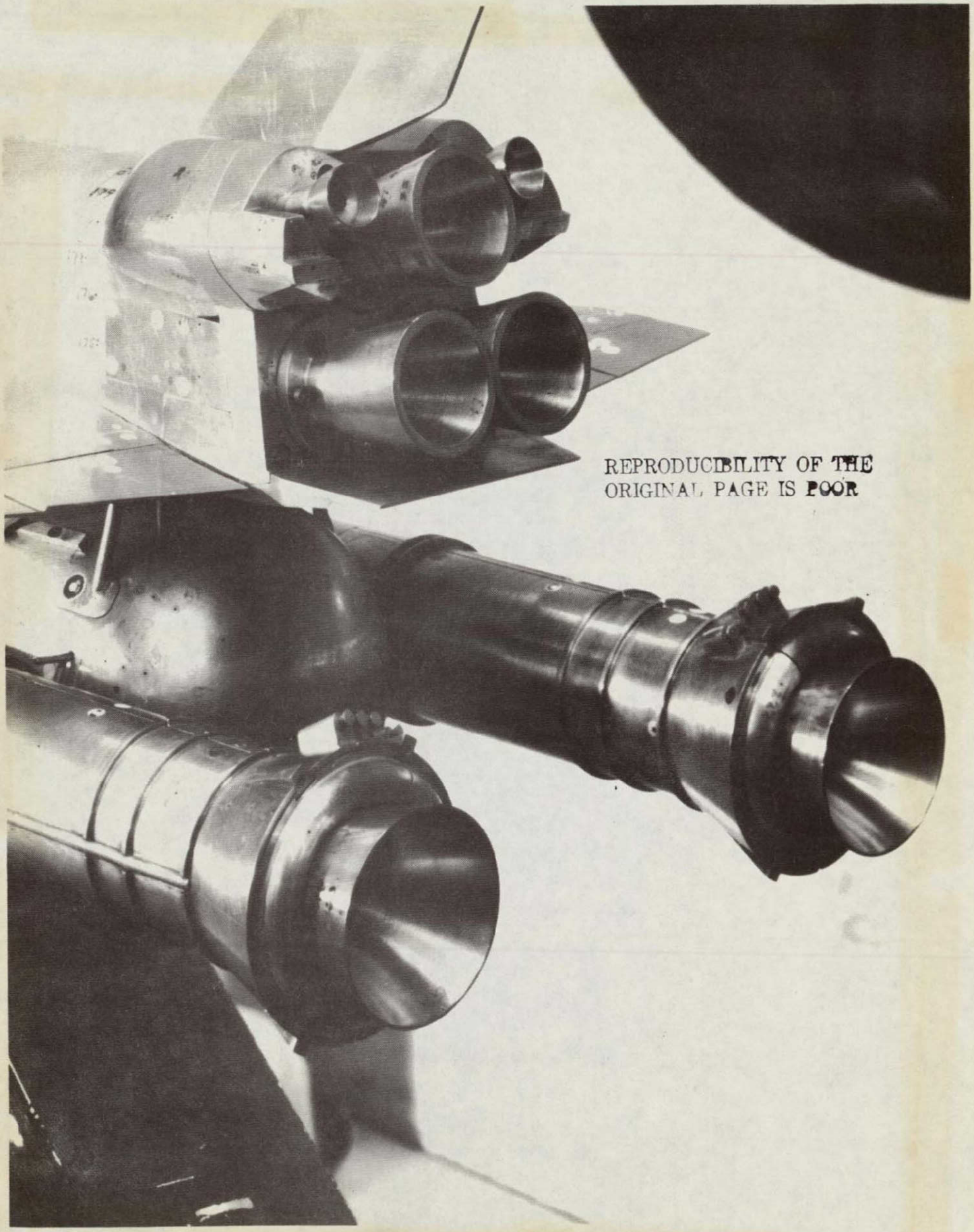

Figure 6-2. IA138 MODEL ORBITER BASE CONFIGURATION

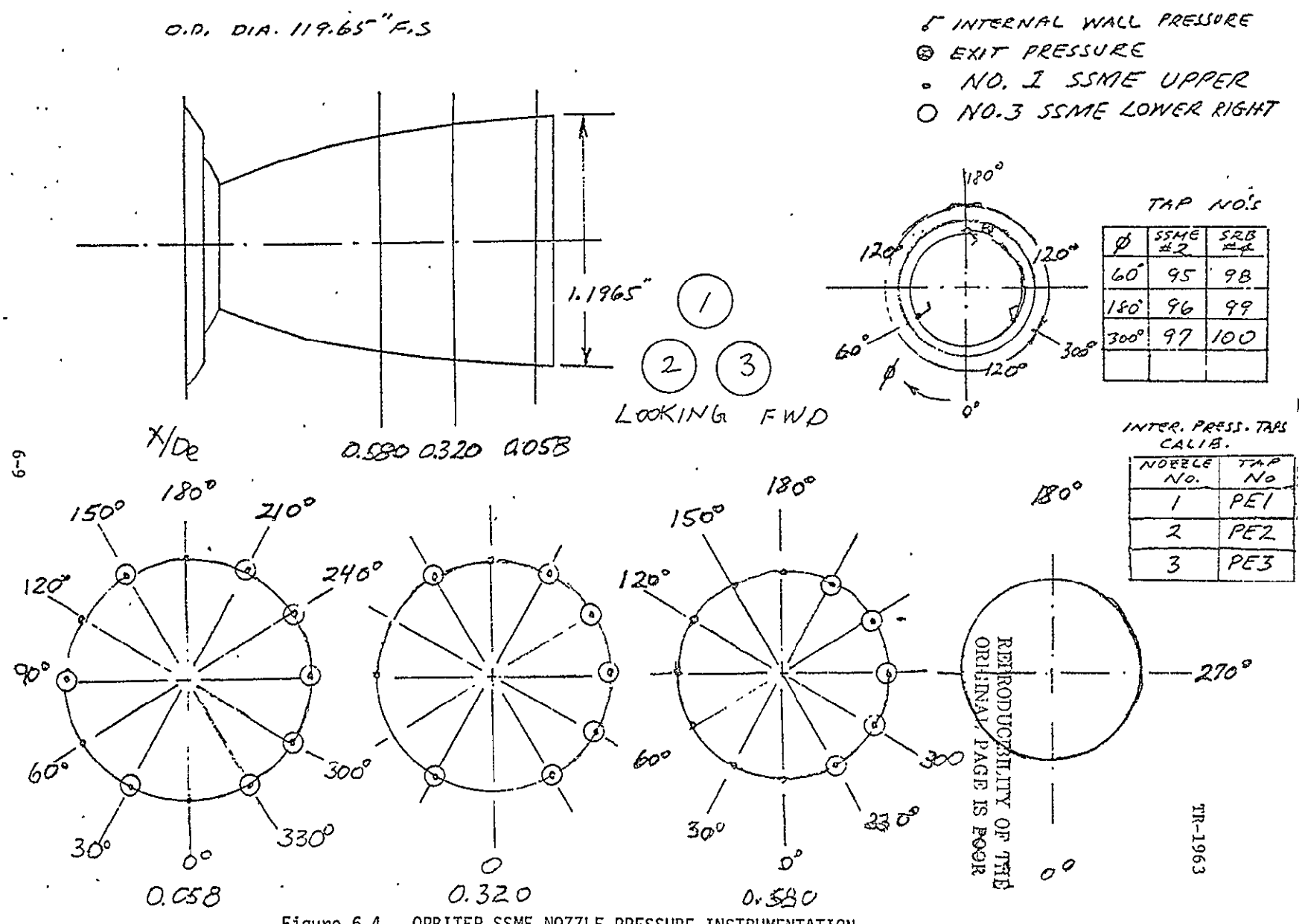

ϕ	SSME #2	SRB #4
60°	95	98
180°	96	99
300°	97	100

NOZZLE NO.	TAP No
1	PE1
2	PE2
3	PE3

Figure 6-4. ORBITER SSME NOZZLE PRESSURE INSTRUMENTATION

BASE INSTRUMENTATION NO. & LOCATION

W.L. (Z_o)	B.L. ($-Y_o$)												℄
	1.30	1.10	1.08	1.07	1.03	.992	.880	.780	.680	.630	.580	.380	.200	0
3.020						318	331						325	307
3.232														306
3.400		334												
3.760			316											305
3.940														304
4.067								313						
4.070												326		
4.150					315									
4.220											329			
4.362														
4.390				323										
4.630	324									330				
4.700							332							
4.880												327		
4.987														302
5.140									328					
5.220							333							
5.320														301

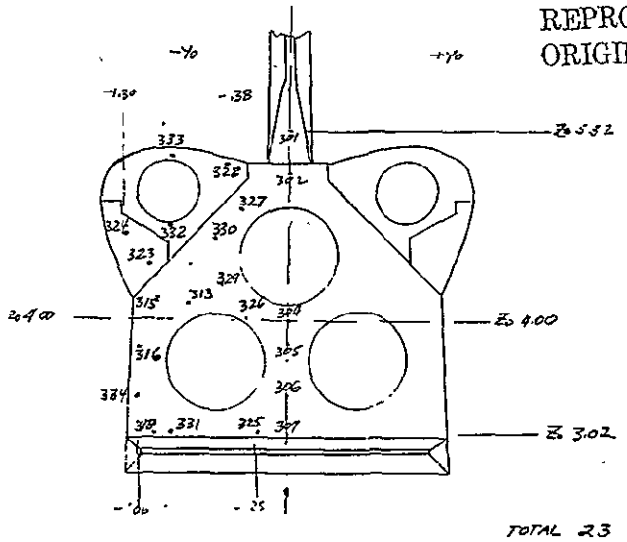

Figure 6-5. ORBITER BASE PRESSURE INSTR. LOCATION.

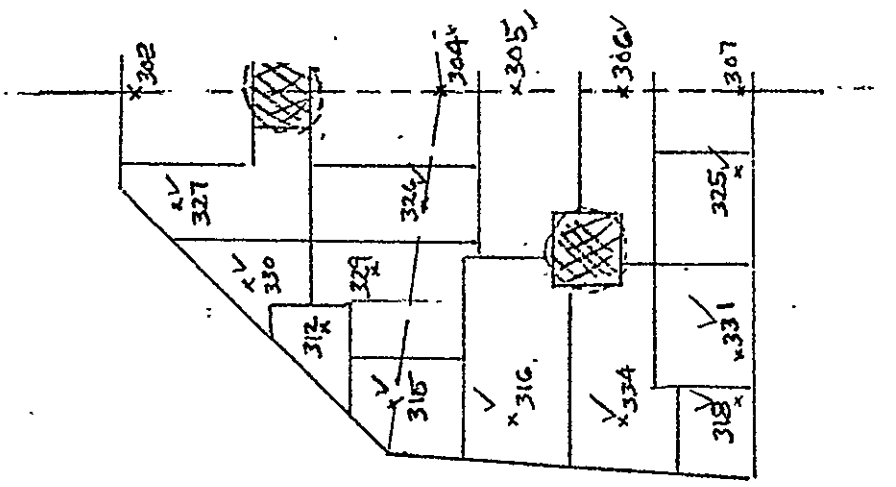

Figure 6-6. ORBITER BASE PLATE-RELATIVE AREAS

ORIFICE	LINE	ITEM	Z	A	X	θ
323	6	3	436.0	18.35	0.0	0.0
324	6	4	465.0	18.35	0.0	0.0
328	6	5	514.0	26.85	0.0	0.0
332	6	6	470.0	26.85	0.0	0.0
333	6	7	522.0	26.85	0.0	0.0
327	6	16	0.0	24.35	1260.5	1.57
315	7	4	0.0	24.35	1260.5	1.57

$\Sigma Ax = 117.25$
$\Sigma Az = 48.7$

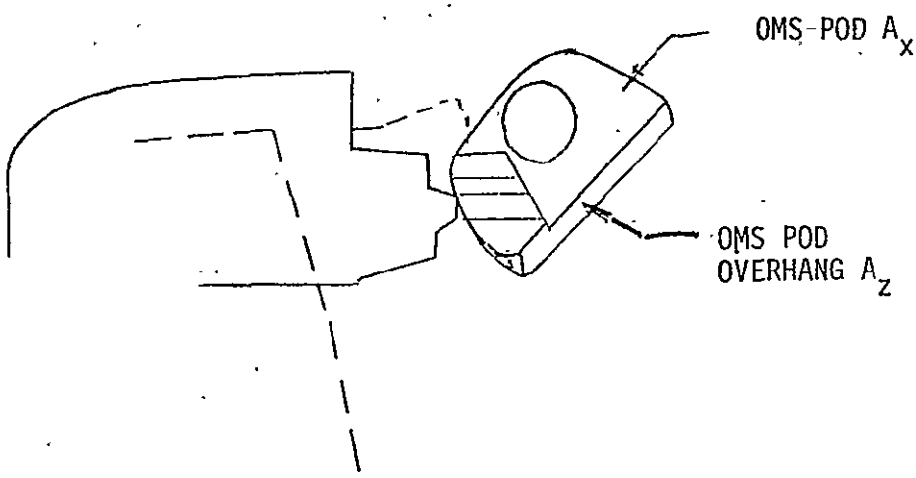

Figure 6-7. OMS POD AREAS

η	X/C_{BF}				LOCATION
	-.10	.20	.60	.95	
.10	405 401	406 402	407 403	408 404	UPPER LOWER
.50	413 409	414 410	415 411	416 412	UPPER LOWER
.90	437 433	438 434	439 435	440 436	UPPER LOWER
				TOTAL	24

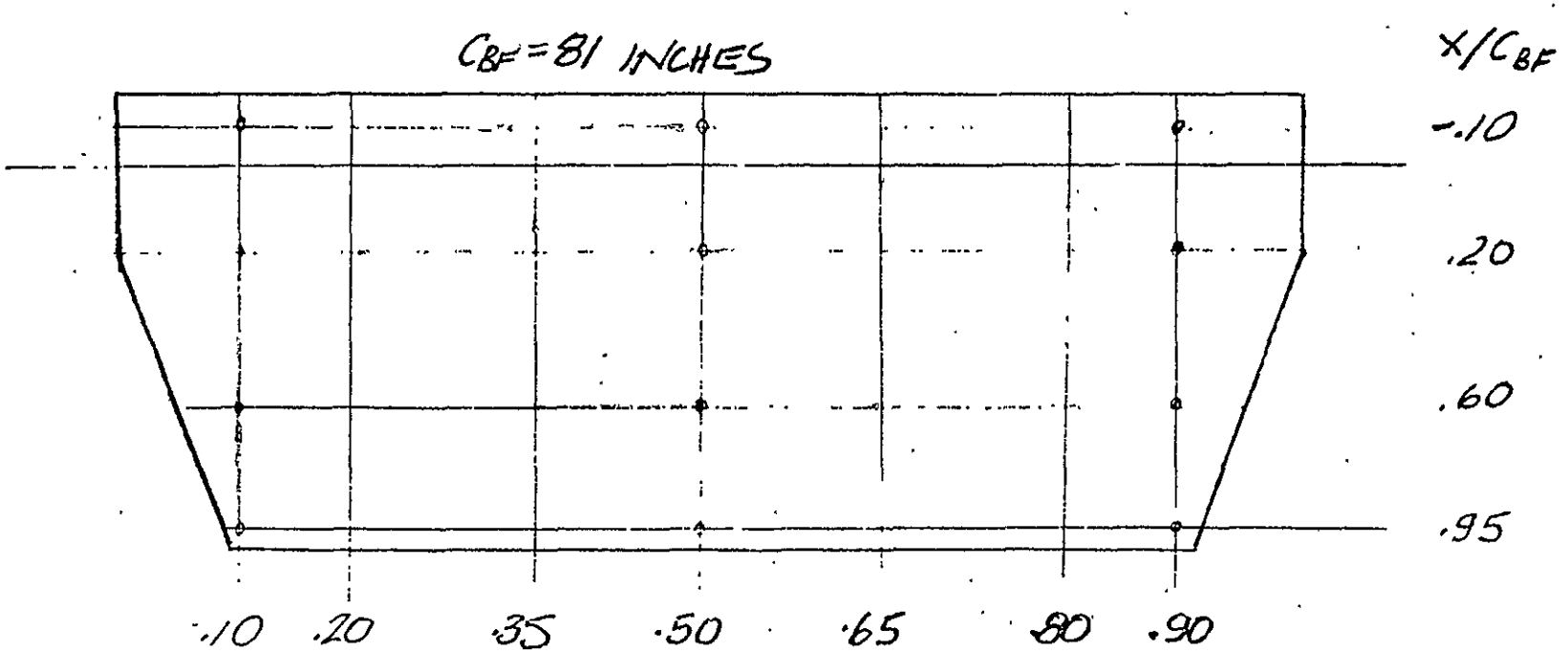

Figure 6-8. ORBITER BODY FLAP PRESSURE INSTRUMENTATION

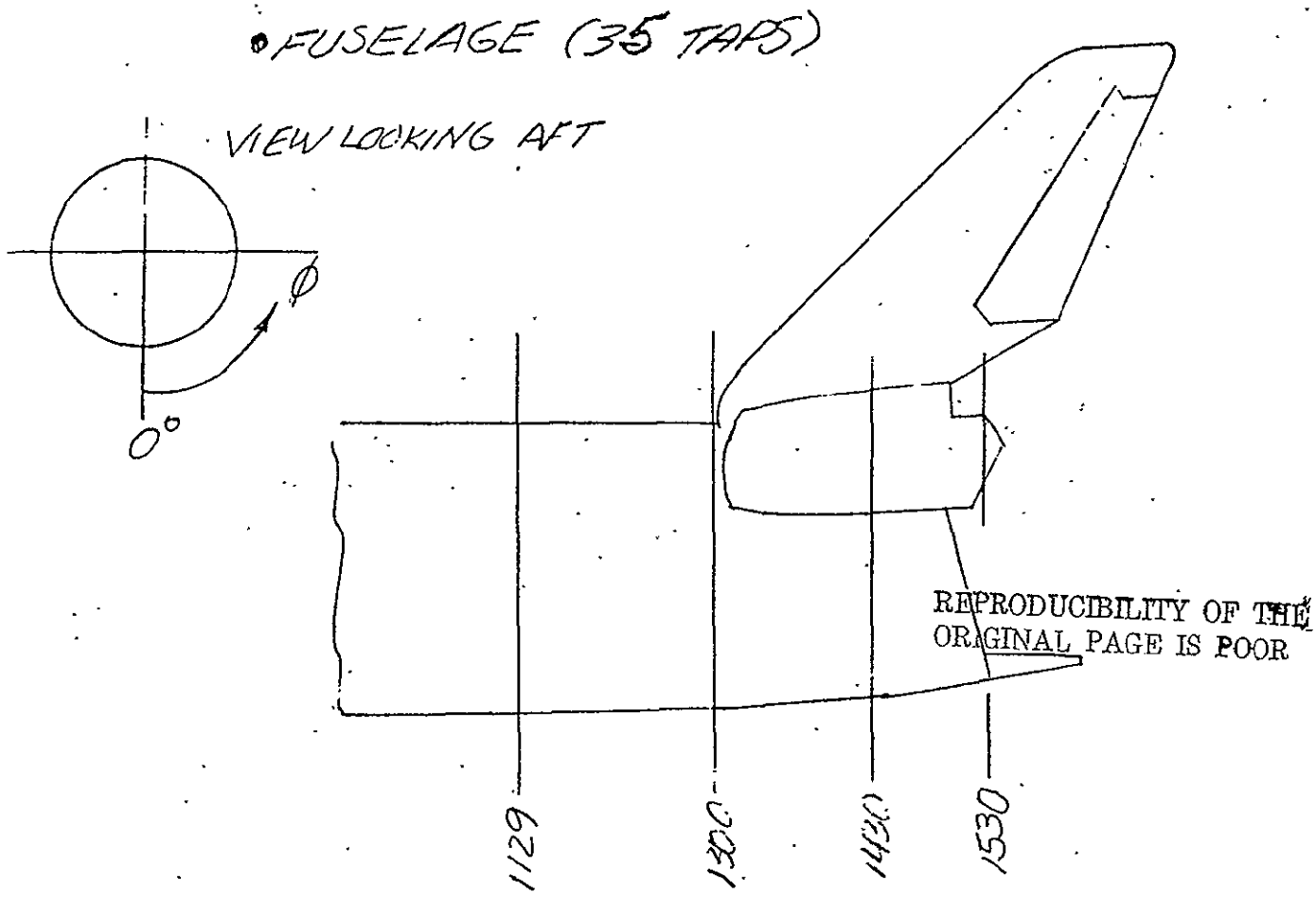

ORB. STA.		ϕ RADIAL LOCATION ~ DEG.											
$X_{o,F.S}$	X_o/L_o	0	20	40	70	90	105	110	120	135	150	165	180
1070	.6288												
1129	.6732		222	223	224	225	226	-	227	228	229	230	231
1215	.7379												
1300	.8019	173	233	174	175	176	177	-	178	179	180	234	181
1375	.8584												
1430	.8998	194	236	195	196	197	198	-	199	200	201	202	-
1480	.9375												
1530a	.9751	-	-	-	-	-	-	214	215	-	-	-	
1530b	.9751	-	-	-	-	-	-	216	217	-	-	-	
										TOTAL			35

Figure 6-9. ORBITER FUSELAGE PRESSURE INSTRUMENTATION

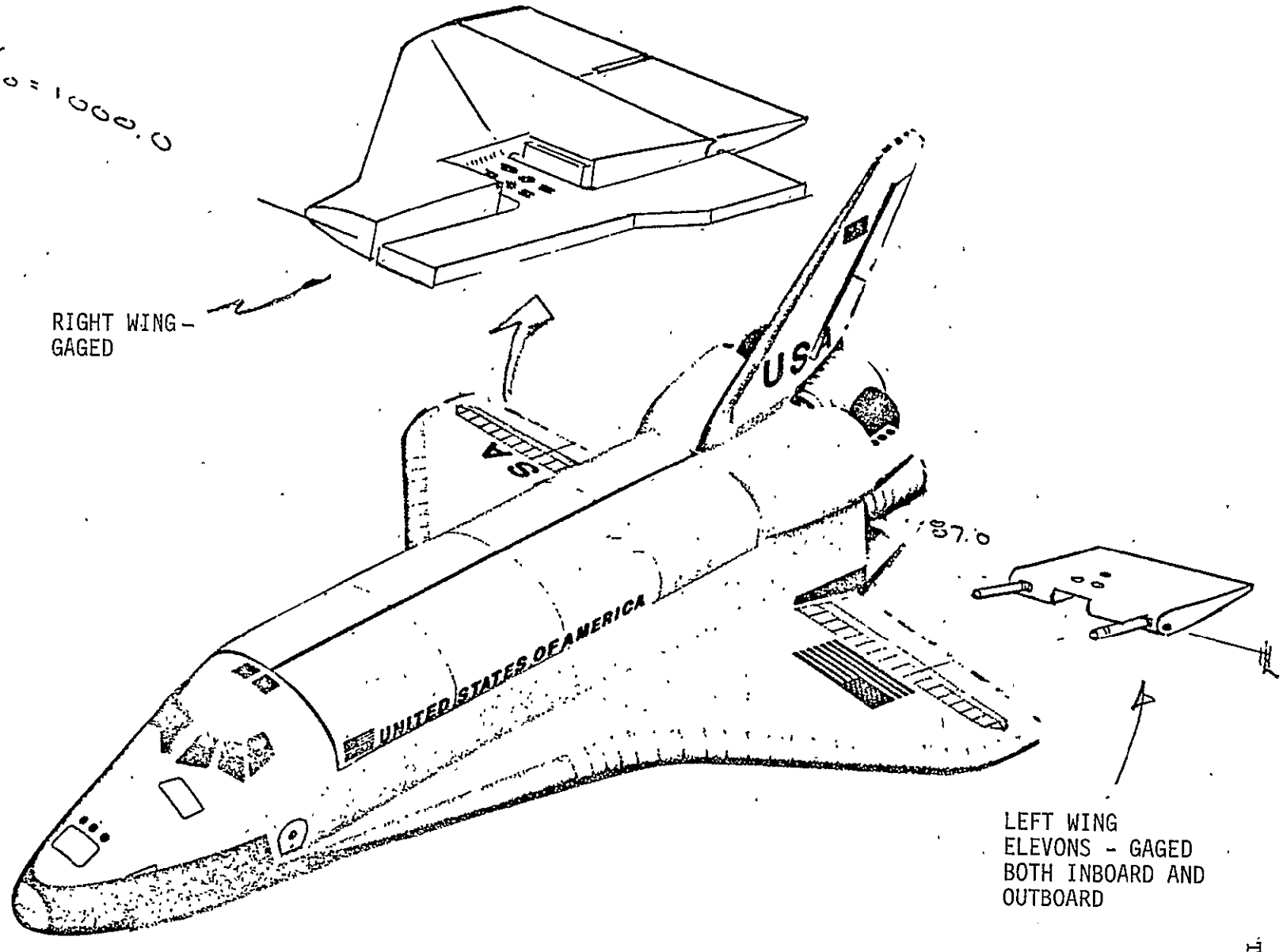

Figure 6-10. GAGED WING AND ELEVONS

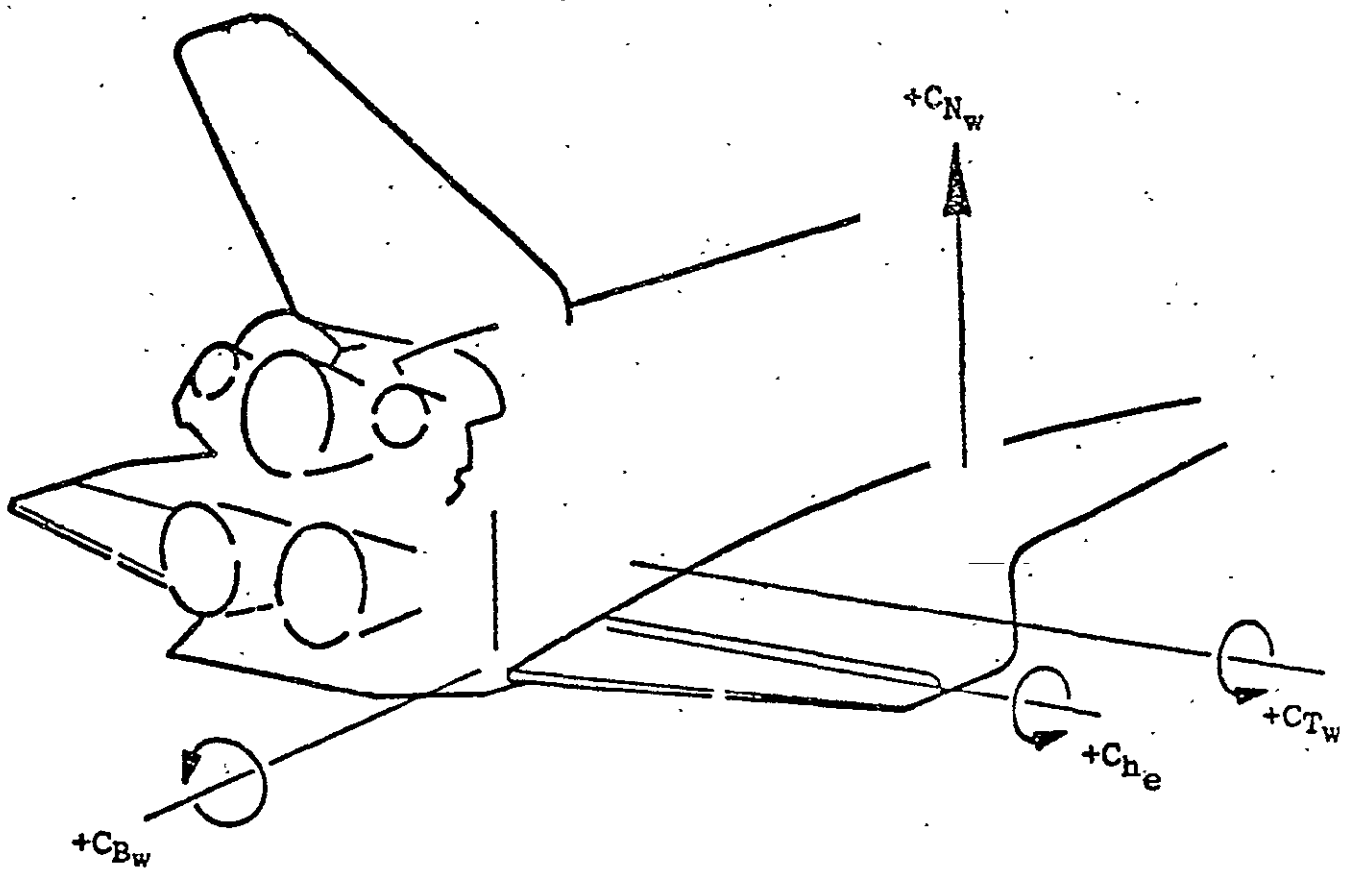

Figure 6-11. WING AND ELEVON FORCE AND MOMENT SIGN CONVENTION

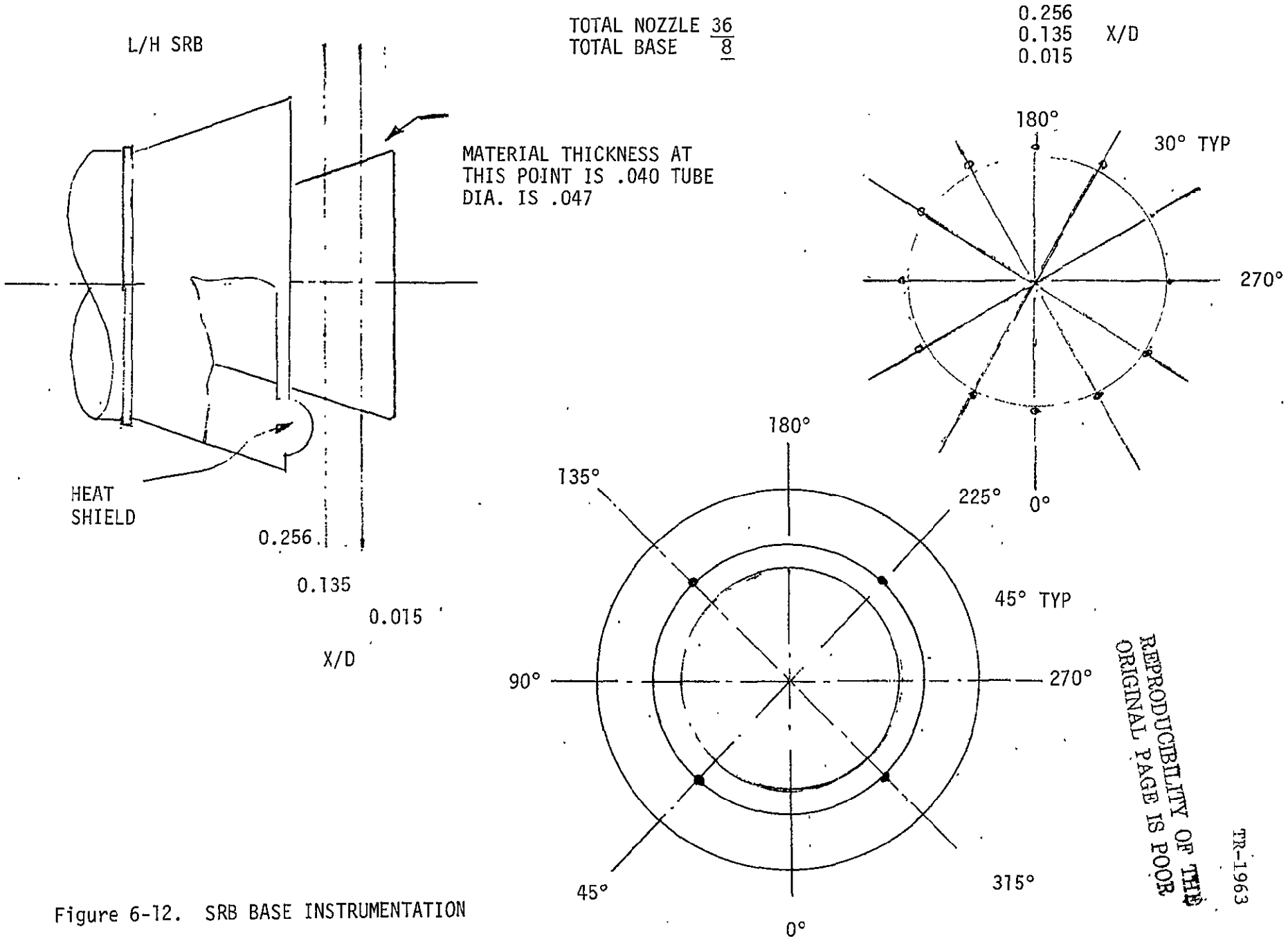

Figure 6-12. SRB BASE INSTRUMENTATION

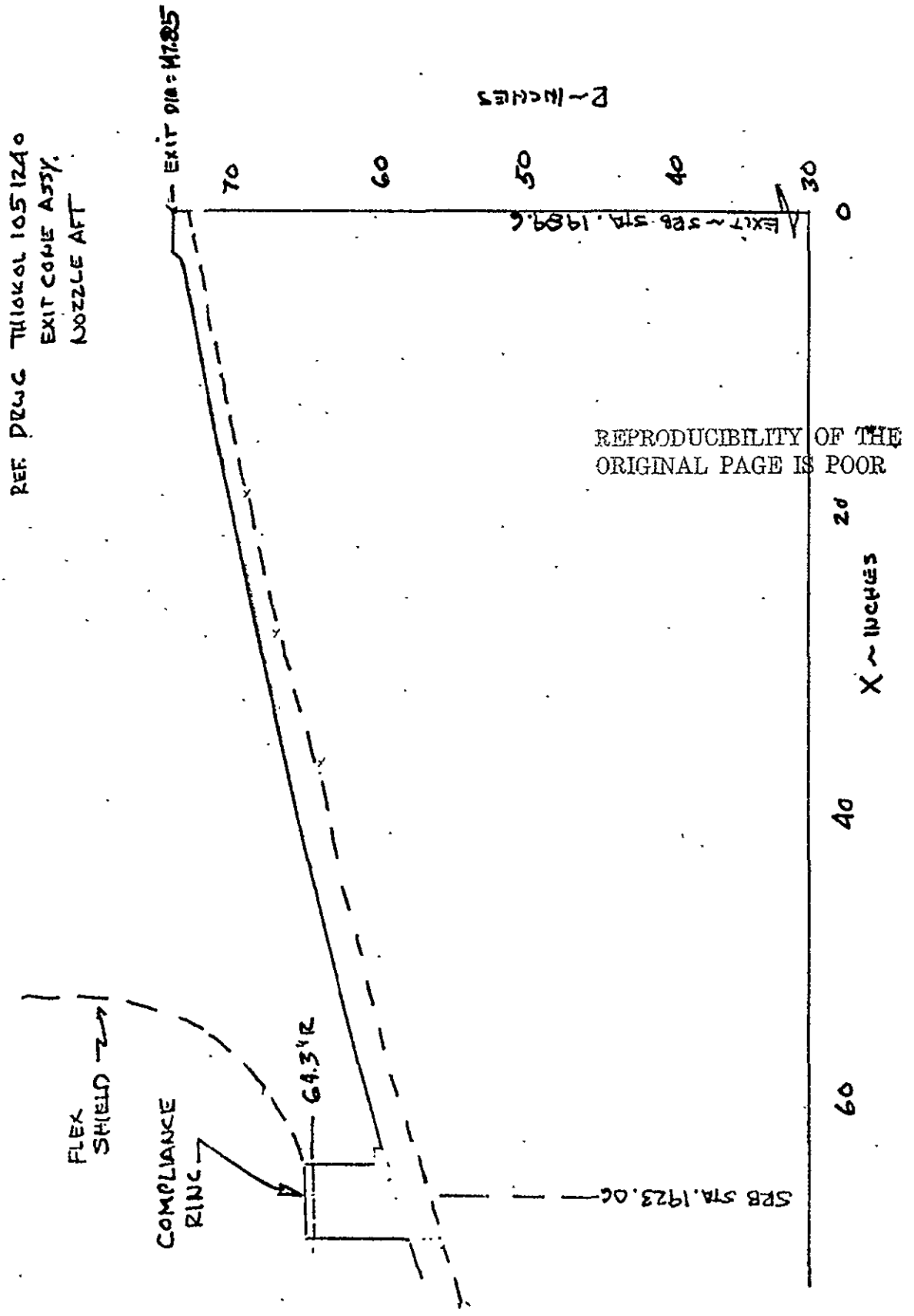

Figure 6-13. SRB NOZZLE CONFIGURATION

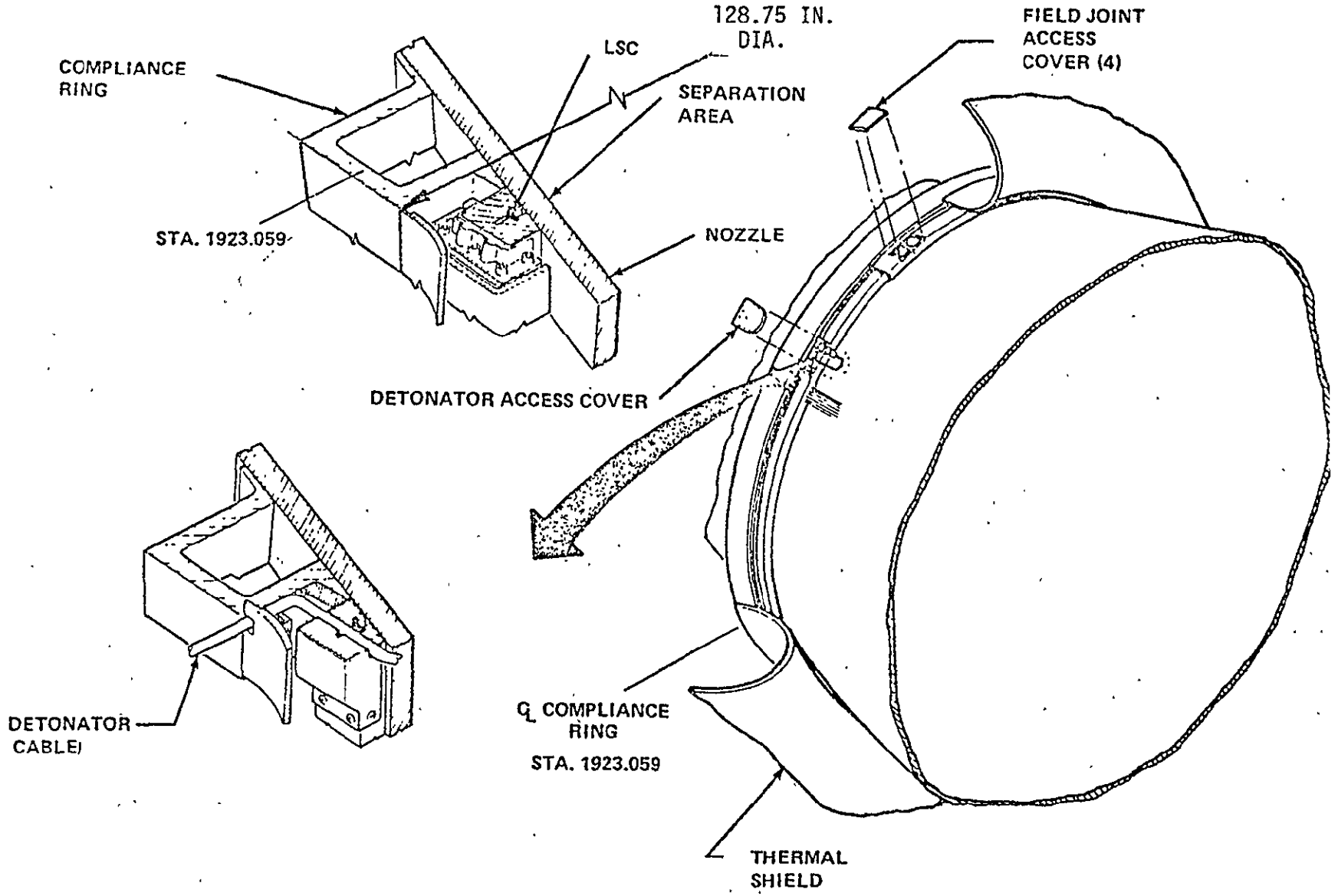

Figure 6-14. SRB NOZZLE HEAT SHIELD AND COMPLIANCE RING

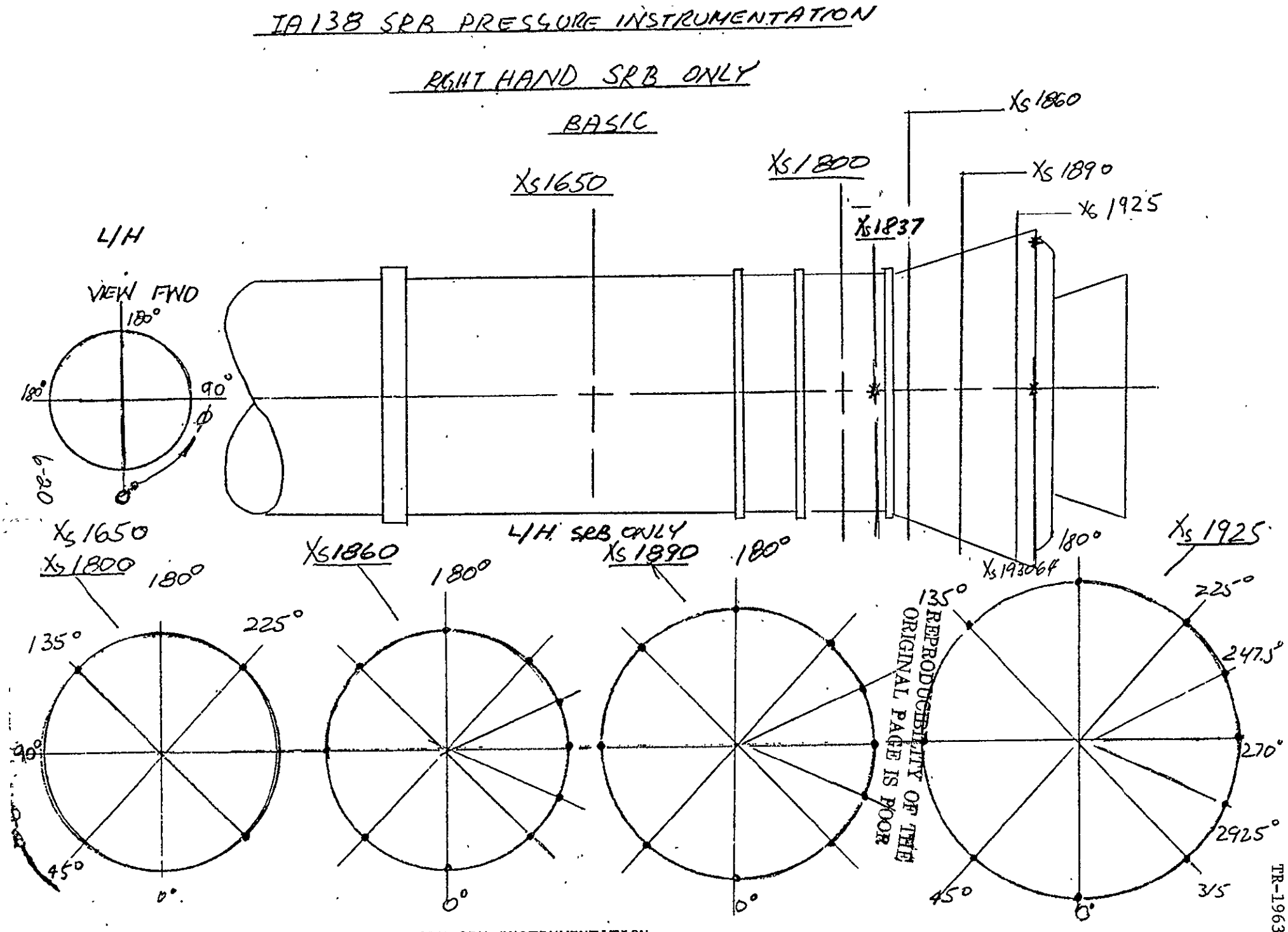

Figure 6-15. SRB FOREBODY INSTRUMENTATION

EXTERNAL TANK BASE

RADIAL LOCATION Ø ~ DEG	RAD.~IN. X_T ~ STA. M.S	X_T 1.655	R_1 1.5656	R_2 1.4812	R_3 1.3902	R_4 1.0509	R_5 .7748	BASE 0
	X_T	20.489	20.8913	21.042	21.1623	21.4477	21.5856	21.7300
0			1502	1516	1530	1546		
15					1531			
30			1503	1517				
45			1501		1533			
60			1504	1518	1534			
67.5			1575	1576	1577			
90			1505	1519	1535	1549	1563	
112.5			1506	1520	1536			
135.0			1507	1521	1537	1551		
157.5			1508	1522				
180.0			1509	1523	1539	1553		
202.5								
225.0								
247.5								
270.0								
300.0								
ET ℄								1574
							TOTAL	34

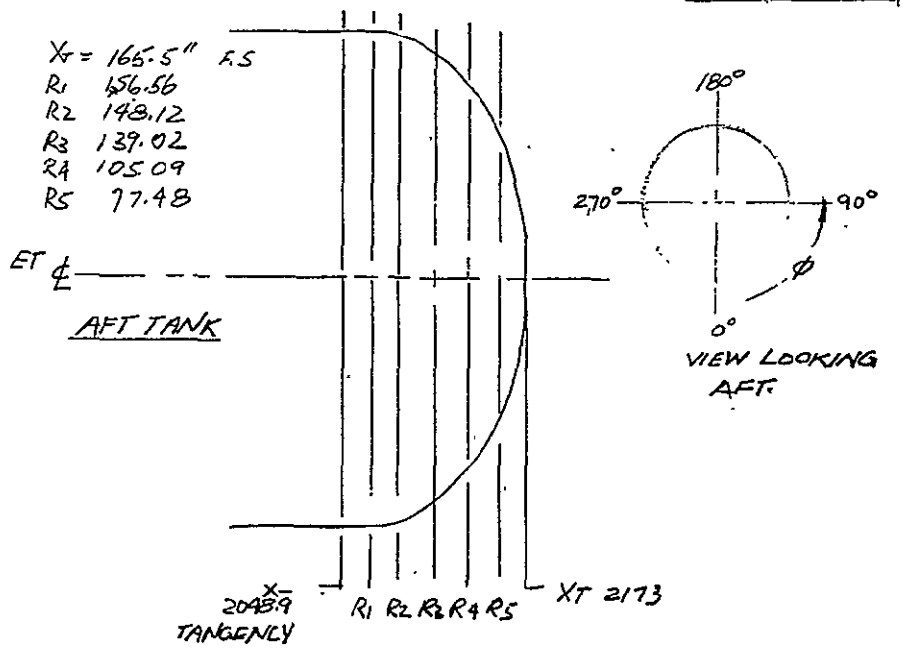

Figure 6-16. EXTERNAL TANK BASE PRESSURE INSTRUMENTATION LOCATION

Table 6-1. SSME #1 PRESSURE INSTRUMENTATION LOCATION AND AREAS

SSME #1

X/D	ORIFICE	θ	TAP LINE ITEM			NOZZLE AXIAL AREA $-FT^2$
	31	0	1	8	17	.287
	32	30	1	9	1	.287
	33	60	1	9	2	.287
	34	90	1	9	3	.287
	35	120	1	9	4	.287
	36	150	1	9	5	.287
.058	37	180	1	9	6	.287
	38	210	1	9	7	.287
	39	240	1	9	8	.287
	40	270	1	9	9	.287
	41	300	1	9	10	.287
	42	330	1	9	11	.287
	43	0	1	9	12	1.11
	44	30	1	9	13	1.11
	45	60	1	9	14	1.11
	46	90	1	9	15	1.11
	47	120	1	9	16	1.11
.32	48	150	1	9	17	1.11
	49	180	1	10	1	1.11
	50	210	1	10	2	1.11
	51	240	1	10	3	1.11
	52	270	1	10	4	1.11
	53	300	1	10	5	1.11
	54	330	1	10	6	1.11
	55	0	1	9	12	2.133
	56	30	1	10	8	2.133
	57	60	1	10	9	2.133
	58	90	1	10	10	2.133
	59	120	1	10	11	2.133
	60	150	1	10	12	2.133
.58	61	180	1	10	1	2.133
	62	210	1	10	14	2.133
	63	240	1	10	15	2.133
	64	270	1	10	4	2.132
	65	300	1	10	17	2.132
	66	330	1	11	1	2.132
					TOTAL	42.357

Table 6-2. SSME #2 PRESSURE INSTRUMENTATION LOCATION AND AREAS

SSME #2

X/D	ORIFICE	θ	TAP	LINE	ITEM	NOZZLE AXIAL AREA ~ FT^2
.058	71	30	2	13	16	.574
	31	90	2	8	17	.574
	73	150	2	13	17	.574
	74	210	2	14	1	.431
	75	240	2	14	2	.287
	76	270	2	14	3	.287
	77	300	2	14	4	.287
	78	330	2	14	5	.431
.32	79	30	2	14	6	2.22
	43	90	2	9	12	2.22
	81	150	2	14	7	2.22
	82	210	2	14	8	1.66
	83	240	2	14	9	1.11
	84	270	2	14	10	1.11
	85	300	2	14	11	1.11
	86	330	2	14	12	1.66
.58	79	30	2	14	6	4.266
	43	90	2	9	12	4.266
	81	150	2	14	7	4.266
	90	210	2	14	13	3.2
	91	240	2	14	14	2.133
	92	270	2	14	15	2.133
	93	300	2	14	16	2.133
	94	330	2	14	17	3.2
					TOTAL	42.352

Table 6-3. SSME #3 PRESSURE INSTRUMENTATION LOCATION AND AREAS

SSME #3

X/D	ORIFICE	θ	TAP LINE ITEM			NOZZLE AXIAL AREA - FT^2
	71	30	3	13	16	.574
	31	90	3	8	17	.574
	73	150	3	13	17	.574
	74	210	3	14	1	.431
.058	75	240	3	14	2	.287
	76	270	3	14	3	.287
	77	300	3	14	4	.287
	78	330	3	14	5	.431
	79	30	3	14	6	2.22
	43	90	3	9	12	2.22
	81	150	3	14	7	2.22
	82	210	3	14	8	1.66
.32	83	240	3	14	9	1.11
	84	270	3	14	10	1.11
	85	300	3	14	11	1.11
	86	330	3	14	12	1.66
	79	30	3	14	6	4.266
	43	90	3	9	12	4.266
	81	150	3	14	7	4.266
.58	90	210	3	14	13	3.2
	91	240	3	14	14	2.133
	92	270	3	14	15	2.133
	93	300	3	14	16	2.133
	94	330	3	14	17	3.2
					TOTAL	42.352

Table 6-4. ORBITER BASE PLATE PRESSURE INSTRUMENTATION LOCATION AND AREAS

ORIFICE	LINE	ITEM	Z	BASE SURFACE AREA	BASE NORMAL AREA
301	7	9	532.0	3.25	2.298
302	6	9	498.7	8.11	7.795
304	6	10	394.0	9.645	9.395
305	6	11	376.0	13.395	13.190
306	6	12	323.2	8.78	8.645
307	6	13	302.0	4.77	4.698
313	7	3	406.7	6.05	5.815
315	7	4	415.0	7.58	7.286
316	7	5	376.0	16.24	15.984
318	7	6	302.0	5.28	5.199
325	6	14	302.0	8.53	8.400
326	6	15	407.0	8.60	8.266
327	6	16	488.0	8.60	8.266
329	6	17	422.0	11.83	11.361
330	7	1	463.0	6.31	6.065
331	7	7	302.0	9.84	9.690
334	7	8	340.0	14.51	14.284
			TOTAL X 2	302.64	293.27
			AREA COMPARISON MINUS A_{301}	-6.50	-4.60
				296.14	288.67
			PLUS NOZZLE BASE PLATE PENETRATION	+11.5	+11.2
			TOTAL	307.64	299.87
			ORBITER BASE DRWG (RI RS009150)	308.3	301.0
			IA119 MODEL DRWG(SSA01261)	306.3	299.014 FT^2

Table 6-5. ORBITER UPPER BODY FLAP PRESSURE INSTRUMENTATION LOCATION AND AREAS

ORIFICE	LINE	ITEM	X	A ~ FT^2
405	7	14	1288.0	3.0
406	7	15	1312.3	26.0
407	7	16	1344.7	21.0
408	7	17	1373.0	5.0
413	8	5	1288.0	5.5
414	8	6	1213.3	9.0
415	8	7	1344.7	15.0
416	8	8	1373.0	7.0
437	8	13	1288.0	3.0
438	8	14	1312.3	26.0
439	8	15	1344.7	21.0
440	8	16	1373.0	5.0

$\Sigma A = 146.5$

Table 6-6. ORBITER FOREBODY AND OMS POD INSTRUMENTATION LOCATION

ORIFICE	LINE	ITEM	AREA	X	Y	θ
222	5	7	29.69	894.0	0.0	0.0
222	5	7	62.94	894.0	50.0	0.0
223	5	8	35.62	894.0	106.0	0.0
224	5	9	58.90	894.0	298.2	90.0
225	5	10	39.54	894.0	336.5	90.0
226	5	11	34.62	894.0	364.8	94.9
227	5	12	35.92	894.0	394.7	118.4
228	5	13	35.15	894.0	414.9	146.2
229	5	14	33.07	894.0	427.2	159.4
230	5	15	31.47	894.0	434.3	169.7
231	5	16	15.44	894.0	436.9	180.0
173	4	1	26.13	1065.0	0.0	0.0
223	5	17	55.39	1065.0	50.6	0.0
174	4	2	32.48	1065.0	105.4	0.0
175	4	3	61.43	1065.0	298.2	90.0
176	4	4	34.75	1065.0	336.5	90.0
177	4	5	30.67	1065.0	364.7	94.4
178	4	6	31.88	1065.0	394.7	118.8
179	4	7	30.96	1065.0	414.9	145.8
180	4	8	29.13	1065.0	427.2	159.2
234	6	1	27.70	1065.0	434.3	169.3
181	4	9	13.59	1065.0	436.9	180.0
194	4	10	25.17	1195.0	0.0	0.0
236	6	2	56.04	1195.0	48.6	0.0
195	4	11	41.94	1195.0	109.9	0.0
196	4	12	88.86	1195.0	294.0	90.0
197	4	13	36.00	1195.0	336.5	90.0
198	4	14	54.38	1195.0	372.1	45.0
199	4	15	45.06	1195.0	419.2	135.0
200	4	16	42.80	1195.0	449.8	135.0
201	4	17	49.09	1195.0	473.8	180.0
202	5	1	42.29	1195.0	451.0	225.0
214	5	2	6.25	1294.0	373.2	45.0
215	5	3	6.25	1294.0	396.4	110.0
216	5	4	15.62	1294.0	390.5	225.0
217	5	5	6.25	1294.0	422.3	290.0
401	8	1	8.5	1288.0	0.0	0.0
433	8	9	9.0	1288.0	88.0	0.0
410	8	2	13.0	1313.2	0.0	0.0
434	8	10	12.0	1313.2	88.0	0.0
411	8	3	8.0	1345.6	0.0	0.0
435	8	11	9.0	1345.6	88.0	0.0
412	8	4	16.0	1373.95	0.0	0.0
436	8	12	8.0	1373.95	88.0	0.0

Table 6-7. LEFT SRB NOZZLE PRESSURE INSTRUMENTATION LOCATION AND AREAS

X/D	ORIFICE	θ	LINE	ITEM	NOZZLE AXIAL AREA - FT^2
	2405	0	16	7	.767
	2406	30	16	8	.767
	2407	60	16	9	.767
	2408	90	16	10	.767
	2409	120	16	11	.767
.256	2410	150	16	12	.767
	2411	180	16	13	.767
	2412	210	16	14	.767
	2413	240	16	15	.767
	2414	270	16	16	.767
	2415	300	16	17	.767
	2416	330	17	1	.767
	2417	0	17	2	1.01
	2418	30	17	3	1.52
	2420	90	17	5	1.52
	2421	120	17	6	1.01
	2422	150	17	7	1.01
.135	2423	180	17	8	1.01
	2424	210	17	9	1.01
	2425	240	17	10	1.01
	2426	270	17	11	1.01
	2427	300	17	12	1.01
	2428	330	17	13	1.01
	2429	0	17	14	.582
	2430	30	17	15	.582
	2431	60	17	16	.582
	2432	90	17	17	.582
.015	2433	120	18	1	.582
	2434	150	18	2	.582
	2435	180	18	3	.582
	2436	210	18	4	.582
	2437	240	18	5	.8733
	2439	300	18	7	.8733
	2440	330	18	8	.582
				TOTAL	28.32

Table 6-8. LEFT SRB FOREBODY PRESSURE INSTRUMENTATION LOCATION

ORIFICE	LINE	ITEM	X_1	X_2	θ_1	θ_2
2151	15	9	1397.6	1432.3	0.0	1.5708
2153	15	10	1397.6	1432.3	1.5708	3.1416
2155	15	11	1397.6	1432.3	3.1416	4.3197
2157	15	12	1397.6	1432.3	4.3197	5.1051
2159	15	13	1397.6	1432.3	5.1051	0.0
2161	15	14	1432.3	1467.3	0.0	1.5708
2163	15	15	1432.3	1467.3	1.5708	3.1416
2165	15	16	1432.3	1467.3	3.1416	4.3197
2167	15	17	1432.3	1467.3	4.3197	5.1051
2169	16	1	1432.3	1467.3	5.1051	0.0
2171	16	2	1467.3	1487.9	0.0	1.5708
2173	16	3	1467.3	1487.9	1.5708	3.1416
2175	16	4	1467.3	1487.9	3.1416	4.3197
2177	16	5	1467.3	1487.9	4.3197	5.1051
2179	16	1	1467.3	1487.9	5.1051	0.0

Table 6-9. EXTERNAL TANK BASE PRESSURE INSTRUMENTATION

ORIFICE	LINE	ITEM	% TOTAL AREA	AREA FT^2	ORIFICE	LINE	ITEM	% TOTAL AREA	AREA FT^2
1501	11	8	.0065	3.882	1530	12	8	.0077	4.60
1502	11	9	.0064	3.82	1531	12	9	.0130	7.764
1503	11	10	.0095	5.674	1533	12	10	.0130	7.764
1504	11	11	.0043	2.568	1534	12	11	.0060	3.583
1505	11	12	.0095	5.674	1535	12	12	.0130	7.764
1506	11	13	.0108	6.450	1536	12	13	.0148	8.840
1507	11	14	.0086	5.136	1537	12	14	.0190	11.34
1508	11	15	.0095	5.674	1539	12	15	.0135	8.06
1509	11	16	.0047	2.807	1546	12	8(16)	.0565	33.75
1516	11	17	.0054	3.22	1549	12	17	.0482	28.79
1517	12	1	.0072	4.300	1551	13	1	.0334	19.94
1518	12	2	.0048	2.867	1553	13	2	.0283	16.90
1519	12	3	.0053	3.165	1563	13	3	.0576	34.40
1520	12	4	.0060	3.583	1574	13	4	.0456	27.24
1521	12	5	.0048	2.867	1575	13	5	.0065	3.882
1522	12	6	.0054	3.225	1576	13	6	.0036	2.150
1523	12	7	.0026	1.583	1577	13	7	.0090	5.375

$\Sigma A = 298.65$

TOTAL AREA = 597.30

Table 6-10. REFERENCE DIMENSIONS

TOTAL VEHICLE	FULL SCALE REFERENCE DIMENSIONS
S_{REF}	2690 ft^2
ℓ_{REF}	1290.3 in.
Wing	
Planform area, S_{REF}	2690 ft^2
MAC, $\bar{c}$	474.81 in.
Span, b	936.68 in.
Elevons	
S_{REF}	210 ft^2
ℓ_{REF}	90.7 in.
Vertical Stabilizer	
S_{REF}	413.25 ft^2
ℓ_{REF}	199.8 in.

The moment reference locations

Total vehicle:	X_T 976, Y_T0, Z_T 400
ORB, ET, SRB:	X_T 976, Y_T0, Z_T 400

COMPONENTS

Wing:	X_o1307, Y_o105, Z_o288
Elevons:	Hingeline at X_o1387
Vertical Tail:	X_o1414.3, Y_o0, Z_o503

Section VII

TEST RESULTS

The results of the integration of the base pressure and forebody power delta's are presented in table form in the Appendix. The output of the Plume Integration computer program contains all the results of the pressure integration including base coefficients, forces and moments and forebody coefficient data from pressure integration along with the gage data.

An example of the printout from a data set is presented below. The data are arranged in 9 sections. Section 1 presents the run numbers, Mach number vehicle configuration and attitude. Section 2 presents the nozzle gas dynamic properties. Section 3 presents the plume gas dynamic similarity parameters. Section 4 presents the values of parameters used to determine the similarity parameters. Section 5 presents the results of the pressure integration over the base of the elements and components. Section 6 presents the average base pressure coefficient for each element. Section 7 presents the nozzle average base pressure coefficients. Section 8 presents the forebody data from the gages. Section 9 presents the forebody data from pressure integration.

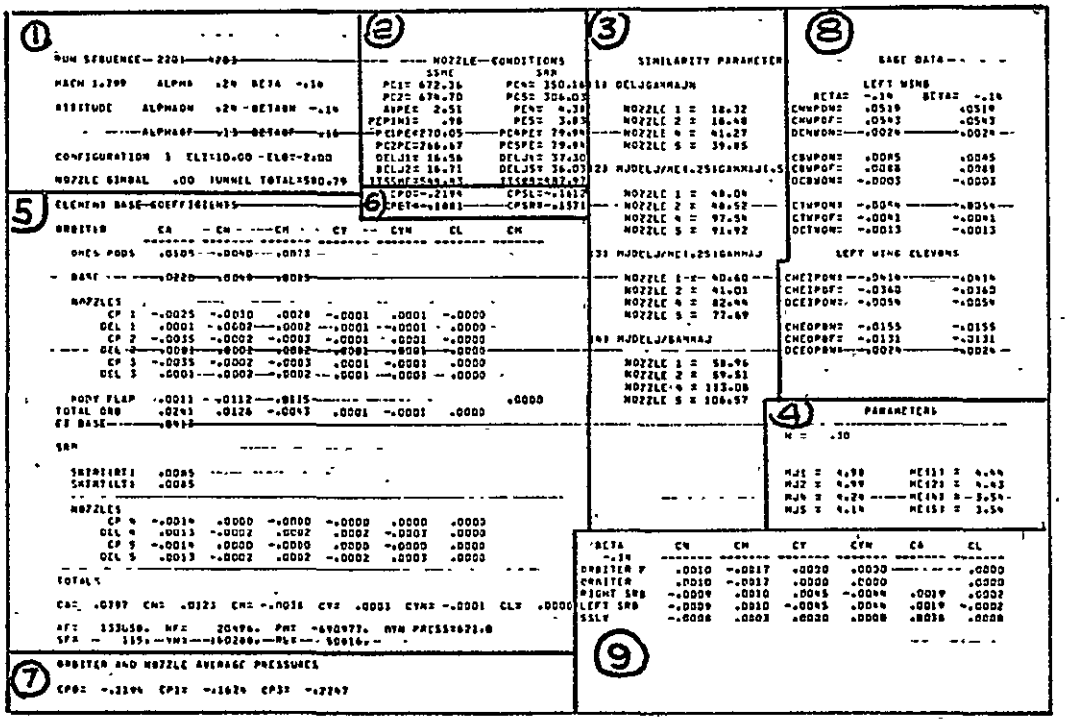

Printouts of each run sequence set is presented in the Appendix. The data sets are grouped for a constant Mach number. The first data set within a Mach group is the power-off runs. The second group contains the variable power runs. The third group contains the various elevon deflections.

It is noted that there is a difference in the power-on model attitude and power-off model attitude for a large portion of the data sets. It was thus necessary to evaluate what effect this had on the base forces and moments and the forebody power deltas. The sensitivity of the base coefficients was determined by plotting the data versus angle of attack and then estimating the error due to an angle of attack error. This procedure is only approximate, but the results showed that the error is less than 2 percent, which is considered well within the accuracy of the measurements and integration technique. Thus the base forces and moments are not considered to be adversely affected by an attitude difference.

The forebody pressure data was similarly evaluated and was found to not be adversibly influenced by the attitude error. The wing and elevon power delta's were evaluated by plotting both the power-off and the power-on gage data versus angle of attack and then evaluating the power delta at a constant angle of attack. It was found that the interpolated wing power delta changed substantially. The interpolated wing power delta was lower than the appendix value and in some cases substantially lower. The elevon hinge moment power-delta was similarly evaluated and found to have about a 10 percent difference from the tabulated value and the interpolated value.

Section VIII

BASE MATH MODEL

A math model of the plume induced aerodynamic characteristics has been developed which can be used in conjunction with the forebody aerodynamic characteristics to evaluate the aerodynamic characteristics of the total space shuttle launch vehicle and each element. Three types of base aerodynamic characteristics have been developed. These include 1. SSLV and element base aerodynamic coefficients for Mach numbers of 1.55, 1.80, 2.20, and 2.50, 2. SSLV base forces and moments versus altitude up to 160,000 ft. and 3. SSLV and element base coefficient tolerances for Mach numbers from 1.55 to 2.50. The math model consists of a description of the base aerodynamic coefficients at a given Mach number and elevon deflection for various α, β values. Gradients are provided giving the change in the aerodynamic characteristics with the primary variable that influences the base flow (inboard elevon deflection).

The base aerodynamic math model is limited to base axial force, normal forces and pitching moments. Lateral-directional forces and moments exist on some base components, but no consistent trend could be identified and thus they are included in the base tolerance model. Base coefficients and tolerances for each element are provided for Mach numbers of 1.55, 1.80, 2.20, and 2.50. These Mach numbers are compatible with the forebody aerodynamic data base. The base aerodynamic coefficient math model is described by the following equation

$$C_{x_i} = [C_{x_i}]_{\alpha,\beta} + [\partial C_{x_i}/\partial \delta_{EI}] \times \Delta\delta_{EI}$$

where $[C_{x_i}]_{\alpha,\beta}$ is a 7x7 matrix for α = -6,-4,-2,0,2,4,6
β = -6,-4,-2,0,2,4,6
elevon deflection corresponds to close schedule 6 (Table 8-1)
i = SSLV, ORBITER, ET, LEFT SRB, RIGHT SRB

$\partial C_{x_i}/\partial \delta_{EI}$ Gradient for inboard elevon deflection - function of Mach number only
i = SSLV, ORBITER, ET

$\Delta\delta_{EI}$ - Change in inboard elevon deflection from math model value to inboard elevon deflection of interest.

Values of the coefficient $[C_{X_i}]_{\alpha,\beta}$ are presented in Tables 8-1 through 8-12 for each element and the total SSLV vehicle. Values of the coefficient gradien are presented in Table 8-13.

Base forces and moments have been determined versus altitude using the base coefficient math model. The base force math model is for the total vehicle and uses the following model,

$$\left.\begin{matrix}F\\M\end{matrix}\right|_{ALT} = \left.\begin{matrix}F\\M\end{matrix}\right|_{\alpha=0} + \left[\frac{\partial F}{\partial \alpha}\right] \times \alpha + \left[\frac{\partial F_X}{\partial \delta_{EI}}\right] \Delta\delta_{EI}$$

where:

$\left.\begin{matrix}F\\M\end{matrix}\right|_{\alpha=0}$ SSLV base force or moment - function of altitude only

$[\partial F/\partial \alpha]$ Gradient for angle of attack - function of altitude only

$[\partial F/\partial \delta_{EI}]$ Gradient for inboard elevon deflection - function of altitude only

α angle of attack

$\Delta\delta_{EI}$ Change in inboard elevon deflection from math model value to inboard elevon deflection of interest

Values of the base axial force, normal force and pitching moment are presented in Tables 8-14 through 8-16. The base force partials are presented in Tables 8-17 through 8-19.

BASE COEFFICIENT TOLERANCES

The base coefficient tolerances are presented in Tables 8-20 and 8-21. The coefficient tolerances cover all altitudes and configurations from the base coefficients presented in the math model to flight data and are to a $\pm 3\sigma$ level The moment tolerances are considered to be only due to force tolerances. The

moment tolerance due to the aerodynamic center location uncertainty being a smaller order of magnitude. The base moment coefficient tolerance equations are presented in Table 8-21.

Approximately 60 percent of the orbiter normal force is due to the orbiter axial force. The orbiter normal force tolerance presented in Table 8-20 was therefore calculated using the orbiter axial force tolerance. The equation used to determine the normal force tolerance is presented at the bottom of Table 8-20. The side force coefficient tolerances are due to side forces that exist on the SSME nozzle bells. Side forces will exist on the nozzle bells during various gimbal patterns and under angle of sideslip conditions. These side forces also produce yawing moments and rolling moments. The majority of the lateral-directional tolerances are due to the orbiter.

The base tolerances include contributions due to 1. test instrumentation uncertainty, 2. simulation parameter uncertainty, 3. Reynolds number characteristics, 4. Model-tunnel testing uncertainties, 5. Pressure integration uncertainties and 6. Math model uncertainties. The tolerances thus cover the uncertainty from the math model to flight data and are to a $\pm 3\sigma$ level. Each tolerance contribution is assumed independent and therefore the contributions are combined using the RSS technique.

The model instrumentation contribution includes the accuracy of the Scanivalve^{R} calculations. The general accuracy is estimated to be $C_P = \pm .013$ for values of C_P in the range of $\pm .5$. The general uncertainty of the measured pressure coefficients was assumed to be 3%.

The simulation parameter uncertainty was assumed to be due to an uncertainty in the exponent. The estimated uncertainty in the exponent is shown in Figure 5-2. The exponent uncertainty was converted to an error in simulati that generally represented a 10 percent uncertainty in base force coefficients The Reynolds number-scale uncertainty was obtained using past flight test to wind-tunnel test results. This factor is a judgement factor and includes the differences between the Saturn V and Titan 3C flight and wind tunnel data, reduced to account for the plume technology program learning curve. This factor

also includes a hot flow simulation uncertainty factor. The Reynolds number-scale uncertainty was generally 10% of the nominal base coefficient.

Model configuration uncertainties includes the effect of the support stings that will influence the flow field at angles of sideslip along with uncertainties due to other model configuration inaccuracies that potentially influence the local flow fields. Uncertainties due to model configuration similitude were approximately 7% of the nominal force coefficients.

Integration uncertainties include the potential error involved in the integration technique and represent approximately 3 percent of the nominal force coefficients.

The math model uncertainty includes the errors of independent variables in the math model of the base forces and moments. Independent variables not included in the math model of the base forces and moments include nozzle gimbal angle and outboard elevon position.

The technique that was used to develop the SSLV base tolerances was to correlate the SRB and ET base tolerances and RSS those to the orbiter base coefficient tolerance. This procedure was used for the base axial force and normal force coefficients. The SSLV base side force coefficient was obtained by using the RSS technique for each element.

The forebody plume induced aerodynamic characteristics have been developed in conjunction with the base plume induced aerodynamic characteristics to allow a complete description of the plume induced characteristics of the Space Shuttle Launch Vehicle. The forebody plume induced aerodynamic characteristics are presented in Section IX.

Table 8-1.

BASE AXIAL FORCE COEFFICIENT

$M_\infty = 1.55$ $\delta_{e_{IO}} = 10/-2$

% SSME POWER = 109%

ELEMENT		α	β -6	-4	-2	0	2	4	6
CA-IOL	1.55	-6.	.0685	.0663	.0642	.0625	.0642	.0663	.0685
CA-IOL	1.55	-4.	.0646	.0632	.0616	.0605	.0616	.0632	.0646
CA-IOL	1.55	-2.	.0629	.0616	.0601	.0591	.0601	.0616	.0629
CA-IOL	1.55	0.	.0614	.0602	.0588	.0579	.0588	.0602	.0614
CA-IOL	1.55	2.	.0595	.0583	.0571	.0561	.0571	.0583	.0595
CA-IOL	1.55	4.	.0575	.0563	.0553	.0543	.0553	.0563	.0575
CA-IOL	1.55	6.	.0557	.0546	.0534	.0525	.0534	.0546	.0557
CA-ORB	1.55	-6.	.0191	.0194	.0198	.0202	.0198	.0194	.0191
CA-ORB	1.55	-4.	.0194	.0197	.0200	.0204	.0200	.0197	.0194
CA-ORB	1.55	-2.	.0195	.0197	.0198	.0200	.0198	.0197	.0195
CA-ORB	1.55	0.	.0196	.0196	.0196	.0196	.0196	.0196	.0196
CA-ORB	1.55	2.	.0194	.0193	.0192	.0191	.0192	.0193	.0194
CA-ORB	1.55	4.	.0191	.0189	.0187	.0185	.0187	.0189	.0191
CA-ORB	1.55	6.	.0189	.0186	.0182	.0179	.0182	.0186	.0189
CA-ET	1.55	-6.	.0386	.0368	.0349	.0331	.0349	.0368	.0386
CA-ET	1.55	-4.	.0365	.0346	.0326	.0307	.0326	.0346	.0365
CA-ET	1.55	-2.	.0363	.0342	.0321	.0301	.0321	.0342	.0363
CA-ET	1.55	0.	.0361	.0340	.0318	.0297	.0318	.0340	.0361
CA-ET	1.55	2.	.0357	.0336	.0315	.0294	.0315	.0336	.0357
CA-ET	1.55	4.	.0351	.0331	.0312	.0292	.0312	.0331	.0351
CA-ET	1.55	6.	.0346	.0327	.0309	.0290	.0309	.0327	.0346
CA-R	1.55	-6.	.0078	.0067	.0056	.0046	.0039	.0034	.0030
CA-R	1.55	-4.	.0072	.0064	.0055	.0047	.0035	.0025	.0015
CA-R	1.55	-2.	.0064	.0058	.0051	.0045	.0031	.0019	.0007
CA-R	1.55	0.	.0057	.0052	.0047	.0043	.0027	.0014	.0000
CA-R	1.55	2.	.0050	.0046	.0042	.0038	.0022	.0008	-.0006
CA-R	1.55	4.	.0044	.0040	.0037	.0033	.0017	.0003	-.0011
CA-R	1.55	6.	.0038	.0035	.0031	.0028	.0012	-.0002	-.0016
CA-L	1.55	-6.	.0030	.0034	.0039	.0046	.0056	.0067	.0078
CA-L	1.55	-4.	.0015	.0025	.0035	.0047	.0055	.0064	.0072
CA-L	1.55	-2.	.0007	.0019	.0031	.0045	.0051	.0058	.0064
CA-L	1.55	0.	.0000	.0014	.0027	.0043	.0047	.0052	.0057
CA-L	1.55	2.	-.0006	.0008	.0022	.0038	.0042	.0046	.0050
CA-L	1.55	4.	-.0011	.0003	.0017	.0033	.0037	.0040	.0044
CA-L	1.55	6.	-.0016	-.0003	.0012	.0028	.0031	.0035	.0039

Table 8-2. $M_\infty = 1.55$ $\delta_{e_{IO}} = 10/-2$

BASE NORMAL FORCE COEFFICIENT % SSME POWER = 109%

ELEMENT		α	β -6	-4	-2	0	2	4	6
CN-IOL	1.55	-6.	.0135	.0135	.0135	.0135	.0135	.0135	.0135
CN-IOL	1.55	-4.	.0139	.0138	.0138	.0136	.0138	.0138	.0139
CN-IOL	1.55	-2.	.0141	.0138	.0136	.0136	.0136	.0138	.0141
CN-IOL	1.55	0.	.0141	.0139	.0135	.0133	.0135	.0139	.0141
CN-IOL	1.55	2.	.0140	.0138	.0137	.0135	.0137	.0138	.0140
CN-IOL	1.55	4.	.0138	.0138	.0138	.0138	.0138	.0138	.0138
CN-IOL	1.55	6.	.0137	.0138	.0139	.0140	.0139	.0138	.0137
CN-ORB	1.55	-6.	.0131	.0132	.0132	.0133	.0132	.0132	.0131
CN-ORB	1.55	-4.	.0138	.0137	.0136	.0134	.0136	.0137	.0138
CN-ORB	1.55	-2.	.0141	.0138	.0136	.0134	.0136	.0138	.0141
CN-ORB	1.55	0.	.0143	.0140	.0136	.0133	.0136	.0140	.0143
CN-ORB	1.55	2.	.0140	.0137	.0135	.0133	.0135	.0137	.0140
CN-ORB	1.55	4.	.0137	.0135	.0134	.0132	.0134	.0135	.0137
CN-ORB	1.55	6.	.0134	.0133	.0132	.0132	.0132	.0133	.0134
CN-ET	1.55	-6.	.0000	.0000	.0000	.0000	.0000	.0000	.0000
CN-ET	1.55	-4.	.0000	.0000	.0000	.0000	.0000	.0000	.0000
CN-ET	1.55	-2.	.0000	.0000	.0000	.0000	.0000	.0000	.0000
CN-ET	1.55	0.	.0000	.0000	.0000	.0000	.0000	.0000	.0000
CN-ET	1.55	2.	.0000	.0000	.0000	.0000	.0000	.0000	.0000
CN-ET	1.55	4.	.0000	.0000	.0000	.0000	.0000	.0000	.0000
CN-ET	1.55	6.	.0000	.0000	.0000	.0000	.0000	.0000	.0000
CN-R	1.55	-6.	.0001	.0001	.0001	.0001	.0002	.0002	.0003
CN-R	1.55	-4.	.0001	.0001	.0001	.0001	.0001	.0000	-.0000
CN-R	1.55	-2.	-.0000	.0000	.0000	.0001	.0000	-.0000	-.0000
CN-R	1.55	0.	-.0002	-.0001	-.0001	-.0000	.0000	-.0000	-.0000
CN-R	1.55	2.	.0001	.0001	.0001	.0001	.0001	-.0000	-.0001
CN-R	1.55	4.	.0003	.0003	.0003	.0003	.0001	-.0000	-.0002
CN-R	1.55	6.	.0006	.0005	.0005	.0004	.0002	-.0000	-.0003
CN-L	1.55	-6.	.0003	.0002	.0002	.0001	.0001	.0001	.0001
CN-L	1.55	-4.	-.0000	.0000	.0001	.0001	.0001	.0001	.0001
CN-L	1.55	-2.	-.0000	-.0000	.0000	.0001	.0000	.0000	-.0000
CN-L	1.55	0.	-.0000	-.0000	.0000	-.0000	-.0001	-.0001	-.0002
CN-L	1.55	2.	-.0001	-.0000	.0001	.0001	.0001	.0001	.0001
CN-L	1.55	4.	-.0002	-.0000	.0001	.0003	.0003	.0003	.0003
CN-L	1.55	6.	-.0003	-.0000	.0002	.0004	.0005	.0005	.0006

Table 8-3. $M_\infty = 1.55$ $\delta_{e_{IO}} = 10/-2$

BASE PITCHING MOMENT COEFFICIENT % SSME POWER = 109%

ELEMENT		α	β = -6	-4	-2	0	2	4	6
CM-IOL	1.55	-6.	-.0063	-.0063	-.0063	-.0062	-.0063	-.0063	-.0063
CM-IOL	1.55	-4.	-.0067	-.0065	-.0064	-.0062	-.0064	-.0065	-.0067
CM-IOL	1.55	-2.	-.0067	-.0065	-.0064	-.0062	-.0064	-.0065	-.0067
CM-IOL	1.55	0.	-.0064	-.0063	-.0061	-.0060	-.0061	-.0063	-.0064
CM-IOL	1.55	2.	-.0065	-.0065	-.0064	-.0063	-.0064	-.0065	-.0065
CM-IOL	1.55	4.	-.0065	-.0066	-.0067	-.0068	-.0067	-.0066	-.0065
CM-IOL	1.55	6.	-.0065	-.0068	-.0070	-.0071	-.0070	-.0068	-.0065
CM-ORB	1.55	-6.	-.0058	-.0059	-.0059	-.0060	-.0059	-.0059	-.0058
CM-ORB	1.55	-4.	-.0063	-.0062	-.0061	-.0060	-.0061	-.0062	-.0063
CM-ORB	1.55	-2.	-.0065	-.0063	-.0062	-.0060	-.0062	-.0063	-.0065
CM-ORB	1.55	0.	-.0066	-.0064	-.0062	-.0060	-.0062	-.0064	-.0066
CM-ORB	1.55	2.	-.0064	-.0063	-.0062	-.0061	-.0062	-.0063	-.0064
CM-ORB	1.55	4.	-.0062	-.0062	-.0062	-.0062	-.0062	-.0062	-.0062
CM-ORB	1.55	6.	-.0060	-.0061	-.0062	-.0063	-.0062	-.0061	-.0060
CM-ET	1.55	-6.	.0000	.0000	.0000	.0000	.0000	.0000	.0000
CM-ET	1.55	-4.	.0000	.0000	.0000	.0000	.0000	.0000	.0000
CM-ET	1.55	-2.	.0000	.0000	.0000	.0000	.0000	.0000	.0000
CM-ET	1.55	0.	.0000	.0000	.0000	.0000	.0000	.0000	.0000
CM-ET	1.55	2.	.0000	.0000	.0000	.0000	.0000	.0000	.0000
CM-ET	1.55	4.	.0000	.0000	.0000	.0000	.0000	.0000	.0000
CM-ET	1.55	6.	.0000	.0000	.0000	.0000	.0000	.0000	.0000
CM-R	1.55	-6.	-.0002	-.0002	-.0002	-.0001	-.0002	-.0002	-.0003
CM-R	1.55	-4.	-.0003	-.0002	-.0002	-.0001	-.0001	-.0001	-.0001
CM-R	1.55	-2.	-.0001	-.0001	-.0001	-.0001	-.0001	-.0001	-.0001
CM-R	1.55	0.	.0002	.0001	.0001	.0000	-.0000	-.0000	.0000
CM-R	1.55	2.	-.0002	-.0002	-.0001	-.0001	-.0001	.0000	.0001
CM-R	1.55	4.	-.0005	-.0004	-.0004	-.0003	-.0001	.0000	.0002
CM-R	1.55	6.	-.0008	-.0007	-.0006	-.0004	-.0002	.0000	.0003
CM-L	1.55	-6.	-.0003	-.0002	-.0002	-.0001	-.0002	-.0002	-.0002
CM-L	1.55	-4.	-.0001	-.0001	-.0001	-.0001	-.0002	-.0002	-.0003
CM-L	1.55	-2.	-.0001	-.0001	-.0001	-.0001	-.0001	-.0001	-.0001
CM-L	1.55	0.	.0000	-.0000	-.0000	.0000	.0001	.0001	.0002
CM-L	1.55	2.	.0001	.0000	-.0001	-.0001	-.0001	-.0002	-.0002
CM-L	1.55	4.	.0002	.0000	-.0001	-.0003	-.0004	-.0004	-.0005
CM-L	1.55	6.	.0003	.0000	-.0002	-.0004	-.0006	-.0007	-.0008

Table 8-4. M_∞ = 1.80 $\delta_{e_{IO}}$ = 10/-5

BASE AXIAL FORCE COEFFICIENT % SSME POWER = 109%

ELEMENT		α	β -6	-4	-2	0	2	4	6
CA-IOL	1.80	-6.	.0467	.0438	.0411	.0383	.0411	.0438	.0467
CA-IOL	1.80	-4.	.0421	.0401	.0382	.0364	.0382	.0401	.0421
CA-IOL	1.80	-2.	.0408	.0391	.0372	.0355	.0372	.0391	.0408
CA-IOL	1.80	0.	.0396	.0380	.0361	.0346	.0361	.0380	.0396
CA-IOL	1.80	2.	.0396	.0378	.0361	.0344	.0361	.0378	.0396
CA-IOL	1.80	4.	.0394	.0378	.0361	.0345	.0361	.0378	.0394
CA-IOL	1.80	6.	.0394	.0376	.0360	.0346	.0360	.0376	.0394
CA-ORB	1.80	-6.	.0140	.0132	.0125	.0118	.0125	.0132	.0140
CA-ORB	1.80	-4.	.0140	.0134	.0128	.0122	.0128	.0134	.0140
CA-ORB	1.80	-2.	.0142	.0138	.0133	.0128	.0133	.0138	.0142
CA-ORB	1.80	0.	.0144	.0141	.0137	.0134	.0137	.0141	.0144
CA-ORB	1.80	2.	.0145	.0142	.0139	.0136	.0139	.0142	.0145
CA-ORB	1.80	4.	.0145	.0143	.0140	.0138	.0140	.0143	.0145
CA-ORB	1.80	6.	.0154	.0149	.0145	.0140	.0145	.0149	.0154
CA-ET	1.80	-6.	.0276	.0258	.0240	.0221	.0240	.0258	.0276
CA-ET	1.80	-4.	.0240	.0228	.0216	.0204	.0216	.0228	.0240
CA-ET	1.80	-2.	.0233	.0219	.0204	.0189	.0204	.0219	.0233
CA-ET	1.80	0.	.0227	.0210	.0192	.0174	.0192	.0210	.0227
CA-ET	1.80	2.	.0234	.0213	.0193	.0172	.0193	.0213	.0234
CA-ET	1.80	4.	.0240	.0217	.0194	.0171	.0194	.0217	.0240
CA-ET	1.80	6.	.0236	.0215	.0194	.0174	.0194	.0215	.0236
CA-K	1.80	-6.	.0051	.0041	.0032	.0022	.0014	.0007	.0000
CA-K	1.80	-4.	.0048	.0038	.0029	.0019	.0009	.0001	-.0007
CA-K	1.80	-2.	.0043	.0035	.0027	.0019	.0008	-.0001	-.0010
CA-K	1.80	0.	.0038	.0032	.0025	.0019	.0007	-.0003	-.0013
CA-K	1.80	2.	.0033	.0028	.0023	.0018	.0006	-.0005	-.0016
CA-K	1.80	4.	.0029	.0025	.0022	.0018	.0005	-.0007	-.0020
CA-K	1.80	6.	.0030	.0025	.0020	.0016	.0001	-.0013	-.0026
CA-L	1.80	-6.	.0000	.0007	.0014	.0022	.0032	.0041	.0051
CA-L	1.80	-4.	-.0007	.0001	.0009	.0019	.0029	.0038	.0048
CA-L	1.80	-2.	-.0010	-.0001	.0008	.0019	.0027	.0035	.0043
CA-L	1.80	0.	-.0013	-.0003	.0007	.0019	.0025	.0032	.0038
CA-L	1.80	2.	-.0016	-.0005	.0006	.0018	.0023	.0028	.0033
CA-L	1.80	4.	-.0020	-.0007	.0005	.0018	.0022	.0025	.0029
CA-L	1.80	6.	-.0026	-.0013	.0001	.0016	.0020	.0025	.0030

Table 8-5. $M_\infty = 1.80$ $\delta_{e_{IO}} = 10/-5$

BASE NORMAL FORCE COEFFICIENT % SSME POWER = 109%

ELEMENT		α	β = -6	-4	-2	0	2	4	6
C_N-IOL	1.80	-6.	.0104	.0102	.0099	.0097	.0099	.0102	.0104
CN-IOL	1.80	-4.	.0105	.0102	.0099	.0096	.0099	.0102	.0105
CN-IOL	1.80	-2.	.0108	.0104	.0101	.0098	.0101	.0104	.0108
CN-IOL	1.80	0.	.0110	.0106	.0102	.0097	.0102	.0106	.0110
CN-IOL	1.80	2.	.0110	.0107	.0104	.0101	.0104	.0107	.0110
CN-IOL	1.80	4.	.0110	.0108	.0105	.0105	.0105	.0108	.0110
CN-IOL	1.80	6.	.0115	.0114	.0112	.0112	.0112	.0114	.0115
CN-ORB	1.80	-6.	.0106	.0101	.0096	.0091	.0096	.0101	.0106
CN-ORB	1.80	-4.	.0109	.0103	.0098	.0092	.0098	.0103	.0109
CN-ORB	1.80	-2.	.0111	.0106	.0101	.0096	.0101	.0106	.0111
CN-ORB	1.80	0.	.0112	.0108	.0103	.0099	.0103	.0108	.0112
CN-ORB	1.80	2.	.0110	.0107	.0104	.0101	.0104	.0107	.0110
CN-ORB	1.80	4.	.0108	.0106	.0104	.0103	.0104	.0106	.0108
CN-ORB	1.80	6.	.0113	.0111	.0108	.0106	.0108	.0111	.0113
CN-ET	1.80	-6.	.0000	.0000	.0000	.0000	.0000	.0000	.0000
CN-ET	1.80	-4.	.0000	.0000	.0000	.0000	.0000	.0000	.0000
CN-ET	1.80	-2.	.0000	.0000	.0000	.0000	.0000	.0000	.0000
CN-ET	1.80	0.	.0000	.0000	.0000	.0000	.0000	.0000	.0000
CN-ET	1.80	2.	.0000	.0000	.0000	.0000	.0000	.0000	.0000
CN-ET	1.80	4.	.0000	.0000	.0000	.0000	.0000	.0000	.0000
CN-ET	1.80	6.	.0000	.0000	.0000	.0000	.0000	.0000	.0000
CN-R	1.80	-6.	-.0005	-.0002	.0000	.0003	.0003	.0003	.0003
CN-R	1.80	-4.	-.0004	-.0002	-.0000	.0002	.0001	.0001	.0000
CN-R	1.80	-2.	-.0003	-.0002	-.0001	.0001	.0001	.0000	.0000
CN-R	1.80	0.	-.0002	-.0002	-.0001	-.0001	-.0000	-.0000	.0000
CN-R	1.80	2.	-.0000	-.0000	-.0000	-.0000	-.0000	-.0000	.0000
CN-R	1.80	4.	.0002	.0002	.0001	.0001	.0000	.0000	-.0000
CN-R	1.80	6.	.0002	.0002	.0002	.0003	.0002	.0001	.0000
CN-L	1.80	-6.	.0003	.0003	.0003	.0003	.0000	-.0002	-.0005
CN-L	1.80	-4.	.0000	.0001	.0001	.0002	-.0000	-.0002	-.0004
CN-L	1.80	-2.	.0000	.0000	.0001	.0001	-.0001	-.0002	-.0003
CN-L	1.80	0.	.0000	-.0000	-.0000	-.0001	-.0001	-.0002	-.0002
CN-L	1.80	2.	.0000	-.0000	-.0000	-.0000	-.0000	-.0000	-.0000
CN-L	1.80	4.	-.0000	.0000	.0000	.0001	.0001	.0002	.0002
CN-L	1.80	6.	.0000	.0001	.0002	.0003	.0002	.0002	.0002

Table 8-6. $M_\infty = 1.80$ $\delta_{e_{IO}} = 10/-5$

BASE PITCHING MOMENT COEFFICIENT % SSME POWER = 109%

ELEMENT		α	β = -6	-4	-2	0	2	4	6
CM-IOL	1.80	-6.	-.0050	-.0050	-.0050	-.0050	-.0050	-.0050	-.0050
CM-IOL	1.80	-4.	-.0049	-.0049	-.0049	-.0049	-.0049	-.0049	-.0049
CM-IOL	1.80	-2.	-.0050	-.0049	-.0049	-.0047	-.0049	-.0049	-.0050
CM-IOL	1.80	0.	-.0051	-.0049	-.0047	-.0045	-.0047	-.0049	-.0051
CM-IOL	1.80	2.	-.0050	-.0049	-.0049	-.0048	-.0049	-.0049	-.0050
CM-IOL	1.80	4.	-.0050	-.0050	-.0049	-.0050	-.0049	-.0050	-.0050
CM-IOL	1.80	6.	-.0053	-.0054	-.0054	-.0056	-.0054	-.0054	-.0053
CM-ORB	1.80	-6.	-.0052	-.0049	-.0047	-.0044	-.0047	-.0049	-.0052
CM-ORB	1.80	-4.	-.0053	-.0050	-.0047	-.0043	-.0047	-.0050	-.0053
CM-ORB	1.80	-2.	-.0054	-.0051	-.0048	-.0045	-.0048	-.0051	-.0054
CM-ORB	1.80	0.	-.0054	-.0052	-.0049	-.0047	-.0049	-.0052	-.0054
CM-ORB	1.80	2.	-.0051	-.0050	-.0049	-.0048	-.0049	-.0050	-.0051
CM-ORB	1.80	4.	-.0048	-.0048	-.0048	-.0048	-.0048	-.0048	-.0048
CM-ORB	1.80	6.	-.0051	-.0051	-.0050	-.0050	-.0050	-.0051	-.0051
CM-ET	1.80	-6.	.0000	.0000	.0000	.0000	.0000	.0000	.0000
CM-ET	1.80	-4.	.0000	.0000	.0000	.0000	.0000	.0000	.0000
CM-ET	1.80	-2.	.0000	.0000	.0000	.0000	.0000	.0000	.0000
CM-ET	1.80	0.	.0000	.0000	.0000	.0000	.0000	.0000	.0000
CM-ET	1.80	2.	.0000	.0000	.0000	.0000	.0000	.0000	.0000
CM-ET	1.80	4.	.0000	.0000	.0000	.0000	.0000	.0000	.0000
CM-ET	1.80	6.	.0000	.0000	.0000	.0000	.0000	.0000	.0000
CM-R	1.80	-6.	.0006	.0003	.0000	-.0003	-.0003	-.0004	-.0004
CM-R	1.80	-4.	.0004	.0002	-.0000	-.0003	-.0002	-.0001	.0000
CM-R	1.80	-2.	.0003	.0002	.0000	-.0001	-.0001	.0000	.0001
CM-R	1.80	0.	.0002	.0002	.0001	.0001	.0001	.0001	.0001
CM-R	1.80	2.	.0000	.0000	.0000	.0000	.0000	.0001	.0001
CM-R	1.80	4.	-.0002	-.0002	-.0001	-.0001	-.0000	.0000	.0000
CM-R	1.80	6.	-.0002	-.0002	-.0002	-.0003	-.0002	-.0001	-.0000
CM-L	1.80	-6.	-.0004	-.0004	-.0003	-.0003	.0000	.0003	.0006
CM-L	1.80	-4.	.0000	-.0001	-.0002	-.0003	-.0000	.0002	.0004
CM-L	1.80	-2.	.0001	.0000	-.0001	-.0001	.0000	.0002	.0003
CM-L	1.80	0.	.0001	.0001	.0001	.0001	.0001	.0002	.0002
CM-L	1.80	2.	.0001	.0001	.0000	.0000	.0000	.0000	.0000
CM-L	1.80	4.	.0000	.0000	-.0000	-.0001	-.0001	-.0002	-.0002
CM-L	1.80	6.	-.0000	-.0001	-.0002	-.0003	-.0002	-.0002	-.0002

Table 8-7. $M_\infty = 2.20$ $\delta_{e_{IO}} = 4/-5$

BASE AXIAL FORCE COEFFICIENT % SSME POWER = 109%

ELEMENT		α	β = -6	-4	-2	0	2	4	6
CA-IOL	2.20	-6.	.0224	.0198	.0174	.0149	.0174	.0198	.0224
CA-IOL	2.20	-4.	.0200	.0179	.0157	.0138	.0157	.0179	.0200
CA-IOL	2.20	-2.	.0186	.0171	.0156	.0142	.0156	.0171	.0186
CA-IOL	2.20	0.	.0169	.0165	.0160	.0158	.0160	.0165	.0169
CA-IOL	2.20	2.	.0158	.0157	.0156	.0152	.0156	.0157	.0158
CA-IOL	2.20	4.	.0153	.0148	.0145	.0142	.0145	.0148	.0153
CA-IOL	2.20	6.	.0157	.0144	.0133	.0122	.0133	.0144	.0157
CA-ORB	2.20	-6.	.0083	.0067	.0051	.0035	.0051	.0067	.0083
CA-ORB	2.20	-4.	.0088	.0074	.0059	.0045	.0059	.0074	.0088
CA-ORB	2.20	-2.	.0086	.0078	.0070	.0062	.0070	.0078	.0086
CA-ORB	2.20	0.	.0083	.0083	.0083	.0083	.0083	.0083	.0083
CA-ORB	2.20	2.	.0080	.0083	.0086	.0088	.0086	.0083	.0080
CA-ORB	2.20	4.	.0079	.0081	.0084	.0086	.0084	.0081	.0079
CA-ORB	2.20	6.	.0076	.0078	.0079	.0079	.0079	.0078	.0078
CA-ET	2.20	-6.	.0115	.0114	.0113	.0112	.0113	.0114	.0115
CA-ET	2.20	-4.	.0089	.0090	.0091	.0093	.0091	.0090	.0089
CA-ET	2.20	-2.	.0084	.0083	.0083	.0082	.0083	.0083	.0084
CA-ET	2.20	0.	.0080	.0079	.0078	.0077	.0078	.0079	.0080
CA-ET	2.20	2.	.0079	.0075	.0071	.0066	.0071	.0075	.0079
CA-ET	2.20	4.	.0080	.0071	.0062	.0054	.0062	.0071	.0080
CA-ET	2.20	6.	.0088	.0075	.0062	.0049	.0062	.0075	.0088
CA-R	2.20	-6.	.0036	.0024	.0013	.0001	-.0003	-.0007	-.0010
CA-R	2.20	-4.	.0039	.0026	.0013	.0000	-.0006	-.0011	-.0016
CA-R	2.20	-2.	.0030	.0020	.0009	-.0001	-.0006	-.0010	-.0014
CA-R	2.20	0.	.0019	.0012	.0005	-.0001	-.0006	-.0009	-.0013
CA-R	2.20	2.	.0013	.0009	.0004	-.0001	-.0005	-.0010	-.0014
CA-R	2.20	4.	.0010	.0007	.0004	.0001	-.0005	-.0011	-.0016
CA-R	2.20	6.	.0013	.0007	.0002	-.0003	-.0010	-.0016	-.0022
CA-L	2.20	-6.	-.0010	-.0007	-.0003	.0001	.0013	.0024	.0036
CA-L	2.20	-4.	-.0016	-.0011	-.0006	.0000	.0013	.0026	.0039
CA-L	2.20	-2.	-.0014	-.0010	-.0006	-.0001	.0009	.0020	.0030
CA-L	2.20	0.	-.0013	-.0009	-.0006	-.0001	.0005	.0012	.0019
CA-L	2.20	2.	-.0014	-.0010	-.0005	-.0001	.0004	.0009	.0013
CA-L	2.20	4.	-.0016	-.0011	-.0005	.0001	.0004	.0007	.0010
CA-L	2.20	6.	-.0022	-.0016	-.0010	-.0003	.0002	.0007	.0013

Table 8-8. $M_\infty = 2.20$ $\delta_{e_{IO}} = 4/-5$

BASE NORMAL FORCE COEFFICIENT % SSME POWER = 109%

ELEMENT		α	β -6	-4	-2	0	2	4	6
CN-IOL	2.20	-6.	.0071	.0065	.0060	.0055	.0060	.0065	.0071
CN-IOL	2.20	-4.	.0073	.0068	.0064	.0060	.0064	.0068	.0073
CN-IOL	2.20	-2.	.0073	.0071	.0068	.0065	.0068	.0071	.0073
CN-IOL	2.20	0.	.0073	.0073	.0073	.0071	.0073	.0073	.0073
CN-IOL	2.20	2.	.0073	.0074	.0074	.0075	.0074	.0074	.0073
CN-IOL	2.20	4.	.0073	.0075	.0076	.0078	.0076	.0075	.0073
CN-IOL	2.20	6.	.0072	.0074	.0074	.0076	.0074	.0074	.0072
CN-ORB	2.20	-6.	.0068	.0061	.0054	.0047	.0054	.0061	.0068
CN-ORB	2.20	-4.	.0077	.0069	.0061	.0054	.0061	.0069	.0077
CN-ORB	2.20	-2.	.0076	.0071	.0066	.0061	.0066	.0071	.0076
CN-ORB	2.20	0.	.0074	.0073	.0071	.0069	.0071	.0073	.0074
CN-ORB	2.20	2.	.0075	.0074	.0073	.0073	.0073	.0074	.0075
CN-ORB	2.20	4.	.0076	.0076	.0075	.0074	.0075	.0076	.0076
CN-ORB	2.20	6.	.0076	.0075	.0073	.0072	.0073	.0075	.0076
CN-ET	2.20	-6.	.0000	.0000	.0000	.0000	.0000	.0000	.0000
CN-ET	2.20	-4.	.0000	.0000	.0000	.0000	.0000	.0000	.0000
CN-ET	2.20	-2.	.0000	.0000	.0000	.0000	.0000	.0000	.0000
CN-ET	2.20	0.	.0000	.0000	.0000	.0000	.0000	.0000	.0000
CN-ET	2.20	2.	.0000	.0000	.0000	.0000	.0000	.0000	.0000
CN-ET	2.20	2.	.0000	.0000	.0000	.0000	.0000	.0000	.0000
CN-ET	2.20	4.	.0000	.0000	.0000	.0000	.0000	.0000	.0000
CN-ET	2.20	6.	.0000	.0000	.0000	.0000	.0000	.0000	.0000
CN-R	2.20	-6.	-.0002	.0000	.0002	.0004	.0004	.0004	.0005
CN-R	2.20	-4.	-.0004	-.0002	.0001	.0003	.0002	.0001	.0000
CN-R	2.20	-2.	-.0003	-.0001	.0001	.0002	.0001	.0001	-.0000
CN-R	2.20	0.	-.0001	-.0000	.0001	.0001	.0001	.0000	-.0000
CN-R	2.20	2.	-.0001	.0000	.0001	.0001	.0000	-.0000	-.0001
CN-R	2.20	4.	-.0001	.0000	.0001	.0002	.0000	-.0001	-.0002
CN-R	2.20	6.	-.0000	.0001	.0001	.0002	.0000	-.0002	-.0004
CN-L	2.20	-6.	.0005	.0004	.0004	.0004	.0002	.0000	-.0002
CN-L	2.20	-4.	.0000	.0001	.0002	.0003	.0001	-.0002	-.0004
CN-L	2.20	-2.	-.0000	.0001	.0001	.0002	.0001	-.0001	-.0003
CN-L	2.20	0.	-.0000	.0000	.0001	.0001	.0001	-.0000	-.0001
CN-L	2.20	2.	-.0001	-.0000	.0000	.0001	.0001	.0000	-.0001
CN-L	2.20	4.	-.0002	-.0001	.0000	.0002	.0001	.0000	-.0001

Table 8-9. M_∞ = 2.20 $\delta_{e_{IO}}$ = 4/-5

% SSME POWER = 109%

BASE PITCHING MOMENT COEFFICIENT

ELEMENT		α	β = -6	-4	-2	0	2	4	6
CM-IOL	2.20	-6.	-.0037	-.0035	-.0034	-.0034	-.0034	-.0035	-.0037
CM-IOL	2.20	-4.	-.0037	-.0036	-.0037	-.0036	-.0037	-.0036	-.0037
CM-IOL	2.20	-2.	-.0037	-.0037	-.0037	-.0036	-.0037	-.0037	-.0037
CM-IOL	2.20	0.	-.0036	-.0036	-.0037	-.0035	-.0037	-.0036	-.0036
CM-IOL	2.20	2.	-.0036	-.0037	-.0037	-.0037	-.0037	-.0037	-.0036
CM-IOL	2.20	4.	-.0036	-.0038	-.0039	-.0041	-.0039	-.0038	-.0036
CM-IOL	2.20	6.	-.0035	-.0037	-.0039	-.0041	-.0039	-.0037	-.0035
CM-ORB	2.20	-6.	-.0034	-.0031	-.0028	-.0026	-.0028	-.0031	-.0034
CM-ORB	2.20	-4.	-.0042	-.0037	-.0033	-.0028	-.0033	-.0037	-.0042
CM-ORB	2.20	-2.	-.0041	-.0037	-.0034	-.0030	-.0034	-.0037	-.0041
CM-ORB	2.20	0.	-.0038	-.0036	-.0035	-.0033	-.0035	-.0036	-.0038
CM-ORB	2.20	2.	-.0038	-.0037	-.0036	-.0035	-.0036	-.0037	-.0038
CM-ORB	2.20	4.	-.0039	-.0039	-.0038	-.0037	-.0038	-.0039	-.0039
CM-ORB	2.20	6.	-.0039	-.0038	-.0038	-.0037	-.0038	-.0038	-.0039
CM-ET	2.20	-6.	.0000	.0000	.0000	.0000	.0000	.0000	.0000
CM-ET	2.20	-4.	.0000	.0000	.0000	.0000	.0000	.0000	.0000
CM-ET	2.20	-2.	.0000	.0000	.0000	.0000	.0000	.0000	.0000
CM-ET	2.20	0.	.0000	.0000	.0000	.0000	.0000	.0000	.0000
CM-ET	2.20	2.	.0000	.0000	.0000	.0000	.0000	.0000	.0000
CM-ET	2.20	4.	.0000	.0000	.0000	.0000	.0000	.0000	.0000
CM-ET	2.20	6.	.0000	.0000	.0000	.0000	.0000	.0000	.0000
CM-R	2.20	-6.	.0002	-.0000	-.0002	-.0004	-.0004	-.0004	-.0005
CM-R	2.20	-4.	.0005	.0002	-.0001	-.0004	-.0003	-.0001	-.0000
CM-R	2.20	-2.	.0003	.0001	-.0001	-.0003	-.0002	-.0001	.0001
CM-R	2.20	0.	.0001	.0000	-.0001	-.0001	-.0001	-.0000	.0001
CM-R	2.20	2.	.0001	-.0000	-.0001	-.0001	-.0000	.0000	.0001
CM-R	2.20	4.	.0001	-.0000	-.0001	-.0002	-.0000	.0001	.0002
CM-R	2.20	6.	.0000	-.0001	-.0001	-.0002	-.0000	.0002	.0004
CM-L	2.20	-6.	-.0005	-.0004	-.0004	-.0004	-.0002	-.0000	.0002
CM-L	2.20	-4.	-.0000	-.0001	-.0003	-.0004	-.0001	.0002	.0005
CM-L	2.20	-2.	.0001	-.0001	-.0002	-.0003	-.0001	.0001	.0003
CM-L	2.20	0.	.0001	-.0000	-.0001	-.0001	-.0001	.0000	.0001
CM-L	2.20	2.	.0001	.0000	-.0000	-.0001	-.0001	-.0000	.0001
CM-L	2.20	4.	.0002	.0001	-.0000	-.0002	-.0001	-.0000	.0001
CM-L	2.20	6.	.0004	.0002	-.0000	-.0002	-.0001	-.0001	.0000

Table 8-10. $M_\infty = 2.50$ $\delta_{e_{IO}} = 0/-2$

BASE AXIAL FORCE COEFFICIENT % SSME POWER = 109%

ELEMENT		α	β -6	-4	-2	0	2	4	6
CA-IOL	2.49	-6.	.0086	.0063	.0043	.0021	.0043	.0063	.0086
CA-IOL	2.49	-4.	.0045	.0032	.0018	.0007	.0018	.0032	.0045
CA-IOL	2.49	-2.	.0037	.0031	.0025	.0017	.0025	.0031	.0037
CA-IOL	2.49	0.	.0031	.0029	.0026	.0024	.0026	.0029	.0031
CA-IOL	2.49	2.	.0009	.0009	.0009	.0010	.0009	.0009	.0009
CA-IOL	2.49	4.	-.0012	-.0011	-.0008	-.0007	-.0008	-.0011	-.0012
CA-IOL	2.49	6.	-.0024	-.0028	-.0033	-.0035	-.0033	-.0028	-.0024
CA-ORB	2.49	-6.	.0085	.0073	.0061	.0049	.0061	.0073	.0085
CA-ORB	2.49	-4.	.0062	.0058	.0053	.0049	.0053	.0058	.0062
CA-ORB	2.49	-2.	.0060	.0058	.0056	.0053	.0056	.0058	.0060
CA-ORB	2.49	0.	.0059	.0058	.0057	.0056	.0057	.0058	.0059
CA-ORB	2.49	2.	.0057	.0055	.0053	.0052	.0053	.0055	.0057
CA-ORB	2.49	4.	.0053	.0051	.0050	.0048	.0050	.0051	.0053
CA-ORB	2.49	6.	.0044	.0046	.0047	.0049	.0047	.0046	.0044
CA-ET	2.49	-6.	.0002	-.0003	-.0007	-.0012	-.0007	-.0003	.0002
CA-ET	2.49	-4.	-.0013	-.0015	-.0018	-.0020	-.0018	-.0015	-.0013
CA-ET	2.49	-2.	-.0013	-.0011	-.0009	-.0008	-.0009	-.0011	-.0013
CA-ET	2.49	0.	-.0013	-.0008	-.0003	.0002	-.0003	-.0008	-.0013
CA-ET	2.49	2.	-.0040	-.0026	-.0012	.0002	-.0012	-.0026	-.0040
CA-ET	2.49	4.	-.0060	-.0042	-.0023	-.0005	-.0023	-.0042	-.0060
CA-ET	2.49	6.	-.0057	-.0051	-.0045	-.0038	-.0045	-.0051	-.0057
CA-R	2.49	-6.	.0015	.0007	-.0000	-.0008	-.0011	-.0014	-.0016
CA-R	2.49	-4.	.0016	.0007	-.0002	-.0011	-.0015	-.0018	-.0020
CA-R	2.49	-2.	.0011	.0003	-.0005	-.0014	-.0017	-.0019	-.0021
CA-R	2.49	0.	.0007	-.0001	-.0009	-.0017	-.0019	-.0020	-.0022
CA-R	2.49	2.	.0008	-.0002	-.0012	-.0022	-.0020	-.0018	-.0016
CA-R	2.49	4.	.0008	-.0003	-.0014	-.0025	-.0021	-.0017	-.0013
CA-R	2.49	6.	.0010	-.0001	-.0012	-.0023	-.0023	-.0022	-.0021
CA-L	2.49	-6.	-.0016	-.0014	-.0011	-.0008	-.0000	.0007	.0015
CA-L	2.49	-4.	-.0020	-.0018	-.0015	-.0011	-.0002	.0007	.0016
CA-L	2.49	-2.	-.0021	-.0019	-.0017	-.0014	-.0005	.0003	.0011
CA-L	2.49	0.	-.0022	-.0020	-.0019	-.0017	-.0009	-.0001	.0007
CA-L	2.49	2.	-.0016	-.0018	-.0020	-.0022	-.0012	-.0002	.0008
CA-L	2.49	4.	-.0013	-.0017	-.0021	-.0025	-.0014	-.0003	.0008
CA-L	2.49	6.	-.0021	-.0022	-.0023	-.0023	-.0012	-.0001	.0010

Table 8-11. $M_\infty = 2.50$ $\delta_{e_{IO}} = 0/-2$

BASE NORMAL FORCE COEFFICIENT % SSME POWER = 109%

ELEMENT		α	β -6	-4	-2	0	2	4	6
CN-IOL	2.49	-6.	.0064	.0058	.0053	.0049	.0053	.0058	.0064
CN-IOL	2.49	-4.	.0055	.0052	.0049	.0048	.0049	.0052	.0055
CN-IOL	2.49	-2.	.0052	.0051	.0050	.0050	.0050	.0051	.0052
CN-IOL	2.49	0.	.0049	.0050	.0051	.0052	.0051	.0050	.0049
CN-IOL	2.49	2.	.0051	.0052	.0051	.0052	.0051	.0052	.0051
CN-IOL	2.49	4.	.0052	.0052	.0051	.0051	.0051	.0052	.0052
CN-IOL	2.49	6.	.0049	.0050	.0050	.0051	.0050	.0050	.0049
CN-ORB	2.49	-6.	.0056	.0051	.0047	.0043	.0047	.0051	.0056
CN-ORB	2.49	-4.	.0050	.0048	.0046	.0044	.0046	.0048	.0050
CN-ORB	2.49	-2.	.0049	.0049	.0049	.0050	.0049	.0049	.0049
CN-ORB	2.49	0.	.0048	.0050	.0052	.0054	.0052	.0050	.0048
CN-ORB	2.49	2.	.0051	.0052	.0052	.0052	.0052	.0052	.0051
CN-ORB	2.49	4.	.0054	.0053	.0052	.0051	.0052	.0053	.0054
CN-ORB	2.49	6.	.0052	.0052	.0051	.0051	.0051	.0052	.0052
CN-ET	2.50	-6.	.0000	.0000	.0000	.0000	.0000	.0000	.0000
CN-ET	2.50	-4.	.0000	.0000	.0000	.0000	.0000	.0000	.0000
CN-ET	2.50	-2.	.0000	.0000	.0000	.0000	.0000	.0000	.0000
CN-ET	2.50	0.	.0000	.0000	.0000	.0000	.0000	.0000	.0000
CN-ET	2.50	2.	.0000	.0000	.0000	.0000	.0000	.0000	.0000
CN-ET	2.50	4.	.0000	.0000	.0000	.0000	.0000	.0000	.0000
CN-ET	2.50	6.	.0000	.0000	.0000	.0000	.0000	.0000	.0000
CN-R	2.49	-6.	.0003	.0003	.0003	.0003	.0003	.0004	.0005
CN-R	2.49	-4.	.0004	.0003	.0002	.0002	.0001	.0001	.0001
CN-R	2.49	-2.	.0003	.0002	.0001	.0000	.0000	-.0000	-.0000
CN-R	2.49	0.	.0002	.0001	.0000	-.0001	-.0001	-.0001	-.0001
CN-R	2.49	2.	.0001	.0001	.0000	-.0000	-.0001	-.0001	-.0001
CN-R	2.49	4.	.0000	.0000	.0000	.0000	-.0001	-.0001	-.0002
CN-R	2.49	6.	.0000	.0000	.0000	.0000	-.0001	-.0002	-.0003
CN-L	2.49	-6.	.0005	.0004	.0003	.0003	.0003	.0003	.0003
CN-L	2.49	-4.	.0001	.0001	.0001	.0002	.0002	.0003	.0004
CN-L	2.49	-2.	-.0000	-.0000	.0000	.0000	.0001	.0002	.0003
CN-L	2.49	0.	-.0001	-.0001	-.0001	-.0001	.0000	.0001	.0002
CN-L	2.49	2.	-.0001	-.0001	-.0001	-.0000	.0000	.0001	.0001
CN-L	2.49	4.	-.0002	-.0001	-.0001	.0000	.0000	.0000	.0000
CN-L	2.49	6.	-.0003	-.0002	-.0001	.0000	.0000	.0000	.0000

Table 8-12. M_∞ = 2.50 $\delta_{e_{IO}}$ = 0/-2

BASE PITCHING MOMENT COEFFICIENT % SSME POWER = 109%

ELEMENT		α	β -6	-4	-2	0	2	4	6
CM-IOL	2.49	-6.	-.0031	-.0029	-.0027	-.0027	-.0027	-.0029	-.0031
CM-IOL	2.49	-4.	-.0029	-.0027	-.0025	-.0025	-.0025	-.0027	-.0029
CM-IOL	2.49	-2.	-.0024	-.0025	-.0025	-.0025	-.0025	-.0025	-.0024
CM-IOL	2.49	0.	-.0021	-.0023	-.0025	-.0027	-.0025	-.0023	-.0021
CM-IOL	2.49	2.	-.0023	-.0024	-.0026	-.0028	-.0026	-.0024	-.0023
CM-IOL	2.49	4.	-.0025	-.0026	-.0027	-.0029	-.0027	-.0026	-.0025
CM-IOL	2.49	6.	-.0026	-.0026	-.0027	-.0027	-.0027	-.0026	-.0026
CM-ORB	2.49	-6.	-.0021	-.0021	-.0021	-.0021	-.0021	-.0021	-.0021
CM-ORB	2.49	-4.	-.0024	-.0023	-.0022	-.0021	-.0022	-.0023	-.0024
CM-ORB	2.49	-2.	-.0021	-.0023	-.0024	-.0025	-.0024	-.0023	-.0021
CM-ORB	2.49	0.	-.0020	-.0023	-.0026	-.0029	-.0026	-.0023	-.0020
CM-ORB	2.49	2.	-.0024	-.0025	-.0026	-.0028	-.0026	-.0025	-.0024
CM-ORB	2.49	4.	-.0027	-.0027	-.0027	-.0027	-.0027	-.0027	-.0027
CM-ORB	2.49	6.	-.0029	-.0028	-.0028	-.0027	-.0028	-.0028	-.0029
CM-ET	2.50	-6.	.0000	.0000	.0000	.0000	.0000	.0000	.0000
CM-ET	2.50	-4.	.0000	.0000	.0000	.0000	.0000	.0000	.0000
CM-ET	2.50	-2.	.0000	.0000	.0000	.0000	.0000	.0000	.0000
CM-ET	2.50	0.	.0000	.0000	.0000	.0000	.0000	.0000	.0000
CM-ET	2.50	2.	.0000	.0000	.0000	.0000	.0000	.0000	.0000
CM-ET	2.50	4.	.0000	.0000	.0000	.0000	.0000	.0000	.0000
CM-ET	2.50	6.	.0000	.0000	.0000	.0000	.0000	.0000	.0000
CM-R	2.49	-6.	-.0005	-.0004	-.0003	-.0003	-.0003	-.0004	-.0005
CM-R	2.49	-4.	-.0004	-.0003	-.0002	-.0002	-.0001	-.0001	-.0001
CM-R	2.49	-2.	-.0003	-.0002	-.0001	-.0000	-.0000	.0000	.0000
CM-R	2.49	0.	-.0002	-.0001	-.0000	.0001	.0001	.0001	.0001
CM-R	2.49	2.	-.0001	-.0000	-.0000	-.0000	.0000	.0001	.0002
CM-R	2.49	4.	.0000	.0000	-.0000	-.0001	.0000	.0001	.0002
CM-R	2.49	6.	-.0000	-.0000	.0000	.0000	.0001	.0002	.0003
CM-L	2.49	-6.	-.0005	-.0004	-.0003	-.0003	-.0003	-.0004	-.0005
CM-L	2.49	-4.	-.0001	-.0001	-.0001	-.0002	-.0002	-.0003	-.0004
CM-L	2.49	-2.	.0000	.0000	-.0000	-.0000	-.0001	-.0002	-.0003
CM-L	2.49	0.	.0001	.0001	.0001	.0001	-.0000	-.0001	-.0002
CM-L	2.49	2.	.0002	.0001	.0000	-.0000	-.0000	-.0000	-.0001
CM-L	2.49	4.	.0002	.0001	.0000	-.0001	-.0000	.0000	.0000
CM-L	2.49	6.	.0003	.0002	.0001	.0000	.0000	-.0000	-.0000

Table 8-13

BASE COEFFICIENT PARTIALS

$\partial C_{X\bar{i}} / \partial \delta_{EI}$

	MACH	SSLV	ORB	ET
C_A	1.55	0	0	0
	1.80	0	0	0
	2.20	0	0	0
	2.50	0	0	0
C_N	1.55	.000075	.000075	0
	1.80	.00004	.00004	0
	2.20	-.00003	-.00003	0
	2.50	-.00008	-.00008	0
C_M	1.55	-.000075	-.000075	0
	1.80	-.00004	-.00004	0
	2.20	.00003	.00003	0
	2.50	.00008	.00008	0

Table 8-14

BASE AXIAL FORCE (LBS)

ALTITUDE (ft)	TOTAL	NOMINAL % SSME POWER LEVEL	ALTITUDE (ft)	TOTAL	NOMINAL % SSME POWER LEVEL
0	0	109	52500	41999	109
4000	41295	109	55000	34543	
6000	112146	109	57500	27620	
8000	148363	109	60000	21255	
10000	162595	107	62500	15582	
12000	178724	101	65000	10328	
14000	193983	95	67500	5494	
16000	209734	88.4	70000	1500	
18000	226100		72500	3000	
19000	240776		75000	-7416	
20000	257649		77500	-9434	
21000	309484		80000	-10837	
22000	341482		85000	-12161	
23000	354185		90000	-12341	
24000	357716		95000	-12191	
25000	338036		100000	-11700	
26000	294479		110000	-10812	
28000	256747		120000	-9258	
30000	230650	88.4	130000	-7641	
34000	193188	93	140000	-7074	
38000	157365	105	145000	-6554	
40000	118714	109	160000	-6334	109
42500	95425				
45000	77572				
47500	62104				
50000	50952	109			

Table 8-15
BASE NORMAL FORCE (LBS)

ALTITUDE (ft)	TOTAL	NOMINAL % SSME POWER LEVEL	ALTITUDE (ft)	TOTAL	NOMINAL % SSME POWER LEVEL
0	0	109	47500	16702	109
4000	14100	109	50000	15285	
6000	18900	109	52500	13946	
8000	22200	109	55000	12578	
10000	24966	107	57500	11347	
12000	26867	101	60000	10061	
14000	28381	95	62500	8943	
16000	30163	88.4	65000	7875	
18000	32278		67500	6716	
19000	33678		70000	5597	
20000	36009		72500	3060	
21000	41054		75000	1175	
22000	48096		77500	742	
23000	50853		80000	391	
24000	51688		85000	-193	
25000	50621		90000	-565	
26000	45343		95000	-791	
28000	40842		100000	-1023	
30000	39239	88.4	110000	-1221	
34000	35678	93	120000	-1380	
38000	28850	105	130000	-1384	
40000	25785	109	140000	-1451	
42500	22034	109	150000	-1500	
45000	19136	109	160000	-1400	109

Table 8-16

BASE PITCHING MOMENT (FT. LBS)

ALTITUDE (ft)	PITCHING MOMENT (ft-lbs)	NOMINAL % SSME POWER LEVEL	ALTITUDE (ft)	PITCHING MOMENT (ft-lbs)	NOMINAL % SSME POWER LEVEL
0	0	109	47500	-842655	109
4000	- 929754	109	50000	-768558	
6000	-1246266	109	52500	-706430	
8000	-1287600	109	55000	-649350	
10000	-1296826	107	57500	-598665	
12000	-1374159	101	60000	-542188	
14000	-1441528	95	62500	-487760	
16000	-1484908	88.4	65000	-433056	
18000	-1535100		67500	-376544	
19000	-1589046		70000	-320178	
20000	-1701877		72500	-160000	
21000	-1937440		75000	-80000	
22000	-2206003		77500	-60000	
23000	-2218121		80000	-39080	
24000	-2187319		85000	-4825	
25000	-2101904		90000	14130	
26000	-1942585		95000	41395	
28000	-1785366		100000	55800	
30000	-1713072	88.4	110000	72303	
34000	-1515453	93	120000	82300	
38000	-1202968	105	130000	84635	
40000	-1163120	109	140000	88920	
42500	-1091025	109	150000	95000	
45000	-987022	109	160000	95000	109

Table 8-17

BASE AXIAL FORCE PARTIALS

ALTITUDE (ft)	$\partial AF/\partial \alpha$ (LB/DEG)	$\partial AF/\partial \delta_{EI}$ (LB/DEG)	$\partial AF/\partial$% SSME POWER (LB/%)
10000	-1331.0	2623.0	73.0
12000	-1361.0	2959.0	71.0
14000	-1536.0	3255.0	62.0
16000	-1823.0	3665.0	43.0
18000	-2454.0	5653.0	26.0
19000	-2667.0	6400.0	23.0
20000	-2716.0	7761.0	31.0
21000	-2021.0	8842.0	107.0
22000	-705.0	9138.0	138.0
23000	1040.0	9098.0	159.0
24000	2461.0	8533.0	167.0
25000	3148.0	6959.0	169.0
26000	2911.0	4350.0	167.0
28000	1627.0	1864.0	142.0
30000	514.0	171.0	158.0
34000	-583.0	87.0	96.0
38000	-1014.0	21.0	-112.0
40000	-1014.0	0	N.A.
42500	-1011.0	↓	↓
45000	-978.0		
47500	-893.0		
50000	-882.0		
52500	-738.0		
55000	-666.0		
57500	-597.0		
60000	-510.0		
62500	-461.0		
65000	-413.0		
67500	-358.0		
70000	-335.0	0	N.A.

Table 8-18

NORMAL FORCE PARTIALS

ALTITUDE (ft)	$\partial NF/\partial \alpha$ (LB/DEG)	$\partial NF/\partial \delta_{EI}$ (LB/DEG)	$\partial NF/\partial$% SSME POWER (LB/%)
10000	-270.0	0.0	20.0
12000	-307.0	0.0	18.0
14000	-318.0	13.0	13.0
16000	-318.0	35.0	9.6
18000	-337.0	176.0	15.0
19000	-381.0	213.0	18.0
20000	-403.0	264.0	39.0
21000	-410.0	276.0	83.0
22000	-352.0	280.0	90.0
23000	0.0	244.0	91.0
24000	328.0	213.0	87.0
25000	845.0	166.0	83.0
26000	886.0	167.0	80.0
28000	551.0	169.0	68.0
30000	282.0	171.0	73.0
34000	139.0	174.0	45.0
38000	131.0	175.0	-47.0
40000	129.0	148.0	N.A.
42500	132.0	121.0	
45000	146.0	103.0	
47500	151.0	76.0	
50000	156.0	41.0	
52500	168.0	16.0	
55000	178.0	-8.0	
57500	179.0	-37.0	
60000	184.0	-50.0	
62500	190.0	-68.0	
65000	194.0	-77.0	
67500	189.0	-88.0	
70000	190.0	-99.0	N.A.

Table 8-19

PITCHING MOMENT PARTIALS

ALTITUDE (ft)	$\partial PM/\partial \alpha$ (FT.LB./DEG.)	$\partial PM/\partial \delta_{EI}$ (FT.LB./DEG.)	$\partial PM/\partial$% SSME POWER (FT.LB./%)
10000	14019.0	0.0	-1070.0
12000	15742.0	0.0	-943.0
14000	16238.0	-1398.0	-638.0
16000	15725.0	-3763.0	-496.0
18000	16013.0	-18920.0	-755.0
19000	18021.0	-22898.0	-898.0
20000	19062.0	-28380.0	-1916.0
21000	19349.0	-29670.0	-4051.0
22000	16082.0	-30100.0	-4354.0
23000	0.0	-26230.0	-4246.0
24000	-13892.0	-22898.0	-3928.0
25000	-44056.0	-17845.0	-3587.0
26000	-37908.0	-17953.0	-4068.0
28000	-24108.0	-18167.0	-3713.0
30000	-12308.0	-18382.0	-4034.0
34000	-5947.0	-18705.0	-2322.0
38000	-5646.0	-18813.0	1667.0
40000	-4690.0	-15946.0	N.A.
42500	-4662.0	-13055.0	
45000	-4612.0	-11069.0	
47500	-4691.0	-8120.0	
50000	-4770.0	-4417.0	
52500	-4824.0	-1723.0	
55000	-4995.0	832.0	
57500	-5136.0	4012.0	
60000	-5178.0	5330.0	
62500	-5242.0	7280.0	
65000	-5274.0	8328.0	
67500	-5510.0	9446.0	
70000	-5584.0	10673.0	N.A.

Table 8-20

IA138
BASE COEFFICIENT TOLERANCES

$\pm\Delta C_A$

MACH NO.	SSLV	ORB	ET	SRB(1)
1.55	.0069	.0032	.0050	.0006
1.8	.0082	.0054	.0050	.0006
2.2	.0078	.0050	.0044	.0008
2.5	.0070	.0040	.0040	.0009

$\pm\Delta C_N$*

*$\Delta C_{N_o} = 0.6\ \Delta C_{A_o}$

MACH NO.	SSLV	ORB	ET	SRB(1)
1.55	.0030	.0019	.0007	.0008
1.8	.0039	.0032	.0009	.0007
2.2	.0037	.0030	.0010	.0006
2.5	.0032	.0024	.0012	.0005

$\pm\Delta C_Y$

MACH NO.	SSLV	ORB	ET	SRB(1)
1.55	.0015	.0012	.0006	.0004
1.8	.0015	.0010	.0008	.0005
2.2	.0017	.0008	.0010	.0008
2.5	.0019	.0006	.0012	.0010

1. $\Delta C_{A_{SSLV}} = \sqrt{(\Delta C_{A_o})^2 + (\Delta C_{A_{ET}} + 2\Delta C_{A_{SRB}})^2}$

2. $\Delta C_{y_{SSLV}} = \sqrt{(\Delta C_{y_o})^2 + (\Delta C_{y_{ET}})^2 + (\Delta C_{A_{SRB}})^2 + (\Delta C_{A_{SRB}})^2}$

3. $\Delta C_{N_o} = 0.6\Delta C_{A_o}$

Table 8-21

BASE MOMENT INCREMENTS

The general equations for the element moment increments are

$$\Delta C_M = \Delta C_N \left(\frac{X_N}{L}\right) + \Delta C_A \left(\frac{Z_A}{L}\right)$$

$$\Delta C_{YN} = \Delta C_Y \left(\frac{X_{YN}}{L}\right)$$

$$\Delta C_\ell = \Delta C_Y \left(\frac{Z_L}{L}\right) + \Delta C_N \left(\frac{Y_L}{L}\right)$$

The SSLV moment increment is determined by the following equations

$$\Delta C_{M_{SSLV}} = \sqrt{(\Delta C_{M_O})^2 + (\Delta C_{M_{ET}} + \Delta C_{M_{RSRB}} + \Delta C_{M_{LSRB}})^2}$$

$$\Delta C_{\underset{\ell}{YN}_{SSLV}} = \sqrt{(\Delta C_{\underset{\ell}{YN}_O})^2 + (\Delta C_{\underset{\ell}{YN}_{ET}})^2 + (\Delta C_{\underset{\ell}{YN}_{RSRB}})^2 + (\Delta C_{\underset{\ell}{YN}_{LSRB}})^2}$$

	ORBITER	ET	SRB RIGHT / LEFT
$\frac{X_N}{L}$ =	.99	.87	1.17
$\frac{Z_A}{L}$ =	.31	0.0	0.0
$\frac{X_{YN}}{L}$ =	1.06	0.87	0.195
$\frac{Y_L}{L}$ =	0.0	0.0	1.17
$\frac{Z_L}{L}$ =	.27	0.03	0.0

NOTE; L = 1290 INCHES

Section IX

FOREBODY PLUME INDUCED MATH MODEL

The nominal forebody plume induced aerodynamic characteristics were small except on the Orbiter fuselage and the inboard elevon. Math models have thus been developed for the SSLV, Orbiter, and the inboard elevon hinge moment. The SSLV and Orbiter normal force, pitching moment and inboard elevon hinge moment coefficient has the following type of math model.

$$\left.\begin{matrix} C_N \\ C_M \\ C_{H_{e_I}} \end{matrix}\right\} = \left.\begin{matrix} C_N \\ \\ \end{matrix}\right|_{\alpha-\beta_{MATRIX}} + \left[\left.\begin{matrix} \partial C_N/\partial\delta_{EI} \\ \\ \end{matrix}\right|_{\substack{\alpha-\beta \\ MATRIX \\ > \\ <}}\right] \times \Delta\delta_{EI} + \left[\left.\begin{matrix} \partial C_N/\partial\delta_{EO} \\ \\ \end{matrix}\right|_{\substack{> \\ <}}\right] \times \Delta\delta_{EO}\Big|_{\substack{\alpha-\beta \\ MATRIX}}$$

where C_N is a 4x7 matrix for $\alpha = +4,0,-4,-8$
$\beta = -6,-4,-2,0,2,4,6$

elevon deflection corresponds to close schedule 6 (Table 9-1 -6,-11)

$\partial C_N/\partial\delta_{EI}\Big|_{\substack{> \\ <}}$ is a 4x7 matrix for $\alpha = +4,0,-4,-8$
$\beta = -6,-4,-2,0,2,4,6$

> gradient for inboard elevon deflections > nominal (Table 9- -7,-12)
< gradient for inboard elevon deflections < nominal (Table 9- -8,-13)

$\partial C_N/\partial\delta_{EO}\Big|_{\substack{> \\ <}}$ is a 4x7 matrix for $\alpha = +4,0,-4,-8$
$\beta = -6,-4,-2,0,2,4,6$

> gradient for outboard elevon deflections > nominal (Table 9 -9,-14)
< gradient for outboard elevon deflections < nominal (Table 9 -10,-15)

$\Delta\delta_{EI}$ - change in inboard elevon deflection from nominal value specif in Table 9-1 to inboard elevon deflection of interest.

$\Delta\delta_{EO}$ - change in outboard elevon deflection from nominal value specified in Table 9-1 to outboard elevon deflection of interest.

The orbiter normal force and pitching moment math models were derived from the results of the pressure integration of the power-delta pressure coefficients The orbiter data used to derive the math model is presented in the tabulated dat in the Appendix - Section 9 (Forebody Pressure Integration) of the printout shee (see Section VII). The SSLV and Orbiter math models are identical since only th plume effects on the Orbiter are included in the math model. The wing data was combined with the Orbiter data. The wing gage power delta presented in the appendix is in error due to the differences in angle of attack from the power-of to the power-on attitude (see Section VII - Test Results). Selected interpolate wing power deltas were found to be significantly less than the tabulated values. The interpolated wing power delta was found to be approximately 3 percent of the power-off wing load and varied from positive to negative values. The nominal wi power delta was thus considered as zero. Interpolated values of the wing power delta are included in the tolerances of the wing and the Orbiter.

The hinge moment math model was derived from the left wing gage data, although the data is presented for the right wing. The left wing gage data used to develop the hinge moment math model is presented in the tabulated data in the appendix in Section 8 (GAGE DATA) of the printout sheet (see Section VII) The hinge moment data was not corrected for α differences (see discussion Section III - Test Results). An error of approximately 10 percent was introduced by not interpolating the data. This error was included in the tolerances.

FOREBODY COEFFICIENT TOLERANCES

Forebody tolerances have been developed for all forebody elements and components. As mentioned above, only the Orbiter and inboard elevon hinge moment had measurable plume induced aerodynamic changes that could be effectivel modeled. The other elements and components have zero nominal math model plume induced aerodynamic characteristics. Tolerances have been developed for all elements and components, however, to account for all possible variations in plum induced aerodynamic characteristics. The forebody element and component force coefficient tolerances are presented as tabled values that are the $\pm 3\sigma$ variation of the nominal coefficient. The $\pm 3\sigma$ variation covers the potential variation of the coefficient from the math model results to expected flight data values.

The SSLV and element force coefficient tolerances are presented in Table 9-21. The moment increment equations are presented in Table 9-22. The component force coefficient tolerances and moment equations are presented in Tables 9-23 and 9-24. The moment tolerances require using equations that include the force coefficient tolerances along with the nominal aerodynamic center in conjunction with the nominal forebody power delta (when $\neq 0$) times the aerodynamic center tolerance.

The forebody tolerances include contributions due to 1. test instrumentation uncertainty, 2. simulation parameter uncertainty, 3. Reynolds number characteristics, 4. Model-tunnel testing uncertainties, 5. Pressure integration uncertainties and 6. Math model uncertainties. Each tolerance contribution is assumed independent and therefore the contributions are combined using the RSS technique. The tolerances thus cover the uncertainty from the math model to flight data and are to a $\pm 3\sigma$ level with a Gussian distribution.

The forebody coefficients are determined using power delta's. Thus the instrumentation accuracy includes two independent measurements that are combined by the RSS techniques. The instrumentation accuracy for a single measurement is estimated to be 3 percent. Thus two measurements would be 4.3 percent. The general uncertainty in the nominal forebody force coefficient due to instrumentation uncertainty was estimated at 50 percent of the calculated nominal forebody coefficient. The similarity parameter uncertainty was estimated to be 30 percent of the nominal, Reynolds number and scale effect was estimated to be 100 percent of the nominal, model uncertainties were estimated to be 30 percent of the nominal, integration uncertainties at 30 percent of the nominal and math model uncertainties were estimated at 20 percent of the nominal value. The net RSS tolerance value for the forebody coefficients are large compared to the nominal math model values. This is because the nominal math model force coefficients are small. If the math model is not used the tolerance would be approximately double the values presented and it was determined that forebody tolerances approaching double the values presented in Table 9-16 would be excessive.

Portions of the forebody have zero nominal plume induced aerodynamic force coefficients in the math model although specific computed values have been determined and are listed in the tabulated data in the appendix (see Section VII). The tolerance analysis discussed above considered the nominal values calculated although the math model nominal force coefficients are zero.

Table 9-1. SSLV AND ORBITER POWER DELTA - NORMAL FORCE COEFFICIENT - FOREBODY

	MACH	α	β -6	-4	-2	0	+2	+4	+6	$\delta_{E_{I/O}}$
CN	1.55	-6.	.0232	.0227	.0223	.0218	.0223	.0227	.0232	10/-2
CN	1.55	-4.	.0267	.0253	.0238	.0224	.0238	.0253	.0267	
CN	1.55	-2.	.0254	.0237	.0221	.0204	.0221	.0237	.0254	
CN	1.55	0.	.0237	.0219	.0200	.0182	.0200	.0219	.0237	
CN	1.55	2.	.0239	.0215	.0192	.0168	.0192	.0215	.0239	
CN	1.55	4.	.0240	.0212	.0184	.0156	.0184	.0212	.0240	
CN	1.55	6.	.0241	.0209	.0176	.0144	.0176	.0209	.0241	
CN	1.80	-6.	.0177	.0202	.0227	.0252	.0227	.0202	.0177	10/-5
CN	1.80	-4.	.0210	.0222	.0234	.0246	.0234	.0222	.0210	
CN	1.80	-2.	.0226	.0228	.0230	.0232	.0230	.0228	.0226	
CN	1.80	0.	.0241	.0234	.0226	.0219	.0226	.0234	.0241	
CN	1.80	2.	.0240	.0234	.0229	.0223	.0229	.0234	.0240	
CN	1.80	4.	.0238	.0235	.0232	.0229	.0232	.0235	.0238	
CN	1.80	6.	.0228	.0223	.0218	.0212	.0218	.0223	.0228	
CN	2.20	-6.	.0216	.0234	.0252	.0270	.0252	.0234	.0216	4/-5
CN	2.20	-4.	.0214	.0231	.0248	.0265	.0248	.0231	.0214	
CN	2.20	-2.	.0202	.0215	.0228	.0241	.0228	.0215	.0202	
CN	2.20	0.	.0190	.0195	.0200	.0205	.0200	.0195	.0190	
CN	2.20	2.	.0188	.0190	.0192	.0194	.0192	.0190	.0188	
CN	2.20	4.	.0189	.0191	.0193	.0195	.0193	.0191	.0189	
CN	2.20	6.	.0189	.0192	.0194	.0197	.0194	.0192	.0189	
CN	2.49	-6.	.0242	.0239	.0236	.0234	.0236	.0239	.0242	0/-2
CN	2.49	-4.	.0264	.0254	.0244	.0233	.0244	.0254	.0264	
CN	2.49	-2.	.0251	.0240	.0229	.0219	.0229	.0240	.0251	
CN	2.49	0.	.0240	.0229	.0217	.0206	.0217	.0229	.0240	
CN	2.49	2.	.0263	.0242	.0221	.0199	.0221	.0242	.0263	
CN	2.49	4.	.0280	.0252	.0224	.0196	.0224	.0252	.0280	
CN	2.49	6.	.0273	.0251	.0229	.0208	.0229	.0251	.0273	

Table 9-2. SSLV AND ORBITER POWER DELTA - NORMAL FORCE COEFFICIENT - FOREBODY INBOARD ELEVON GRADIENT - δ_{EI} GREATER THAN NOMINAL

	MACH	α	β -6	-4	-2	0	+2	+4	+6
CN	1.55	-6.	.0008	.0005	.0003	.0000	.0003	.0005	.0008
CN	1.55	-4.	-.0013	-.0010	-.0006	-.0003	-.0006	-.0010	-.0013
CN	1.55	-2.	-.0024	-.0016	-.0007	.0001	-.0007	-.0016	-.0024
CN	1.55	0.	-.0032	-.0020	-.0007	.0006	-.0007	-.0020	-.0032
CN	1.55	2.	-.0026	-.0017	-.0007	.0002	-.0007	-.0017	-.0026
CN	1.55	4.	-.0020	-.0014	-.0007	-.0001	-.0007	-.0014	-.0020
CN	1.55	6.	-.0027	-.0014	-.0002	.0011	-.0002	-.0014	-.0027
CN	1.80	-6.	-.0001	-.0007	-.0013	-.0019	-.0013	-.0007	-.0001
CN	1.80	-4.	-.0010	-.0013	-.0016	-.0019	-.0016	-.0013	-.0010
CN	1.80	-2.	-.0017	-.0019	-.0020	-.0022	-.0020	-.0019	-.0017
CN	1.80	0.	-.0025	-.0024	-.0024	-.0024	-.0024	-.0024	-.0025
CN	1.80	2.	-.0024	-.0026	-.0028	-.0030	-.0028	-.0026	-.0024
CN	1.80	4.	-.0023	-.0027	-.0032	-.0037	-.0032	-.0027	-.0023
CN	1.80	6.	-.0018	-.0021	-.0024	-.0027	-.0024	-.0021	-.0018
CN	2.19	-6.	.0000	-.0002	-.0004	-.0006	-.0004	-.0002	.0000
CN	2.19	-4.	.0003	-.0001	-.0004	-.0007	-.0004	-.0001	.0003
CN	2.19	-2.	.0005	.0001	-.0002	-.0006	-.0002	.0001	.0005
CN	2.19	0.	.0007	.0004	.0000	-.0003	.0000	.0004	.0007
CN	2.19	2.	.0007	.0004	.0001	-.0002	.0001	.0004	.0007
CN	2.19	4.	.0006	.0003	.0001	-.0002	.0001	.0003	.0006
CN	2.19	6.	.0006	.0003	.0000	-.0002	.0000	.0003	.0006
CN	2.49	-6.	.0002	.0001	-.0000	-.0002	-.0000	.0001	.0002
CN	2.49	-4.	.0000	-.0001	-.0002	-.0003	-.0002	-.0001	.0000
CN	2.49	-2.	-.0000	-.0001	-.0003	-.0004	-.0003	-.0001	-.0000
CN	2.49	0.	-.0000	-.0002	-.0003	-.0005	-.0003	-.0002	-.0000
CN	2.49	2.	-.0001	-.0002	-.0003	-.0005	-.0003	-.0002	-.0001
CN	2.49	4.	-.0002	-.0003	-.0004	-.0005	-.0004	-.0003	-.0002
CN	2.49	6.	-.0006	-.0004	-.0002	-.0001	-.0002	-.0004	-.0006

Table 9-3. SSLV AND ORBITER POWER DELTA - NORMAL FORCE COEFFICIENT - FOREBODY INBOARD ELEVON GRADIENT - δ_{EI} LESS THAN NOMINAL

			β						
	MACH	α	-6	-4	-2	0	+2	+4	+6
CN	1.55	-6.	-.0019	-.0008	.0002	.0013	.0002	-.0008	-.0019
CN	1.55	-4.	-.0009	-.0002	.0005	.0012	.0005	-.0002	-.0009
CN	1.55	-2.	-.0001	.0004	.0008	.0013	.0008	.0004	-.0001
CN	1.55	0.	.0008	.0009	.0011	.0012	.0011	.0009	.0008
CN	1.55	2.	.0001	.0004	.0006	.0009	.0006	.0004	.0001
CN	1.55	4.	-.0003	.0000	.0003	.0006	.0003	.0000	-.0003
CN	1.55	6.	-.0016	-.0009	-.0002	.0006	-.0002	-.0009	-.0016
CN	1.80	-6.	.0003	.0004	.0005	.0006	.0005	.0004	.0003
CN	1.80	-4.	.0004	.0004	.0004	.0005	.0004	.0004	.0004
CN	1.80	-2.	.0002	.0003	.0004	.0006	.0004	.0003	.0002
CN	1.80	0.	-.0000	.0002	.0004	.0007	.0004	.0002	-.0000
CN	1.80	2.	-.0002	.0002	.0005	.0009	.0005	.0002	-.0002
CN	1.80	4.	-.0004	.0001	.0006	.0011	.0006	.0001	-.0004
CN	1.80	6.	-.0000	.0002	.0003	.0005	.0003	.0002	-.0000
CN	2.19	-6.	-.0005	-.0002	.0002	.0006	.0002	-.0002	-.0005
CN	2.19	-4.	-.0006	-.0004	-.0001	.0001	-.0001	-.0004	-.0006
CN	2.19	-2.	-.0008	-.0006	-.0004	-.0002	-.0004	-.0006	-.0008
CN	2.19	0.	-.0010	-.0008	-.0006	-.0003	-.0006	-.0008	-.0010
CN	2.19	2.	-.0011	-.0008	-.0006	-.0003	-.0006	-.0008	-.0011
CN	2.19	4.	-.0011	-.0008	-.0005	-.0002	-.0005	-.0008	-.0011
CN	2.19	6.	-.0009	-.0007	-.0004	-.0001	-.0004	-.0007	-.0009
CN	2.49	-6.	-.0002	-.0001	.0000	.0002	.0000	-.0001	-.0002
CN	2.49	-4.	-.0000	.0001	.0002	.0003	.0002	.0001	-.0000
CN	2.49	-2.	.0000	.0001	.0003	.0004	.0003	.0001	.0000
CN	2.49	0.	.0000	.0002	.0003	.0005	.0003	.0002	.0000
CN	2.49	2.	.0001	.0002	.0003	.0005	.0003	.0002	.0001
CN	2.49	4.	.0002	.0003	.0004	.0005	.0004	.0003	.0002
CN	2.49	6.	.0006	.0004	.0002	.0001	.0002	.0004	.0006

Table 9-4. SSLV AND ORBITER POWER DELTA - NORMAL FORCE COEFFICIENT - FOREBODY OUTBOARD ELEVON GRADIENT - δ_{EO} GREATER THAN NOMINAL

	MACH	α	β -6	-4	-2	0	+2	+4	+6
CN	1.55	-6.	-.0007	-.0003	.0001	.0004	.0001	-.0003	-.0007
CN	1.55	-4.	.0002	.0003	.0004	.0005	.0004	.0003	.0002
CN	1.55	-2.	.0005	.0005	.0005	.0005	.0005	.0005	.0005
CN	1.55	0.	.0009	.0007	.0005	.0004	.0005	.0007	.0009
CN	1.55	2.	.0006	.0006	.0005	.0004	.0005	.0006	.0006
CN	1.55	4.	.0005	.0005	.0004	.0004	.0004	.0005	.0005
CN	1.55	6.	.0002	.0003	.0004	.0005	.0004	.0003	.0002
CN	1.80	-6.	-.0000	-.0004	-.0007	-.0011	-.0007	-.0004	-.0000
CN	1.80	-4.	-.0008	-.0010	-.0012	-.0013	-.0012	-.0010	-.0008
CN	1.80	-2.	-.0016	-.0015	-.0015	-.0014	-.0015	-.0015	-.0016
CN	1.80	0.	-.0023	-.0021	-.0018	-.0015	-.0018	-.0021	-.0023
CN	1.80	2.	-.0015	-.0016	-.0018	-.0019	-.0018	-.0016	-.0015
CN	1.80	4.	-.0006	-.0012	-.0018	-.0024	-.0018	-.0012	-.0006
CN	1.80	6.	-.0008	-.0009	-.0009	-.0010	-.0009	-.0009	-.0008
CN	2.20	-6.	.0005	-.0000	-.0006	-.0011	-.0006	-.0000	.0005
CN	2.20	-4.	.0002	-.0001	-.0005	-.0008	-.0005	-.0001	.0002
CN	2.20	-2.	.0011	.0004	-.0002	-.0009	-.0002	.0004	.0011
CN	2.20	0.	.0021	.0011	.0002	-.0008	.0002	.0011	.0021
CN	2.20	2.	.0023	.0013	.0003	-.0006	.0003	.0013	.0023
CN	2.20	4.	.0023	.0013	.0003	-.0007	.0003	.0013	.0023
CN	2.20	6.	.0023	.0013	.0003	-.0007	.0003	.0013	.0023
CN	2.49	-6.	.0005	.0003	.0002	.0000	.0002	.0003	.0005
CN	2.49	-4.	-.0001	-.0001	-.0000	.0000	-.0000	-.0001	-.0001
CN	2.49	-2.	-.0002	-.0001	-.0000	.0001	-.0000	-.0001	-.0002
CN	2.49	0.	-.0002	-.0001	-.0000	.0001	-.0000	-.0001	-.0002
CN	2.49	2.	-.0004	-.0002	-.0001	-.0000	-.0001	-.0002	-.0004
CN	2.49	4.	-.0004	-.0003	-.0002	-.0001	-.0002	-.0003	-.0004
CN	2.49	6.	-.0001	-.0001	-.0001	-.0002	-.0001	-.0001	-.0001

Table 9-5. SSLV AND ORBITER POWER DELTA - NORMAL FORCE COEFFICIENT - FOREBODY OUTBOARD ELEVON GRADIENT - δ_{EO} LESS THAN NOMINAL

	MACH	α	β -6	-4	-2	0	+2	+4	+6
CN	1.55	-6.	-.0007	-.0003	.0001	.0004	.0001	-.0003	-.0007
CN	1.55	-4.	.0002	.0003	.0004	.0005	.0004	.0003	.0002
CN	1.55	-2.	.0005	.0005	.0005	.0005	.0005	.0005	.0005
CN	1.55	0.	.0009	.0007	.0005	.0004	.0005	.0007	.0009
CN	1.55	2.	.0006	.0006	.0005	.0004	.0005	.0006	.0006
CN	1.55	4.	.0005	.0005	.0004	.0004	.0004	.0005	.0005
CN	1.55	6.	.0002	.0003	.0004	.0005	.0004	.0003	.0002
CN	1.80	-6.	-.0022	-.0005	.0012	.0029	.0012	-.0005	-.0022
CN	1.80	-4.	-.0013	.0002	.0017	.0032	.0017	.0002	-.0013
CN	1.80	-2.	.0014	.0020	.0026	.0032	.0026	.0020	.0014
CN	1.80	0.	.0042	.0038	.0035	.0032	.0035	.0038	.0042
CN	1.80	2.	.0029	.0033	.0037	.0041	.0037	.0033	.0029
CN	1.80	4.	.0017	.0028	.0039	.0049	.0039	.0028	.0017
CN	1.80	6.	.0016	.0020	.0024	.0028	.0024	.0020	.0016
CN	2.20	-6.	-.0007	.0001	.0010	.0018	.0010	.0001	-.0007
CN	2.20	-4.	-.0006	-.0000	.0005	.0011	.0005	-.0000	-.0006
CN	2.20	-2.	-.0012	-.0005	.0001	.0008	.0001	-.0005	-.0012
CN	2.20	0.	-.0020	-.0011	-.0001	.0008	-.0001	-.0011	-.0020
CN	2.20	2.	-.0022	-.0013	-.0003	.0006	-.0003	-.0013	-.0022
CN	2.20	4.	-.0022	-.0014	-.0005	.0004	-.0005	-.0014	-.0022
CN	2.20	6.	-.0020	-.0012	-.0004	.0004	-.0004	-.0012	-.0020
CN	2.49	-6.	-.0006	-.0004	-.0002	.0000	-.0002	-.0004	-.0006
CN	2.49	-4.	-.0000	-.0000	.0000	.0000	.0000	-.0000	-.0000
CN	2.49	-2.	-.0002	-.0002	-.0001	-.0001	-.0001	-.0002	-.0002
CN	2.49	0.	-.0004	-.0003	-.0002	-.0001	-.0002	-.0003	-.0004
CN	2.49	2.	-.0002	-.0001	.0000	.0001	.0000	-.0001	-.0002
CN	2.49	4.	-.0001	.0001	.0002	.0003	.0002	.0001	-.0001
CN	2.49	6.	.0001	.0001	.0001	.0001	.0001	.0001	.0001

Table 9-6. SSLV AND ORBITER POWER DELTA - PITCHING MOMENT COEFFICIENT - FOREBODY

	MACH	α	β -6	-4	-2	0	+2	+4	+6	$\delta E_{I/O}$
CM	1.55	-6.	-.0222	-.0217	-.0213	-.0208	-.0213	-.0217	-.0222	10/-2
CM	1.55	-4.	-.0252	-.0239	-.0225	-.0212	-.0225	-.0239	-.0252	
CM	1.55	-2.	-.0242	-.0226	-.0211	-.0195	-.0211	-.0226	-.0242	
CM	1.55	0.	-.0228	-.0211	-.0194	-.0177	-.0194	-.0211	-.0228	
CM	1.55	2.	-.0229	-.0207	-.0186	-.0165	-.0186	-.0207	-.0229	
CM	1.55	4.	-.0229	-.0204	-.0178	-.0153	-.0178	-.0204	-.0229	
CM	1.55	6.	-.0229	-.0200	-.0170	-.0141	-.0170	-.0200	-.0229	
CM	1.80	-6.	-.0172	-.0194	-.0216	-.0238	-.0216	-.0194	-.0172	10/-5
CM	1.80	-4.	-.0199	-.0209	-.0219	-.0229	-.0219	-.0209	-.0199	
CM	1.80	-2.	-.0211	-.0213	-.0215	-.0216	-.0215	-.0213	-.0211	
CM	1.80	0.	-.0223	-.0217	-.0210	-.0203	-.0210	-.0217	-.0223	
CM	1.80	2.	-.0224	-.0218	-.0211	-.0205	-.0211	-.0218	-.0224	
CM	1.80	4.	-.0224	-.0219	-.0213	-.0208	-.0213	-.0219	-.0224	
CM	1.80	6.	-.0213	-.0208	-.0203	-.0199	-.0203	-.0208	-.0213	
CM	2.20	-6.	-.0210	-.0227	-.0243	-.0260	-.0243	-.0227	-.0210	4/-5
CM	2.20	-4.	-.0207	-.0223	-.0240	-.0256	-.0240	-.0223	-.0207	
CM	2.20	-2.	-.0197	-.0209	-.0221	-.0232	-.0221	-.0209	-.0197	
CM	2.20	0.	-.0186	-.0191	-.0195	-.0198	-.0195	-.0191	-.0188	
CM	2.20	2.	-.0189	-.0188	-.0187	-.0187	-.0187	-.0188	-.0189	
CM	2.20	4.	-.0191	-.0190	-.0188	-.0186	-.0188	-.0190	-.0191	
CM	2.20	6.	-.0190	-.0189	-.0188	-.0187	-.0188	-.0189	-.0190	
CM	2.49	-6.	-.0230	-.0229	-.0228	-.0227	-.0228	-.0229	-.0230	0/-2
CM	2.49	-4.	-.0252	-.0244	-.0235	-.0226	-.0235	-.0244	-.0252	
CM	2.49	-2.	-.0240	-.0230	-.0221	-.0212	-.0221	-.0230	-.0240	
CM	2.49	0.	-.0229	-.0220	-.0210	-.0200	-.0210	-.0220	-.0229	
CM	2.49	2.	-.0252	-.0232	-.0213	-.0193	-.0213	-.0232	-.0252	
CM	2.49	4.	-.0268	-.0242	-.0216	-.0190	-.0216	-.0242	-.0268	
CM	2.49	6.	-.0261	-.0241	-.0221	-.0202	-.0221	-.0241	-.0261	

Table 9-7. SSLV AND ORBITER POWER DELTA - PITCHING MOMENT COEFFICIENT - FOREBODY INBOARD ELEVON GRADIENT - δ_{EI} GREATER THAN NOMINAL

	MACH	α	β -6	-4	-2	0	+2	+4	+6
CM	1.55	-6.	-.0008	-.0006	-.0003	-.0001	-.0003	-.0006	-.0008
CM	1.55	-4.	.0011	.0008	.0005	.0002	.0005	.0008	.0011
CM	1.55	-2.	.0019	.0012	.0005	-.0001	.0005	.0012	.0019
CM	1.55	0.	.0026	.0016	.0005	-.0005	.0005	.0016	.0026
CM	1.55	2.	.0021	.0013	.0006	-.0002	.0006	.0013	.0021
CM	1.55	4.	.0016	.0011	.0006	.0001	.0006	.0011	.0016
CM	1.55	6.	.0022	.0011	.0001	-.0010	.0001	.0011	.0022
CM	1.80	-6.	.0000	.0005	.0011	.0016	.0011	.0005	.0000
CM	1.80	-4.	.0006	.0009	.0012	.0015	.0012	.0009	.0006
CM	1.80	-2.	.0011	.0013	.0015	.0017	.0015	.0013	.0011
CM	1.80	0.	.0017	.0018	.0018	.0019	.0018	.0018	.0017
CM	1.80	2.	.0018	.0020	.0022	.0023	.0022	.0020	.0018
CM	1.80	4.	.0019	.0022	.0025	.0028	.0025	.0022	.0019
CM	1.80	6.	.0014	.0016	.0018	.0021	.0018	.0016	.0014
CM	2.19	-6.	-.0000	.0002	.0004	.0006	.0004	.0002	-.0000
CM	2.19	-4.	-.0002	.0001	.0004	.0007	.0004	.0001	-.0002
CM	2.19	-2.	-.0004	-.0001	.0003	.0006	.0003	-.0001	-.0004
CM	2.19	0.	-.0006	-.0003	.0000	.0003	.0000	-.0003	-.0006
CM	2.19	2.	-.0005	-.0003	-.0000	.0002	-.0000	-.0003	-.0005
CM	2.19	4.	-.0004	-.0002	-.0000	.0002	-.0000	-.0002	-.0004
CM	2.19	6.	-.0004	-.0002	.0000	.0002	.0000	-.0002	-.0004
CM	2.49	-6.	-.0002	-.0001	.0000	.0002	.0000	-.0001	-.0002
CM	2.49	-4.	-.0001	.0001	.0002	.0003	.0002	.0001	-.0001
CM	2.49	-2.	-.0000	.0001	.0003	.0004	.0003	.0001	-.0000
CM	2.49	0.	.0000	.0002	.0003	.0005	.0003	.0002	.0000
CM	2.49	2.	.0001	.0002	.0003	.0004	.0003	.0002	.0001
CM	2.49	4.	.0002	.0003	.0004	.0005	.0004	.0003	.0002
CM	2.49	6.	.0006	.0004	.0002	.0001	.0002	.0004	.0006

Table 9-8. SSLV AND ORBITER POWER DELTA - PITCHING MOMENT COEFFICIENT - FOREBODY INBOARD ELEVON GRADIENT - δ_{EI} LESS THAN NOMINAL

	MACH	α	β -6	-4	-2	0	+2	+4	+6
CM	1.55	-6.	.0017	.0008	-.0001	-.0010	-.0001	.0008	.0017
CM	1.55	-4.	.0010	.0003	-.0003	-.0009	-.0003	.0003	.0010
CM	1.55	-2.	.0003	-.0001	-.0006	-.0010	-.0006	-.0001	.0003
CM	1.55	0.	-.0005	-.0006	-.0008	-.0009	-.0008	-.0006	-.0005
CM	1.55	2.	-.0000	-.0002	-.0005	-.0007	-.0005	-.0002	-.0000
CM	1.55	4.	.0001	-.0000	-.0002	-.0004	-.0002	-.0000	.0001
CM	1.55	6.	.0011	.0006	.0001	-.0003	.0001	.0006	.0011
CM	1.80	-6.	-.0002	-.0003	-.0004	-.0005	-.0004	-.0003	-.0002
CM	1.80	-4.	-.0002	-.0003	-.0003	-.0003	-.0003	-.0003	-.0002
CM	1.80	-2.	-.0000	-.0002	-.0003	-.0004	-.0003	-.0002	-.0000
CM	1.80	0.	.0001	-.0001	-.0003	-.0004	-.0003	-.0001	.0001
CM	1.80	2.	.0002	-.0000	-.0003	-.0006	-.0003	-.0000	.0002
CM	1.80	4.	.0003	-.0000	-.0004	-.0007	-.0004	-.0000	.0003
CM	1.80	6.	.0001	-.0000	-.0001	-.0003	-.0001	-.0000	.0001
CM	2.19	-6.	.0004	.0001	-.0002	-.0005	-.0002	.0001	.0004
CM	2.19	-4.	.0005	.0004	.0002	-.0000	.0002	.0004	.0005
CM	2.19	-2.	.0007	.0005	.0004	.0002	.0004	.0005	.0007
CM	2.19	0.	.0008	.0007	.0005	.0004	.0005	.0007	.0008
CM	2.19	2.	.0009	.0007	.0005	.0004	.0005	.0007	.0009
CM	2.19	4.	.0009	.0007	.0005	.0003	.0005	.0007	.0009
CM	2.19	6.	.0007	.0005	.0004	.0002	.0004	.0005	.0007
CM	2.49	-6.	.0002	.0001	-.0000	-.0002	-.0000	.0001	.0002
CM	2.49	-4.	.0001	-.0001	-.0002	-.0003	-.0002	-.0001	.0001
CM	2.49	-2.	.0000	-.0001	-.0003	-.0004	-.0003	-.0001	.0000
CM	2.49	0.	-.0000	-.0002	-.0003	-.0005	-.0003	-.0002	-.0000
CM	2.49	2.	-.0001	-.0002	-.0003	-.0004	-.0003	-.0002	-.0001
CM	2.49	4.	-.0002	-.0003	-.0004	-.0005	-.0004	-.0003	-.0002
CM	2.49	6.	-.0006	-.0004	-.0002	-.0001	-.0002	-.0004	-.0006

Table 9-9. SSLV AND ORBITER POWER DELTA - PITCHING MOMENT COEFFICIENT - FOREBODY OUTBOARD ELEVON GRADIENT - δ_{EO} GREATER THAN NOMINAL

	MACH	α	β -6	-4	-2	0	+2	+4	+6
CM	1.55	-6.	.0007	.0003	-.0000	-.0004	-.0000	.0003	.0007
CM	1.55	-4.	-.0001	-.0002	-.0003	-.0004	-.0003	-.0002	-.0001
CM	1.55	-2.	-.0004	-.0004	-.0004	-.0004	-.0004	-.0004	-.0004
CM	1.55	0.	-.0007	-.0006	-.0004	-.0003	-.0004	-.0006	-.0007
CM	1.55	2.	-.0005	-.0005	-.0004	-.0004	-.0004	-.0005	-.0005
CM	1.55	4.	-.0004	-.0004	-.0003	-.0003	-.0003	-.0004	-.0004
CM	1.55	6.	-.0002	-.0003	-.0004	-.0005	-.0004	-.0003	-.0002
CM	1.80	-6.	-.0000	.0003	.0006	.0009	.0006	.0003	-.0000
CM	1.80	-4.	.0005	.0007	.0009	.0010	.0009	.0007	.0005
CM	1.80	-2.	.0011	.0011	.0011	.0011	.0011	.0011	.0011
CM	1.80	0.	.0018	.0016	.0014	.0011	.0014	.0016	.0018
CM	1.80	2.	.0012	.0012	.0013	.0014	.0013	.0012	.0012
CM	1.80	4.	.0005	.0009	.0013	.0017	.0013	.0009	.0005
CM	1.80	6.	.0006	.0006	.0006	.0006	.0006	.0006	.0006
CM	2.20	-6.	-.0003	.0001	.0005	.0009	.0005	.0001	-.0003
CM	2.20	-4.	-.0001	.0002	.0004	.0007	.0004	.0002	-.0001
CM	2.20	-2.	-.0009	-.0003	.0003	.0008	.0003	-.0003	-.0009
CM	2.20	0.	-.0017	-.0009	-.0001	.0008	-.0001	-.0009	-.0017
CM	2.20	2.	-.0018	-.0010	-.0002	.0005	-.0002	-.0010	-.0018
CM	2.20	4.	-.0018	-.0010	-.0002	.0005	-.0002	-.0010	-.0018
CM	2.20	6.	-.0018	-.0010	-.0002	.0006	-.0002	-.0010	-.0018
CM	2.49	-6.	-.0005	-.0003	-.0002	-.0000	-.0002	-.0003	-.0005
CM	2.49	-4.	.0001	.0000	-.0000	-.0000	-.0000	.0000	.0001
CM	2.49	-2.	.0001	.0001	-.0000	-.0001	-.0000	.0001	.0001
CM	2.49	0.	.0002	.0001	-.0000	-.0001	-.0000	.0001	.0002
CM	2.49	2.	.0003	.0002	.0001	.0000	.0001	.0002	.0003
CM	2.49	4.	.0004	.0003	.0002	.0001	.0002	.0003	.0004
CM	2.49	6.	.0001	.0001	.0001	.0001	.0001	.0001	.0001

Table 9-10. SSLV AND ORBITER POWER DELTA - PITCHING MOMENT COEFFICIENT - FOREBODY OUTBOARD ELEVON GRADIENT - δ_{EO} LESS THAN NOMINAL

	MACH	α	β -6	-4	-2	0	+2	+4	+6
CM	1.55	-6.	.0007	.0003	-.0000	-.0004	-.0000	.0003	.0007
CM	1.55	-4.	-.0001	-.0002	-.0003	-.0004	-.0003	-.0002	-.0001
CM	1.55	-2.	-.0004	-.0004	-.0004	-.0004	-.0004	-.0004	-.0004
CM	1.55	0.	-.0007	-.0006	-.0004	-.0003	-.0004	-.0006	-.0007
CM	1.55	2.	-.0005	-.0005	-.0004	-.0004	-.0004	-.0005	-.0005
CM	1.55	4.	-.0004	-.0004	-.0003	-.0003	-.0003	-.0004	-.0004
CM	1.55	6.	-.0002	-.0003	-.0004	-.0005	-.0004	-.0003	-.0002
CM	1.80	-6.	.0018	.0004	-.0010	-.0024	-.0010	.0004	.0018
CM	1.80	-4.	.0012	-.0000	-.0013	-.0025	-.0013	-.0000	.0012
CM	1.80	-2.	-.0010	-.0015	-.0020	-.0025	-.0020	-.0015	-.0010
CM	1.80	0.	-.0033	-.0031	-.0028	-.0025	-.0028	-.0031	-.0033
CM	1.80	2.	-.0024	-.0026	-.0029	-.0031	-.0029	-.0026	-.0024
CM	1.80	4.	-.0016	-.0022	-.0029	-.0036	-.0029	-.0022	-.0016
CM	1.80	6.	-.0011	-.0014	-.0017	-.0020	-.0017	-.0014	-.0011
CM	2.20	-6.	.0005	-.0001	-.0008	-.0015	-.0008	-.0001	.0005
CM	2.20	-4.	.0004	-.0000	-.0005	-.0010	-.0005	-.0000	.0004
CM	2.20	-2.	.0009	.0004	-.0002	-.0007	-.0002	.0004	.0009
CM	2.20	0.	.0016	.0008	.0001	-.0007	.0001	.0008	.0016
CM	2.20	2.	.0017	.0010	.0002	-.0005	.0002	.0010	.0017
CM	2.20	4.	.0016	.0010	.0004	-.0003	.0004	.0010	.0016
CM	2.20	6.	.0015	.0010	.0004	-.0002	.0004	.0010	.0015
CM	2.49	-6.	.0006	.0004	.0002	-.0000	.0002	.0004	.0006
CM	2.49	-4.	.0000	.0000	-.0000	-.0000	-.0000	.0000	.0000
CM	2.49	-2.	.0003	.0002	.0001	.0001	.0001	.0002	.0003
CM	2.49	0.	.0005	.0003	.0002	.0001	.0002	.0003	.0005
CM	2.49	2.	.0003	.0002	-.0000	-.0002	-.0000	.0002	.0003
CM	2.49	4.	.0001	-.0000	-.0001	-.0003	-.0001	-.0000	.0001
CM	2.49	6.	-.0001	-.0001	-.0001	-.0001	-.0001	-.0001	-.0001

Table 9-11. INBOARD ELEVON - HINGE MOMENT COEFFICIENT - POWER DELTA

	MACH	α	β -6	-4	-2	0	+2	+4	+6	$\delta E_{I/O}$
DCHEI	1.55	-6.	-.0157	-.0128	-.0099	-.0069	-.0049	-.0034	-.0020	10/-2
DCHEI	1.55	-4.	-.0163	-.0124	-.0085	-.0046	-.0036	-.0033	-.0029	
DCHEI	1.55	-2.	-.0159	-.0104	-.0069	-.0034	-.0028	-.0026	-.0024	
DCHEI	1.55	0.	-.0111	-.0083	-.0054	-.0025	-.0020	-.0019	-.0018	
DCHEI	1.55	2.	-.0102	-.0074	-.0047	-.0019	-.0014	-.0011	-.0008	
DCHEI	1.55	4.	-.0091	-.0065	-.0040	-.0014	-.0007	-.0003	.0001	
DCHEI	1.55	6.	-.0081	-.0057	-.0033	-.0009	-.0000	.0005	.0011	
DCHEI	1.80	-6.	-.0160	-.0140	-.0121	-.0101	-.0071	-.0046	-.0020	10/-5
DCHEI	1.80	-4.	-.0149	-.0128	-.0106	-.0085	-.0070	-.0057	-.0045	
DCHEI	1.80	-2.	-.0129	-.0112	-.0094	-.0076	-.0062	-.0050	-.0039	
DCHEI	1.80	0.	-.0110	-.0095	-.0081	-.0067	-.0054	-.0044	-.0033	
DCHEI	1.80	2.	-.0097	-.0084	-.0071	-.0058	-.0055	-.0052	-.0050	
DCHEI	1.80	4.	-.0084	-.0072	-.0061	-.0049	-.0055	-.0061	-.0068	
DCHEI	1.80	6.	-.0062	-.0056	-.0051	-.0045	-.0052	-.0059	-.0067	
DCHEI	2.20	-6.	-.0165	-.0157	-.0149	-.0140	-.0102	-.0067	-.0032	4/-5
DCHEI	2.20	-4.	-.0179	-.0156	-.0132	-.0109	-.0070	-.0035	-.0001	
DCHEI	2.20	-2.	-.0153	-.0128	-.0103	-.0078	-.0046	-.0019	.0009	
DCHEI	2.20	0.	-.0123	-.0098	-.0072	-.0046	-.0022	-.0002	.0018	
DCHEI	2.20	2.	-.0094	-.0073	-.0052	-.0031	-.0015	-.0000	.0014	
DCHEI	2.20	4.	-.0064	-.0050	-.0037	-.0024	-.0013	-.0003	.0007	
DCHEI	2.20	6.	-.0055	-.0043	-.0032	-.0021	-.0016	-.0012	-.0009	
DCHEI	2.49	-6.	-.0208	-.0168	-.0129	-.0089	-.0079	-.0072	-.0066	0/-2
DCHEI	2.49	-4.	-.0224	-.0178	-.0131	-.0085	-.0068	-.0054	-.0041	
DCHEI	2.49	-2.	-.0221	-.0170	-.0120	-.0069	-.0054	-.0044	-.0034	
DCHEI	2.49	0.	-.0216	-.0162	-.0108	-.0054	-.0043	-.0035	-.0028	
DCHEI	2.49	2.	-.0186	-.0138	-.0091	-.0043	-.0042	-.0044	-.0046	
DCHEI	2.49	4.	-.0152	-.0113	-.0074	-.0036	-.0043	-.0051	-.0060	
DCHEI	2.49	6.	-.0102	-.0082	-.0062	-.0043	-.0047	-.0052	-.0057	

Table 9-12. INBOARD ELEVON POWER DELTA - HINGE MOMENT COEFFICIENT
INBOARD ELEVON GRADIENT - δ_{EI} GREATER THAN NOMINAL

	MACH	α	β -6	-4	-2	0	+2	+4	+6
DCHEI	1.55	-6.	.0014	.0011	.0008	.0005	-.0006	-.0014	-.0023
DCHEI	1.55	-4.	.0021	.0014	.0007	-.0001	-.0005	-.0009	-.0012
DCHEI	1.55	-2.	.0016	.0010	.0005	-.0001	-.0001	-.0001	-.0000
DCHEI	1.55	0.	.0009	.0006	.0003	.0000	.0004	.0007	.0011
DCHEI	1.55	2.	.0008	.0005	.0002	-.0001	.0000	.0002	.0004
DCHEI	1.55	4.	.0007	.0004	.0000	-.0003	-.0003	-.0003	-.0004
DCHEI	1.55	6.	.0003	-.0002	-.0008	-.0013	-.0010	-.0007	-.0004
DCHEI	1.80	-6.	.0014	.0017	.0021	.0024	.0021	.0018	.0015
DCHEI	1.80	-4.	.0010	.0013	.0016	.0019	.0021	.0023	.0024
DCHEI	1.80	-2.	.0007	.0012	.0016	.0020	.0020	.0019	.0018
DCHEI	1.80	0.	.0005	.0010	.0016	.0021	.0019	.0016	.0013
DCHEI	1.80	2.	.0004	.0008	.0011	.0015	.0016	.0018	.0019
DCHEI	1.80	4.	.0003	.0005	.0007	.0009	.0014	.0019	.0024
DCHEI	1.80	6.	-.0002	.0003	.0007	.0012	.0014	.0015	.0016
DCHEI	2.19	-6.	.0003	.0005	.0007	.0009	.0011	.0012	.0013
DCHEI	2.19	-4.	.0008	.0008	.0009	.0010	.0007	.0005	.0003
DCHEI	2.19	-2.	.0010	.0009	.0008	.0007	.0003	-.0000	-.0004
DCHEI	2.19	0.	.0013	.0009	.0005	.0002	-.0002	-.0005	-.0009
DCHEI	2.19	2.	.0011	.0007	.0003	-.0000	-.0004	-.0007	-.0010
DCHEI	2.19	4.	.0007	.0005	.0002	-.0001	-.0004	-.0007	-.0010
DCHEI	2.19	6.	.0006	.0003	.0001	-.0002	-.0004	-.0006	-.0007
DCHEI	2.49	-6.	.0000	.0000	.0000	.0000	.0002	.0003	.0004
DCHEI	2.49	-4.	.0004	.0003	.0003	.0002	.0001	.0001	.0001
DCHEI	2.49	-2.	.0007	.0006	.0004	.0003	.0001	.0001	-.0000
DCHEI	2.49	0.	.0010	.0008	.0006	.0004	.0001	-.0000	-.0002
DCHEI	2.49	2.	.0011	.0008	.0005	.0002	-.0000	-.0002	-.0003
DCHEI	2.49	4.	.0010	.0007	.0004	.0000	-.0002	-.0003	-.0005
DCHEI	2.49	6.	.0007	.0004	.0000	-.0003	-.0003	-.0002	-.0001

Table 9-13. INBOARD ELEVON POWER DELTA - HINGE MOMENT COEFFICIENT
INBOARD ELEVON GRADIENT - δ_{EI} LESS THAN NOMINAL

	MACH	α	β -6	-4	-2	0	+2	+4	+6
DCHEI	1.55	-6.	.0027	.0016	.0005	-.0006	.0007	.0021	.0034
DCHEI	1.55	-4.	.0018	.0010	.0001	-.0008	.0006	.0019	.0031
DCHEI	1.55	-2.	.0019	.0011	.0003	-.0006	.0002	.0010	.0018
DCHEI	1.55	0.	.0022	.0013	.0004	-.0005	-.0002	.0001	.0004
DCHEI	1.55	2.	.0017	.0009	.0001	-.0006	-.0002	.0002	.0006
DCHEI	1.55	4.	.0009	.0004	-.0001	-.0006	-.0002	.0003	.0008
DCHEI	1.55	6.	.0008	.0002	-.0004	-.0009	-.0002	.0004	.0011
DCHEI	1.80	-6.	.0002	.0001	-.0001	-.0002	-.0003	-.0004	-.0004
DCHEI	1.80	-4.	.0005	.0003	.0001	-.0000	-.0002	-.0003	-.0004
DCHEI	1.80	-2.	.0005	.0002	-.0001	-.0003	-.0004	-.0004	-.0003
DCHEI	1.80	0.	.0005	.0002	-.0002	-.0006	-.0005	-.0004	-.0003
DCHEI	1.80	2.	.0003	.0000	-.0003	-.0005	-.0005	-.0004	-.0003
DCHEI	1.80	4.	.0000	-.0001	-.0003	-.0004	-.0004	-.0004	-.0003
DCHEI	1.80	6.	.0001	-.0000	-.0002	-.0003	-.0004	-.0005	-.0005
DCHEI	2.19	-6.	.0006	.0003	-.0001	-.0004	-.0003	-.0002	-.0001
DCHEI	2.19	-4.	.0004	.0003	.0002	.0001	.0003	.0005	.0006
DCHEI	2.19	-2.	.0006	.0005	.0003	.0002	.0005	.0008	.0011
DCHEI	2.19	0.	.0010	.0007	.0003	.0000	.0005	.0011	.0016
DCHEI	2.19	2.	.0011	.0007	.0004	-.0000	.0004	.0009	.0013
DCHEI	2.19	4.	.0011	.0007	.0004	.0001	.0003	.0005	.0007
DCHEI	2.19	6.	.0007	.0005	.0003	.0001	.0002	.0003	.0004
DCHEI	2.49	-6.	-.0000	-.0000	-.0000	-.0000	-.0002	-.0003	-.0004
DCHEI	2.49	-4.	-.0004	-.0003	-.0003	-.0002	-.0001	-.0001	-.0001
DCHEI	2.49	-2.	-.0007	-.0006	-.0004	-.0003	-.0001	-.0001	.0000
DCHEI	2.49	0.	-.0010	-.0008	-.0006	-.0004	-.0001	.0000	.0002
DCHEI	2.49	2.	-.0011	-.0008	-.0005	-.0002	.0000	.0002	.0003
DCHEI	2.49	4.	-.0010	-.0007	-.0004	-.0000	.0002	.0003	.0005
DCHEI	2.49	6.	-.0007	-.0004	-.0000	.0003	.0003	.0002	.0001

Table 9-14. INBOARD ELEVON POWER DELTA - HINGE MOMENT COEFFICIENT OUTBOARD ELEVON GRADIENT - δ_{EO} GREATER THAN NOMINAL

			β						
	MACH	α	-6	-4	-2	0	+2	+4	+6
DCHEI	1.55	-6.	.0004	.0001	-.0001	-.0004	-.0000	.0004	.0008
DCHEI	1.55	-4.	-.0004	-.0003	-.0002	-.0001	.0001	.0003	.0005
DCHEI	1.55	-2.	-.0001	-.0001	-.0001	-.0001	-.0000	.0000	.0001
DCHEI	1.55	0.	.0002	.0001	-.0000	-.0002	-.0002	-.0002	-.0002
DCHEI	1.55	2.	.0002	.0000	-.0001	-.0002	-.0002	-.0002	-.0002
DCHEI	1.55	4.	.0002	.0000	-.0001	-.0002	-.0002	-.0002	-.0001
DCHEI	1.55	6.	.0002	-.0000	-.0002	-.0004	-.0003	-.0001	.0000
DCHEI	1.80	-6.	.0000	.0005	.0009	.0014	.0015	.0016	.0016
DCHEI	1.80	-4.	-.0011	-.0003	.0005	.0013	.0016	.0017	.0019
DCHEI	1.80	-2.	-.0007	.0000	.0008	.0015	.0015	.0015	.0015
DCHEI	1.80	0.	-.0003	.0004	.0010	.0017	.0015	.0013	.0010
DCHEI	1.80	2.	.0000	.0005	.0009	.0014	.0015	.0015	.0016
DCHEI	1.80	4.	.0003	.0006	.0008	.0011	.0015	.0018	.0021
DCHEI	1.80	6.	-.0000	.0003	.0006	.0009	.0011	.0014	.0016
DCHEI	2.20	-6.	-.0004	.0000	.0004	.0008	.0010	.0010	.0011
DCHEI	2.20	-4.	.0002	.0003	.0005	.0006	.0005	.0002	.0000
DCHEI	2.20	-2.	-.0000	.0002	.0004	.0006	.0002	-.0003	-.0007
DCHEI	2.20	0.	-.0001	.0001	.0003	.0005	-.0002	-.0009	-.0016
DCHEI	2.20	2.	-.0000	.0001	.0002	.0003	-.0005	-.0012	-.0019
DCHEI	2.20	4.	.0000	.0001	.0001	.0002	-.0007	-.0015	-.0023
DCHEI	2.20	6.	.0002	.0001	.0000	-.0001	-.0007	-.0013	-.0020
DCHEI	2.49	-6.	.0000	.0001	.0001	.0001	.0001	.0002	.0002
DCHEI	2.49	-4.	-.0001	-.0000	.0001	.0001	.0002	.0002	.0002
DCHEI	2.49	-2.	-.0002	-.0001	.0000	.0001	.0002	.0003	.0004
DCHEI	2.49	0.	-.0002	-.0001	.0000	.0002	.0003	.0005	.0006
DCHEI	2.49	2.	-.0001	.0000	.0002	.0003	.0004	.0006	.0008
DCHEI	2.49	4.	.0000	.0001	.0002	.0003	.0005	.0007	.0009
DCHEI	2.49	6.	-.0001	.0000	.0001	.0003	.0004	.0006	.0008

Table 9-15. INBOARD ELEVON POWER DELTA - HINGE MOMENT COEFFICIENT
OUTBOARD ELEVON GRADIENT - δ_{EO} LESS THAN NOMINAL

	MACH	α	β -6	-4	-2	0	+2	+4	+6
DCHEI	1.55	-6.	.0004	.0001	-.0001	-.0004	-.0000	.0004	.0008
DCHEI	1.55	-4.	-.0004	-.0003	-.0002	-.0001	.0001	.0003	.0005
DCHEI	1.55	-2.	-.0001	-.0001	-.0001	-.0001	-.0000	.0000	.0001
DCHEI	1.55	0.	.0002	.0001	-.0000	-.0002	-.0002	-.0002	-.0002
DCHEI	1.55	2.	.0002	.0000	-.0001	-.0002	-.0002	-.0002	-.0002
DCHEI	1.55	4.	.0002	.0000	-.0001	-.0002	-.0002	-.0002	-.0001
DCHEI	1.55	6.	.0002	-.0000	-.0002	-.0004	-.0003	-.0001	.0000
DCHEI	1.80	-6.	.0018	-.0001	-.0020	-.0039	-.0024	-.0009	.0007
DCHEI	1.80	-4.	.0023	.0007	-.0008	-.0024	-.0022	-.0019	-.0016
DCHEI	1.80	-2.	.0022	.0006	-.0010	-.0026	-.0024	-.0020	-.0016
DCHEI	1.80	0.	.0019	.0003	-.0013	-.0029	-.0025	-.0020	-.0015
DCHEI	1.80	2.	.0009	-.0002	-.0014	-.0025	-.0029	-.0031	-.0032
DCHEI	1.80	4.	.0000	-.0007	-.0015	-.0022	-.0032	-.0040	-.0048
DCHEI	1.80	6.	.0009	-.0002	-.0013	-.0024	-.0027	-.0029	-.0031
DCHEI	2.20	-6.	.0014	.0004	-.0005	-.0015	-.0012	-.0009	-.0006
DCHEI	2.20	-4.	-.0001	-.0003	-.0006	-.0008	-.0002	.0003	.0008
DCHEI	2.20	-2.	-.0001	-.0002	-.0004	-.0005	.0001	.0007	.0013
DCHEI	2.20	0.	-.0001	-.0002	-.0003	-.0004	.0003	.0011	.0018
DCHEI	2.20	2.	-.0000	-.0001	-.0002	-.0003	.0005	.0013	.0020
DCHEI	2.20	4.	-.0000	-.0001	-.0001	-.0002	.0007	.0015	.0023
DCHEI	2.20	6.	-.0001	-.0001	-.0001	-.0001	.0005	.0010	.0016
DCHEI	2.49	-6.	.0001	.0001	.0001	.0001	-.0000	-.0001	-.0002
DCHEI	2.49	-4.	.0002	.0002	.0002	.0001	.0001	-.0000	-.0001
DCHEI	2.49	-2.	-.0000	.0001	.0002	.0003	.0001	-.0001	-.0003
DCHEI	2.49	0.	-.0002	.0000	.0002	.0003	.0001	-.0001	-.0004
DCHEI	2.49	2.	-.0001	-.0000	-.0000	-.0000	-.0001	-.0001	-.0002
DCHEI	2.49	4.	.0000	-.0001	-.0002	-.0003	-.0002	-.0001	-.0000
DCHEI	2.49	6.	.0000	-.0000	-.0001	-.0002	-.0003	-.0003	-.0003

Table 9-16. OUTBOARD ELEVON - HINGE MOMENT COEFFICIENT POWER DELTA

	MACH	α	β -6	-4	-2	0	+2	+4	+6	$\delta E_{I/O}$
DCHEO	1.55	-6.	-.0007	.0007	.0021	.0035	.0065	.0090	.0115	10/-2
DCHEO	1.55	-4.	-.0005	.0008	.0021	.0034	.0056	.0074	.0092	
DCHEO	1.55	-2.	-.0005	.0009	.0023	.0037	.0054	.0069	.0083	
DCHEO	1.55	0.	-.0005	.0010	.0025	.0040	.0053	.0064	.0074	
DCHEO	1.55	2.	-.0004	.0012	.0027	.0042	.0053	.0062	.0070	
DCHEO	1.55	4.	-.0002	.0013	.0029	.0044	.0053	.0059	.0065	
DCHEO	1.55	6.	-.0001	.0015	.0030	.0046	.0052	.0057	.0061	
DCHEO	1.80	-6.	-.0103	-.0079	-.0054	-.0029	.0041	.0103	.0165	10/-5
DCHEO	1.80	-4.	-.0083	-.0068	-.0053	-.0038	.0009	.0051	.0092	
DCHEO	1.80	-2.	-.0075	-.0059	-.0043	-.0028	.0007	.0037	.0068	
DCHEO	1.80	0.	-.0068	-.0050	-.0033	-.0016	.0006	.0025	.0044	
DCHEO	1.80	2.	-.0063	-.0046	-.0028	-.0010	.0013	.0034	.0054	
DCHEO	1.80	4.	-.0059	-.0041	-.0023	-.0005	.0020	.0043	.0065	
DCHEO	1.80	6.	-.0040	-.0025	-.0011	.0003	.0030	.0054	.0079	
DCHEO	2.20	-6.	-.0083	-.0062	-.0042	-.0021	-.0009	.0001	.0011	4/-5
DCHEO	2.20	-4.	-.0050	-.0048	-.0046	-.0044	-.0040	-.0037	-.0033	
DCHEO	2.20	-2.	-.0041	-.0045	-.0048	-.0051	-.0046	-.0041	-.0035	
DCHEO	2.20	0.	-.0040	-.0043	-.0047	-.0051	-.0045	-.0039	-.0034	
DCHEO	2.20	2.	-.0038	-.0042	-.0047	-.0051	-.0044	-.0038	-.0031	
DCHEO	2.20	4.	-.0036	-.0041	-.0047	-.0052	-.0044	-.0036	-.0027	
DCHEO	2.20	6.	-.0039	-.0043	-.0046	-.0050	-.0051	-.0053	-.0054	
DCHEO	2.49	-6.	-.0154	-.0094	-.0034	.0026	-.0017	-.0062	-.0106	0/-2
DCHEO	2.49	-4.	-.0106	-.0069	-.0032	.0006	-.0017	-.0041	-.0066	
DCHEO	2.49	-2.	-.0082	-.0055	-.0027	.0000	-.0018	-.0036	-.0054	
DCHEO	2.49	0.	-.0060	-.0042	-.0024	-.0005	-.0018	-.0032	-.0045	
DCHEO	2.49	2.	-.0049	-.0037	-.0024	-.0011	-.0025	-.0038	-.0051	
DCHEO	2.49	4.	-.0041	-.0033	-.0025	-.0018	-.0030	-.0042	-.0055	
DCHEO	2.49	6.	-.0044	-.0039	-.0034	-.0029	-.0033	-.0038	-.0043	

Table 9-17. OUTBOARD ELEVON - HINGE MOMENT COEFFICIENT POWER DELTA
INBOARD ELEVON GRADIENT - δ_{EI} GREATER THAN NOMINAL

	MACH	α	β -6	-4	-2	0	+2	+4	+6
DCHEO	1.55	-6.	.0005	-.0015	-.0034	-.0054	-.0081	-.0103	-.0124
DCHEO	1.55	-4.	-.0007	-.0023	-.0039	-.0056	-.0078	-.0096	-.0113
DCHEO	1.55	-2.	-.0005	-.0021	-.0037	-.0053	-.0074	-.0090	-.0106
DCHEO	1.55	0.	-.0003	-.0019	-.0035	-.0051	-.0069	-.0084	-.0099
DCHEO	1.55	2.	-.0009	-.0020	-.0031	-.0042	-.0063	-.0081	-.0099
DCHEO	1.55	4.	-.0014	-.0021	-.0028	-.0035	-.0057	-.0077	-.0097
DCHEO	1.55	6.	-.0003	-.0019	-.0034	-.0049	-.0063	-.0075	-.0086
DCHEO	1.80	-6.	.0059	.0042	.0024	.0006	-.0056	-.0112	-.0167
DCHEO	1.80	-4.	.0047	.0030	.0014	-.0003	-.0040	-.0071	-.0103
DCHEO	1.80	-2.	.0044	.0025	.0007	-.0012	-.0039	-.0062	-.0086
DCHEO	1.80	0.	.0041	.0020	-.0000	-.0021	-.0039	-.0054	-.0069
DCHEO	1.80	2.	.0031	.0015	-.0002	-.0018	-.0039	-.0057	-.0076
DCHEO	1.80	4.	.0022	.0009	-.0003	-.0016	-.0040	-.0061	-.0082
DCHEO	1.80	6.	.0011	.0001	-.0008	-.0018	-.0040	-.0061	-.0082
DCHEO	2.19	-6.	.0033	.0025	.0016	.0008	.0002	-.0002	-.0006
DCHEO	2.19	-4.	.0014	.0013	.0012	.0010	.0010	.0009	.0008
DCHEO	2.19	-2.	.0009	.0009	.0010	.0010	.0010	.0009	.0009
DCHEO	2.19	0.	.0007	.0007	.0008	.0008	.0008	.0008	.0008
DCHEO	2.19	2.	.0005	.0006	.0008	.0009	.0008	.0007	.0006
DCHEO	2.19	4.	.0003	.0006	.0008	.0011	.0008	.0006	.0003
DCHEO	2.19	6.	.0004	.0006	.0008	.0010	.0010	.0011	.0011
DCHEO	2.49	-6.	.0058	.0026	-.0006	-.0037	-.0040	-.0041	-.0041
DCHEO	2.49	-4.	.0036	.0014	-.0007	-.0028	-.0032	-.0036	-.0039
DCHEO	2.49	-2.	.0028	.0010	-.0008	-.0025	-.0031	-.0035	-.0039
DCHEO	2.49	0.	.0021	.0006	-.0008	-.0023	-.0029	-.0034	-.0039
DCHEO	2.49	2.	.0011	.0000	-.0011	-.0022	-.0027	-.0032	-.0037
DCHEO	2.49	4.	.0003	-.0005	-.0013	-.0020	-.0025	-.0029	-.0033
DCHEO	2.49	6.	-.0015	-.0007	.0001	.0009	-.0009	-.0027	-.0044

Table 9-18. OUTBOARD ELEVON - HINGE MOMENT COEFFICIENT POWER DELTA INBOARD ELEVON GRADIENT - δ_{EI} LESS THAN NOMINAL

			β						
	MACH	α	-6	-4	-2	0	+2	+4	+6
DCHEO	1.55	-6.	-.0023	-.0011	.0002	.0014	.0052	.0085	.0117
DCHEO	1.55	-4.	-.0000	.0002	.0004	.0006	.0043	.0076	.0108
DCHEO	1.55	-2.	-.0002	.0004	.0009	.0014	.0043	.0069	.0095
DCHEO	1.55	0.	-.0003	.0005	.0013	.0021	.0044	.0063	.0082
DCHEO	1.55	2.	-.0014	-.0002	.0010	.0022	.0042	.0060	.0077
DCHEO	1.55	4.	-.0023	-.0007	.0009	.0025	.0042	.0056	.0070
DCHEO	1.55	6.	-.0037	-.0017	.0003	.0023	.0040	.0052	.0065
DCHEO	1.80	-6.	-.0030	-.0022	-.0013	-.0004	.0011	.0024	.0037
DCHEO	1.80	-4.	-.0021	-.0014	-.0008	-.0001	.0008	.0017	.0025
DCHEO	1.80	-2.	-.0017	-.0011	-.0005	.0001	.0009	.0015	.0022
DCHEO	1.80	0.	-.0013	-.0008	-.0002	.0003	.0009	.0014	.0019
DCHEO	1.80	2.	-.0009	-.0004	-.0000	.0004	.0010	.0016	.0022
DCHEO	1.80	4.	-.0004	-.0001	.0001	.0004	.0011	.0018	.0025
DCHEO	1.80	6.	-.0003	-.0000	.0002	.0005	.0011	.0016	.0022
DCHEO	2.19	-6.	-.0001	-.0006	-.0010	-.0015	-.0043	-.0069	-.0095
DCHEO	2.19	-4.	.0000	-.0008	-.0016	-.0024	-.0039	-.0053	-.0066
DCHEO	2.19	-2.	.0000	-.0008	-.0017	-.0026	-.0036	-.0044	-.0053
DCHEO	2.19	0.	.0000	-.0008	-.0016	-.0024	-.0032	-.0038	-.0044
DCHEO	2.19	2.	-.0002	-.0009	-.0016	-.0024	-.0030	-.0036	-.0041
DCHEO	2.19	4.	-.0004	-.0011	-.0017	-.0023	-.0029	-.0035	-.0040
DCHEO	2.19	6.	-.0006	-.0012	-.0017	-.0023	-.0038	-.0052	-.0066
DCHEO	2.49	-6.	-.0058	-.0026	.0006	.0037	.0040	.0041	.0041
DCHEO	2.49	-4.	-.0036	-.0014	.0007	.0028	.0032	.0036	.0039
DCHEO	2.49	-2.	-.0028	-.0010	.0008	.0025	.0031	.0035	.0039
DCHEO	2.49	0.	-.0021	-.0006	.0008	.0023	.0029	.0034	.0039
DCHEO	2.49	2.	-.0011	-.0000	.0011	.0022	.0027	.0032	.0037
DCHEO	2.49	4.	-.0003	.0005	.0013	.0020	.0025	.0029	.0033
DCHEO	2.49	6.	.0015	.0007	-.0001	-.0009	.0009	.0027	.0044

Table 9-19. OUTBOARD ELEVON - HINGE MOMENT COEFFICIENT POWER DELTA
OUTBOARD ELEVON GRADIENT - δ_{EO} GREATER THAN NOMINAL

	MACH	α	β -6	-4	-2	0	+2	+4	+6
DCHEO	1.55	-6.	.0007	.0003	-.0001	-.0005	-.0001	.0004	.0008
DCHEO	1.55	-4.	.0008	.0004	-.0001	-.0005	-.0003	-.0001	.0001
DCHEO	1.55	-2.	.0007	.0003	-.0001	-.0005	-.0004	-.0002	.0000
DCHEO	1.55	0.	.0005	.0002	-.0001	-.0005	-.0004	-.0003	-.0001
DCHEO	1.55	2.	.0004	.0001	-.0001	-.0004	-.0004	-.0004	-.0003
DCHEO	1.55	4.	.0001	.0000	-.0000	-.0001	-.0003	-.0005	-.0006
DCHEO	1.55	6.	.0000	-.0000	-.0001	-.0001	-.0004	-.0006	-.0008
DCHEO	1.80	-6.	.0040	.0030	.0020	.0010	-.0014	-.0035	-.0057
DCHEO	1.80	-4.	.0027	.0023	.0018	.0013	-.0001	-.0014	-.0027
DCHEO	1.80	-2.	.0021	.0017	.0012	.0008	-.0001	-.0009	-.0017
DCHEO	1.80	0.	.0015	.0011	.0007	.0002	-.0001	-.0004	-.0007
DCHEO	1.80	2.	.0012	.0008	.0005	.0001	-.0004	-.0008	-.0012
DCHEO	1.80	4.	.0009	.0006	.0003	.0001	-.0006	-.0012	-.0018
DCHEO	1.80	6.	.0010	.0006	.0002	-.0002	-.0010	-.0018	-.0026
DCHEO	2.20	-6.	.0028	.0021	.0014	.0007	.0003	-.0000	-.0004
DCHEO	2.20	-4.	.0017	.0016	.0015	.0015	.0013	.0012	.0011
DCHEO	2.20	-2.	.0014	.0015	.0016	.0017	.0015	.0014	.0012
DCHEO	2.20	0.	.0013	.0014	.0016	.0017	.0015	.0013	.0011
DCHEO	2.20	2.	.0013	.0014	.0016	.0017	.0015	.0013	.0010
DCHEO	2.20	4.	.0012	.0014	.0016	.0017	.0015	.0012	.0009
DCHEO	2.20	6.	.0013	.0014	.0015	.0017	.0017	.0018	.0018
DCHEO	2.49	-6.	.0024	.0025	.0027	.0028	.0056	.0082	.0107
DCHEO	2.49	-4.	.0021	.0022	.0023	.0025	.0046	.0065	.0084
DCHEO	2.49	-2.	.0015	.0018	.0022	.0025	.0043	.0059	.0075
DCHEO	2.49	0.	.0010	.0015	.0020	.0025	.0039	.0053	.0067
DCHEO	2.49	2.	.0007	.0013	.0018	.0024	.0038	.0051	.0065

Table 9-20. OUTBOARD ELEVON - HINGE MOMENT COEFFICIENT POWER DELTA
OUTBOARD ELEVON GRADIENT - δ_{EO} LESS THAN NOMINAL

	MACH	α	β -6	-4	-2	0	+2	+4	+6
DCHEO	1.55	-6.	.0007	.0003	-.0001	-.0005	-.0001	.0004	.0008
DCHEO	1.55	-4.	.0008	.0004	-.0001	-.0005	-.0003	-.0001	.0001
DCHEO	1.55	-2.	.0007	.0003	-.0001	-.0005	-.0004	-.0002	.0000
DCHEO	1.55	0.	.0005	.0002	-.0001	-.0005	-.0004	-.0003	-.0001
DCHEO	1.55	2.	.0004	.0001	-.0001	-.0004	-.0004	-.0004	-.0003
DCHEO	1.55	4.	.0001	.0000	-.0000	-.0001	-.0003	-.0005	-.0006
DCHEO	1.55	6.	.0000	-.0000	-.0001	-.0001	-.0004	-.0006	-.0008
DCHEO	1.80	-6.	-.0064	-.0051	-.0037	-.0024	.0018	.0056	.0094
DCHEO	1.80	-4.	-.0040	-.0035	-.0030	-.0026	.0001	.0025	.0049
DCHEO	1.80	-2.	-.0035	-.0030	-.0024	-.0019	-.0001	.0014	.0030
DCHEO	1.80	0.	-.0032	-.0025	-.0018	-.0011	-.0003	.0003	.0010
DCHEO	1.80	2.	-.0032	-.0025	-.0019	-.0012	.0001	.0013	.0025
DCHEO	1.80	4.	-.0032	-.0026	-.0019	-.0012	.0006	.0023	.0040
DCHEO	1.80	6.	-.0025	-.0019	-.0013	-.0007	.0017	.0038	.0060
DCHEO	2.20	-6.	-.0015	-.0005	.0005	.0015	-.0020	-.0053	-.0087
DCHEO	2.20	-4.	.0005	-.0000	-.0006	-.0012	-.0028	-.0043	-.0058
DCHEO	2.20	-2.	.0009	-.0001	-.0010	-.0020	-.0025	-.0029	-.0034
DCHEO	2.20	0.	.0007	-.0001	-.0009	-.0017	-.0019	-.0019	-.0020
DCHEO	2.20	2.	.0009	.0001	-.0008	-.0016	-.0017	-.0017	-.0017
DCHEO	2.20	4.	.0013	.0004	-.0005	-.0014	-.0016	-.0017	-.0019
DCHEO	2.20	6.	.0011	.0003	-.0005	-.0013	-.0010	-.0008	-.0006
DCHEO	2.49	-6.	-.0075	-.0051	-.0028	-.0004	-.0012	-.0021	-.0030
DCHEO	2.49	-4.	-.0051	-.0034	-.0018	-.0001	-.0004	-.0008	-.0012
DCHEO	2.49	-2.	-.0041	-.0027	-.0014	-.0000	-.0001	-.0003	-.0004
DCHEO	2.49	0.	-.0031	-.0021	-.0010	.0001	.0002	.0002	.0003
DCHEO	2.49	2.	-.0027	-.0018	-.0008	.0002	.0002	.0001	.0001
DCHEO	2.49	4.	-.0022	-.0014	-.0006	.0002	.0002	.0001	-.0000
DCHEO	2.49	6.	-.0011	-.0007	-.0003	.0001	.0002	.0002	.0002

Table 9-21

FOREBODY FORCE COEFFICIENT TOLERANCES - SSLV AND ELEMENTS

MACH NO.	SSLV	ORB	ET	SRB(1)
		$\pm\Delta C_A$		
1.55	.0143	.0015	.0015	.0100
1.80	.0171	.0016	.0016	.0120
2.20	.0171	.0017	.0017	.0120
2.50	.0186	.0018	.0018	.0130
		$\pm\Delta C_N$		
1.55	.0271	.0162	.0050	.0150
1.80	.0302	.0192	.0060	.0160
2.20	.0276	.0162	.0070	.0150
2.50	.0255	.0157	.0080	.0130
		$\pm\Delta C_Y$		
1.55	.0256	.0030	.0008	.0180
1.80	.0355	.0030	.0012	.0250
2.20	.0383	.0025	.0014	.0270
2.50	.0340	.0020	.0016	.0240

Table 9-22

FOREBODY MOMENT INCREMENT EQUATIONS - SSLV AND ELEMENTS

ELEMENTS

$$\Delta C_M = \sqrt{\left[\Delta C_N \left(\frac{X_N}{L}\right)\right]^2 + \left[C_N \left(\frac{\Delta X_N}{L}\right)\right]^2 + \left[\Delta C_A \left(\frac{Z_A}{L}\right)\right]^2}$$

$$\Delta C_{YN} = \sqrt{\left[\Delta C_Y \left(\frac{X_{YN}}{L}\right)\right]^2 + \left[\Delta C_A \left(\frac{Y_{ZL}}{L}\right)\right]^2}$$

$$\Delta C_{\ell} = \sqrt{\left[\Delta C_Y \left(\frac{Z_L}{L}\right)\right]^2 + \left[\Delta C_N \left(\frac{Y_L}{L}\right)\right]^2}$$

SSLV TYPICAL

$$\Delta C_{M_{SSLV}} = \sqrt{(\Delta C_{M_o})^2 + (\Delta C_{M_{ET}})^2 + (\Delta C_{M_{RSRB}})^2 + (\Delta C_{M_{LSRB}})^2}$$

MACH	ORB $\frac{X_N}{L}$	$\frac{\Delta X_N}{L}$	$\frac{X_{YN}}{L}$	$\frac{Z_L}{L}$	$\frac{Y_{ZL}}{L}$	$\frac{Y_L}{L}$	$\frac{Z_A}{L}$	ET $\frac{X_N}{L}$	$\frac{\Delta X_N}{L}$	$\frac{X_{YN}}{L}$	$\frac{Z_L}{L}$	$\frac{Y_{ZL}}{L}$	$\frac{Y_L}{L}$	$\frac{Z_A}{L}$
1.55	.99	.02	1.0	.44	0	0	.26	.8	0	.8	.03	.03	.03	.03
1.80	.99	.02	1.0	.44	0	0	.26	.8	0	.8	.03	.03	.03	.03
2.20	.99	.02	1.0	.44	0	0	.26	.8	0	.8	.03	.03	.03	.03
2.50	.99	.02	1.0	.44	0	0	.26	.8	0	.8	.03	.03	.03	.03

MACH	SRB RIGHT LEFT $\frac{X_N}{L}$	$\frac{\Delta X_N}{L}$	$\frac{X_{YN}}{L}$	$\frac{Z_L}{L}$	$\frac{Y_{ZL}}{L}$	$\frac{Y_L}{L}$	$\frac{Z_A}{L}$
1.55	1.10	0	1.10	0	.194	.194	.02
1.80	1.10	0	1.10	0	.194	.194	.02
2.20	1.10	0	1.10	0	.194	.194	.02
2.50	1.10	0	1.10	0	.194	.194	.02

NOTE: L = 1290 INCHES

Table 9-23

FOREBODY FORCE TOLERANCES — COMPONENTS

WING TOLERANCES		VERTICAL TAIL TOLERANCES
MACH	$\pm\Delta$CNW	$\pm\Delta$CYV
1.55	.010	.010
1.80	.012	.012
2.20	.010	.012
2.50	.010	.013

Table 9-24

FOREBODY MOMENT EQUATIONS — COMPONENTS

WING

$$\Delta C_{BW} = \Delta C_{NW} \left(\frac{y_w}{b}\right)$$

$$\Delta C_{TW} = \Delta C_{NW} \left(\frac{x_w}{\bar{c}}\right)$$

VERTICAL TAIL

$$\Delta C_{BV} = \sqrt{\left[\Delta C_{YV}\left(\frac{Z_V}{L}\right)\right]^2 + \left[C_{YV}\left(\frac{\Delta Z_V}{L}\right)\right]^2}$$

$$\Delta C_{TV} = \sqrt{\left[\Delta C_{YV}\left(\frac{X_V}{L}\right)\right]^2 + \left[C_{YV}\left(\frac{\Delta X_V}{L}\right)\right]^2}$$

HINGE MOMENT

$$\Delta CHEI = \Delta CHEI$$

$$\Delta CHEO = \Delta CHEO$$

MACH	WING[1] $\frac{y_w}{b}$	WING[1] $\frac{x_w}{\bar{c}}$	VERTICAL[2] $\frac{Z_V}{L}$	VERTICAL[2] $\frac{\Delta Z_V}{L}$	VERTICAL[2] $\frac{X_V}{L}$	VERTICAL[2] $\frac{\Delta X_V}{L}$	$\pm\Delta$CHEI	$\pm\Delta$CHEO
1.55	.110	-.32	.45	.30	.40	.10	.0030	.0050
1.80	.110	-.32	.45	.30	.40	.10	.0030	.0060
2.20	.110	-.32	.45	.30	.40	.10	.0060	.0060
2.50	.110	-.32	.47	.30	.40	.10	.0030	.0080

1 For Wing

b = 936.68"

c = 474.81"

2 Vertical

L = 199.8 in.

Section X

CONCLUSIONS

Problems with the IA138 test were mainly limited to differences in the model attitude for the power-off and power-on runs. This difference mainly influenced the wing gage data. It is estimated that the wing power delta's are most severely influenced by this problem.

There was a measurable change in the performance of the SSME nozzles approximately half way through the test that should be investigated. The change in performance is approximately within the tolerance level of the instrumentation, however it is a consistent change.

The base axial forces and base pressures show some unexpected slight variations that may be due to the change in performance of the SSME nozzles. The majority of the base pressure data appeared to be consistent.

The major independent variables that change the plume induced aerodynamic characteristics are angle of attack, angle of sideslip, inboard elevon deflection and SRB and SSME power level.

Section XI

RECOMMENDATIONS

It is recommended that the SSME nozzle performance be studied to evaluate the change in performance that occurred during the test.

It is also recommended that the test data be evaluated using the new similarity parameters and a new math model of the plume induced base and forebody aerodynamic characteristics be developed.

Section XII

REFERENCES

1. Marroquin, J., "Pretest Information for Test IA138 of the 0.010-Scale 75-OTS Jet Plume Space Shuttle Model in the 9x7-Foot Leg of the NASA/ARC Unitary Plan Wind Tunnel", Document SD78-SH-0133, Rockwell International, Space Division, June 12, 1978.

2. Informal notes and figures, some from RI memo SAS/WTO/74-367.

3. Program 7413, "Shuttle Nozzle Calibration 75-OTS for IA82B and C, Test Log" Rocket Nozzle Wind Tunnel, Rocketdyne, dated 24 September 1974.

4. Program 7413, "Rocket Nozzle Test Facility Pressure Transducer Calibration Data", Rocketdyne, dated 17 October 1974.

5. Program 7502, "75-OTS SRB Nozzle Calibration IA-82 B&C Test Log," Rocket Nozzle Wind Tunnel, Rocketdyne, dated 17 October 1974.

6. Program 7502, "Rocket Nozzle Test Facility Pressure Transducer Calibration Data", Rocketdyne, dated 29 October 1974.

7. Crowder, R. S., "75-OTS Nozzle Calibration Requirements (SRB) for IA82B and C", Internal letter #SAS/WTO/74-184, Rockwell International, dated 10 Octob 1974.

8. Andrews, C. D., "MSFC Input for RI/SD SSLV Wind Tunnel Tests IA119/IA138 NASA Memo ED32-77-13, dated February 23, 1977.

9. Boyle, W. W., "Plume Technology Program Base Pressure Similarity Parameters NSI Memo M-9230-76-45, dated July 1976.

10. Sims, Joseph L., "Plume Simulation Technology", MSFC Systems Dynamics Laboratory, Viewgraph presentation, dated January 1979.